**EGE UNIVERSITY GRADUATE SCHOOL OF
NATURAL AND APPLIED SCIENCES**

(MSc THESIS)

APPLICATION OF ADVANCED OXIDATION AND NOVEL BIOLOGICAL METHODS FOR TREATMENT OF TEREPHTHALIC ACID PLANT WASTEWATER

Gülen TEKİN

Supervisor : Prof. Dr. Süheyda ATALAY

Chemical Engineering Department

Discipline Code : 603.02.00
Presentation Date: 13.01.2015

Bornova-İZMİR

2015

Gülen Tekin tarafından yüksek lisans tezi olarak sunulan "Application of Advanced Oxidation and Novel Biological Methods For Treatment of Terephthalic Acid Plant Wastewater" başlıklı bu çalışma E.Ü. Lisansüstü Eğitim ve Öğretim Yönetmeliği ile E.Ü. Fen Bilimleri Enstitüsü Eğitim ve Öğretim Yönergesi'nin ilgili hükümleri uyarınca tarafımızdan değerlendirilerek savunmaya değer bulunmuş ve 13.01.2015 tarihinde yapılan tez savunma sınavında aday oybirliği/~~oyçokluğu~~ ile başarılı bulunmuştur.

Jüri Üyeleri:		**İmza**
Jüri Başkanı	**: Prof. Dr. Süheyda ATALAY**	
Raportör Üye	**: Prof. Dr. Ferhan S. ATALAY**	
Üye	**: Prof. Dr. Murat ELİBOL**	

EGE ÜNİVERSİTESİ FEN BİLİMLERİ ENSTİTÜSÜ

ETİK KURALLARA UYGUNLUK BEYANI

E.Ü. Lisansüstü Eğitim ve Öğretim Yönetmeliğinin ilgili hükümleri uyarınca Yüksek Lisans Tezi / Doktora Tezi olarak sunduğum "Application of Advanced Oxidation and Novel Biological Methods For Treatment of Terephthalic Acid Plant Wastewater" başlıklı bu tezin kendi çalışmam olduğunu, sunduğum tüm sonuç, doküman, bilgi ve belgeleri bizzat ve bu tez çalışması kapsamında elde ettiğimi, bu tez çalışmasıyla elde edilmeyen bütün bilgi ve yorumlara atıf yaptığımı ve bunları kaynaklar listesinde usulüne uygun olarak verdiğimi, tez çalışması ve yazımı sırasında patent ve telif haklarını ihlal edici bir davranışımın olmadığını, bu tezin herhangi bir bölümünü bu üniversite veya diğer bir üniversitede başka bir tez çalışması içinde sunmadığımı, bu tezin planlanmasından yazımına kadar bütün safhalarda bilimsel etik kurallarına uygun olarak davrandığımı ve aksinin ortaya çıkması durumunda her türlü yasal sonucu kabul edeceğimi beyan ederim.

13/ 01 / 2015

Gülen Tekin

ÖZET

TEREFTALİK ASİT FABRİKASI ATIKSULARININ ARITILMASINDA İLERİ OKSİDASYON VE YENİ BİYOLOJİK YÖNTEMLERİN UYGULANMASI

TEKİN, Gülen

Yüksek Lisans Tezi, Kimya Mühendisliği Anabilim Dalı
Tez Danışmanı: Prof. Dr. Süheyda ATALAY
Ocak 2015, 138 sayfa

Bu tez kapsamında, tereftalik asit fabrikası atıksuyunun ceviz kabuklarından hazırlanan katalizörler varlığında çeşitli ileri oksidasyon yöntemleri ve yenilikçi bir biyolojik oksidasyon yöntemi ile giderimi araştırılmıştır.

Tereftalik asit fabrikası atıksuyunu yansıtması için giderimi hedeflenen bileşikler tereftalik asit (TPA), benzoik asit (BA) ve p-toluik asit (p-Tol) olarak seçilmiştir. Benzoik asit için Fenton benzeri oksidasyon, katalitik ıslak hava oksidasyonu, fotokatalitik oksidasyon, foto-Fenton benzeri oksidasyon gibi çeşitli ileri oksidasyon yöntemleri ile biyolojik oksidasyon yöntem ile giderimi araştırılmıştır. Tereftalik asit ve p-toluik asitin; Fenton benzeri oksidasyon, fotokatalitik oksidasyon ve foto-Fenton-benzeri oksidasyon yöntemleri ile giderimi incelenmiştir.

İlk aşama olarak metal tutturulan ceviz kabuğu temelli katalizörlerin hazırlanması ve karakterizasyonu gerçekleştirilmiştir. Ceviz kabuklarından fiziksel ve kimyasal (asidik, nötral ve bazik) olmak üzere farklı aktivasyon yöntemleri ile hazırlanan aktif karbon (AK) yapısına % 10 oranında demir (Fe) veya demir-titanyum dioksit (Fe-TiO_2 (1:99)) tutturularak Fe/AK ve Fe-TiO_2/AK katalizörler elde edilmiştir.

Çalışmanın ikinci aşamasında her bir bileşik ve bu bileşiklere uygulanan tüm yöntemler için en etkin katalizörler belirlenmiştir. Uygun katalizör belirlenmesinden sonra optimum çalışma koşullarını saptamak amacıyla tüm model bileşikler için uygulanan yöntemler test edilmiştir. Başlangıç konsantrasyonu tüm deneylerde tüm model bileşikler için 50 mg/L olarak sabit tutulmuştur.

Benzoik asit için ulaşılan en yüksek giderim; fotokatalitik ve foto-Fenton benzeri oksidasyon için seçilen nötral aktivasyon ile hazırlanan Fe-TiO_2/AK katalizör varlığında foto-Fenton-benzeri oksidasyon ile optimum çalışma koşullarında 80 dakika sonunda % 95 olarak bulunmuştur.

Tereftalik asit için en yüksek giderim yine en uygun katalizör olarak seçilen nötral Fe-TiO_2/AK varlığında optimum çalışma koşullarında 120 dakika sonunda % 90 olarak bulunmuştur.

Son olarak p-toluik asit için de diğer model bileşiklerle benzer şekilde en uygun katalizör nötral Fe-TiO_2/AK seçilmiş ve bu katalizör varlığında gerçekleştirilen deneylerde en yüksek giderim, fotokatalitik oksidasyon ile optimum çalışma koşullarında 60 dakika sonunda % 90 olarak bulunmuştur.

Çalışmanın üçüncü aşamasında benzoik asitin biyolojik oksidasyonla giderimi ceviz kabuğu temelli biyokatalizörler varlığında gerçekleştirilmiştir. Seçilen *P.chrysosporium* ve *T.versicolor* mikroorganizmalarının ceviz kabuğu üzerine immobilize edilerek hazırlanan biyokatalizörlerin seçimlilik deneyleri sonucunda *P.chrysosporium* tutturulmuş ceviz kabukları parametrik çalışma için uygun bulunmuştur. Bu biyokatalizör varlığında optimum çalışma koşulları ile 4.gün sonunda % 90'a varan benzoik asit giderimi sağlanmıştır.

Çalışmanın sonunda elde edilen sonuçlar ışığında katalitik aktivite anlamında nötral ve bazik aktivasyon yöntemleri, fiziksel ve asidik aktivasyon yöntemlerine göre daha başarılı bulunmuştur. Seçilen tüm bileşikler için en umut vaat eden yöntemin ise daha yüksek giderim miktarları ve hızları sağlaması nedeniyle fotokatalitik oksidasyon ve foto-Fenton benzeri oksidasyon yöntemleri olduğuna karar verilmiştir. Benzoik asit için en yüksek giderimin sağlandığı yöntemler olan fotokatalitik oksidasyion ve foto-Fenton benzeri oksidasyon ile biyolojik oksidasyon kıyaslandığında aynı giderim sonuçlarına (90–95 %) fotokatalitik oksidasyon veya foto-Fenton benzeri oksidasyon ile 2 saatte ulaşılırken biyolojik oksidasyon ile 4 gün gibi uzun sürelerde ulaşıldığı sonucuna varılmıştır.

Anahtar Sözcükler: Benzoik asit, biyolojik oksidasyon, ceviz kabuğu, endüstriyel atıksu arıtımı**,** ileri oksidasyon yöntemleri, p-toluik asit, tereftalik asit.

ABSTRACT

APPLICATION OF ADVANCED OXIDATION AND NOVEL BIOLOGICAL OXIDATION METHODS FOR TREATMENT OF TEREPHTHALIC ACID PLANT WASTEWATER

TEKİN, Gülen

MSc in Chemical Eng.
Supervisor: Prof. Dr. Süheyda ATALAY
January 2015, 138 pages

In this study, treatment of terephthalic acid wastewater by various advanced oxidation methods and biological oxidation using walnut shells based catalysts has been studied.

The target compounds to represent terephthalic acid wastewater were selected as terephthalic acid (TPA), benzoic acid (BA) and p-toluic acid (p-Tol). Degradation of BA by various advanced oxidation methods such as Fenton-like oxidation, catalytic wet air oxidation, photocatalytic oxidation, photo-Fenton-like oxidation and by biological oxidation was investigated. Degradation of terephthalic acid and p-toluic acid by photocatalytic and photo-Fenton-like oxidation were also investigated.

The first part was preparation and characterization of metal doped walnut shells based catalysts. Iron (Fe) or iron-titanium dioxide (Fe-TiO_2 (1:99)) with a weight ratio of 10 % were doped to the activated carbon (AC) prepared from walnut shells by physical and different chemical activation methods such as acidic, neutral and basic activation. After metal doping Fe/AC and Fe-TiO_2/AC catalysts were obtained.

In the second part of the study, first catalyst screening experiments were performed to each target compound for methods applied to determine the most efficient catalyst. Then parametric studies were performed to determine optimum values of operating conditions. Initial concentration was kept constant as 50 mg/L for each target compound.

For benzoic acid, neutral Fe-TiO_2/AC catalyst was selected for photocatalytic and photo-Fenton-like oxidation and highest degradation efficiency for BA, % 95 degradation was accomplished by photo-Fenton-like oxidation in 80 minutes at optimum operating conditions.

For terephthalic acid, neutral Fe-TiO_2/AC catalyst was determined from catalyst screening experiments for photocatalytic and photo-Fenton-like oxidation and highest degradation efficiency for TPA in the presence of this catalyst was accomplished with a degradation efficiency of 90 % in 120 minutes at optimum operating conditions.

For p-toluic acid, neutral Fe-TiO_2/AC catalyst same as other target compounds was determined for photocatalytic and photo-Fenton-like oxidation. Highest degradation efficiency for p-Tol in the presence of this catalyst was accomplished with a degradation efficiency of 70 % in 60 minutes at optimum operating conditions.

In the third part of the study, biological oxidation of benzoic acid in the presence of biocatalysts based on walnut shells was investigated. *P.chrysosporium* and *T.versicolor* were selected as microorganisms and immobilized on walnut shells. *P.chrysosporium* immobilized on walnut shells were determined as more successful in biocatalyst screening experiments and in presence of this biocatalyst, up to 90 % degradation was achieved at optimum conditions in 4 days.

As a conclusion, neutral and basic activation were considered as more successful than physical and acidic activation based on catalytic performances. Photocatalytic oxidation and photo-Fenton-like oxidations were determined as the most promising methods with higher degradation efficiencies and degradation rates for all target compounds. Comparing biological oxidation, photocatalytic oxidation, and photo-Fenton-like oxidation of BA in which highest degradation efficiencies were obtained for BA, the same degradation efficiency (90–95 %) was achieved in two hours by photocatalytic oxidation and photo-Fenton-like oxidation where it was achieved in four days by biological oxidation.

Keywords: Advanced oxidation methods, benzoic acid, biological oxidation industrial wastewater treatment, p-toluic acid, terephthalic acid, walnut shells.

ACKNOWLEDGMENT

I would like to express my gratitude to my supervisor Prof. Dr. Süheyda ATALAY for her precious guidance and patience during this study.

I also would like to thank Assist. Prof. Dr. Gülin AYTİMUR ERSÖZ for her valuable suggestions in this study.

I also would like to thank Prof. Dr. Derya AYTİMUR, Prof. Dr. Jale YANIK, and PhD. Student Gözde DUMAN for their support and help in this study.

I also would like to thank my mother Nurgül ÇİMEN, my grandmother Nurten ÇİMEN, my aunt Zeliha TEKİN and my friend Ezgi ENGİN for their patience, tolerance and precious supports during this study.

This project is supported by Ege University Scientific Research Project Office with Project number of 12-MÜH-033.

TABLE OF CONTENTS

Page

ÖZET vii

ABSTRACT ix

ACKNOWLEDGMENT xi

LIST OF FIGURES xvii

LIST OF TABLES xxiii

1.0 INTRODUCTION 1

2.0 THEORETICAL BACKGROUND 4

2.1. Terephthalic Acid Wastewater 4

2.2 Advanced Oxidation Processes 6

2.2.1 Fenton-like oxidation 9

2.2.2 Catalytic wet air oxidation 9

2.2.3 Photocatalytic oxidation 10

2.3 Biological Oxidation 11

2.3.1 Cell immobilization 12

2.4 Heterogeneous Catalysis 12

2.4.1 Activated carbon as catalyst support 13

2.4.2 Activated carbon production 14

3.0 LITERATURE SURVEY 16

3.1 Studies About TPA and Derivatives by Biological Methods 16

3.2 Studies About TPA and Derivatives by AOPs 17

TABLE OF CONTENTS (Continued)

Page

3.3 Studies About Fe Supported on Activated Carbon Catalysts 19

4.0 FOREWORD TO STUDY..... 23

4.1 The Choice of Pollutants..... 23

4.2 The Choice of Methods and Catalyst..... 24

4.2.1 The choice of AOPs and biological oxidation 24

4.2.2 The choice of catalyst 25

5.0 EXPERIMENTAL STUDY..... 26

5.1 Catalyst Preparation 29

5.1.1 Catalyst preparation for chemical oxidation 29

5.1.2 Catalyst preparation for biolocigal oxidation..... 34

5.2 Catalyst Characterization 36

5.3 Experimental Setups and Procedures..... 36

5.3.1 Experimental setups 36

5.3.2 Experimental procedures..... 39

5.3.3 Analysis..... 41

5.4 Catalyst Screening Experiments 42

5.4.1 Catalyst screening experiments for Fenton-like oxidation 42

5.4.2 Catalyst screening experiments for catalytic wet air oxidation 43

5.4.3 Catalyst screening experiments for photocatalytic oxidation 44

TABLE OF CONTENTS (Continued)

Page

5.4.4 Catalyst screening experiments for biological oxidation.....45

5.5 Parametric Study Experiments 45

5.5.1 Parametric study for benzoic acid.....46

5.5.2 Parametric study for terephthalic acid 49

5.5.3 Parametric study for p-toluic acid.....50

6.0 RESULTS AND DISCUSSION.....52

6.1 Catalyst Characterization.....52

6.1.1 SEM analysis 52

6.1.2 XRD analysis.....55

6.1.3 BET analysis.....59

6.2 Benzoic Acid Degradation.....62

6.2.1 Fenton-like oxidation.....62

6.2.2 Catalytic wet air oxidation.....69

6.2.3 Photocatalytic and photo-Fenton-like oxidation.....76

6.2.4 Biological oxidation.....88

6.3 Terephthalic Acid Degradation.....91

6.3.1 Fenton-like oxidation.....91

6.3.2 Photocatalytic and photo-Fenton-like oxidation.....92

6.4 p-Toluic Acid Degradation.....103

6.4.1 Fenton-like oxidation.....103

TABLE OF CONTENTS (Continued)

Page

6.4.2 Photocatalytic oxidation..... 103

7.0 GENERAL CONSIDERATIONS 115

8.0 CONCLUSIONS..... 118

REFERENCES..... 125

RESUME 136

LIST OF FIGURES

Figure		Page
2.1	Advanced oxidation processes based on oxidant type	8
5.1	Schematic representation of experimental study	28
5.2	Schematic representation of activated carbon preparation	31
5.3	Schematic representation of Fe/AC preperation	32
5.4	Schematic representation of Fe-TiO_2/AC preparation	34
5.5	Schematic overview of catalyst preparation for biological oxidation	35
5.6	The schematic view (a) and picture of experimental setup (b) of catalytic wet air oxidation	37
5.7	The schematic view (a) and picture of experimental setup (b) of catalytic wet air oxidation	38
5.8	The schematic view (a) and picture of experimental setup (b) of photocatalytic oxidation	38
5.9	Experimental setup for biological oxidation experiments	39
6.1	SEM images of activated carbons at 20000x times magnifications: (a) physical activation, (b) acidic activation, (c) neutral activation, (d) basic activation	53
6.2	SEM images of Fe/AC at 20000x times magnifications: (a) physical activation, (b) acidic activation, (c) neutral activation, (d) basic activation.	54

LIST OF FIGURES (Continued)

Figure — Page

6.3 SEM images of Fe-TiO_2/AC at 20000x times magnifications: (a) physical activation, (b) neutral activation, (c) acidic activation. 55

6.4 XRD patterns of physically activated carbon and Fe/AC catalyst 55

6.5 XRD patterns of acidic activated carbon and Fe/AC catalyst ... 56

6.6 XRD patterns of neutrally activated carbon and Fe/AC catalyst 56

6.7 XRD patterns of basic activated carbon and Fe/AC catalyst 57

6.8 XRD patterns of physically activated carbon and Fe-TiO_2/AC catalyst 57

6.9 XRD patterns of acidic activated carbon and Fe-TiO_2/AC catalyst 58

6.10 XRD patterns of neutrally activated carbon and Fe-TiO_2/AC catalyst 58

6.11 Degradation efficiencies obtained by physical Fe/AC ([BA]=50 ppm, T=25°C, pH=4) 62

6.12 Degradation efficiencies obtained by acidic Fe/AC ([BA]=50 ppm, T=25°C, pH=4) 63

6.13 Degradation efficiencies obtained by neutral Fe/AC ([BA]=50 ppm, T=25°C, pH=4) 64

6.14 Degradation efficiencies obtained by basic Fe/AC ([BA]=50 ppm, T=25°C, pH=4) 64

6.15 Effect of catalyst loading for basic Fe/AC ([BA]=50 ppm, [H_2O_2]=3 mM, T=25°C, pH=4) 66

6.16 Effect of hydrogen peroxide concentration for basic Fe/AC ([BA]=50 ppm, [Catalyst]=0.3 g/L, T=25°C, pH=4) 67

LIST OF FIGURES (Continued)

Figure — Page

6.17 Effect of initial pH for basic Fe/AC ([BA]=50 ppm, [Catalyst]=0.3 g/L, [H_2O_2]=2 mM, T=25°C) 69

6.18 Degradation efficiencies obtained by physical Fe/AC for different temperature and pressure ([BA]=50ppm, [Catalyst]=0.25-0.5 g/L, pH=4, v_{air}=0.92 mL/min)..... 70

6.19 Degradation efficiencies obtained by acidic Fe/AC for different temperature and pressure ([BA]=50ppm, [Catalyst]=0.25-0.5 g/L, pH=4, v_{air}=0.92 mL/min)..... 71

6.20 Degradation efficiencies obtained by neutral Fe/AC for different temperature and pressure ([BA]=50ppm, [Catalyst]=0.25-0.5g/L, pH=4, v_{air}=0.92 mL/min)..... 71

6.21 Degradation efficiencies obtained by basic Fe/AC for different temperature and pressure ([BA]=50ppm, [Catalyst]=0.25-0.5 g/L, pH=4, v_{air}=0.92 mL/min)..... 72

6.22 Effect of catalyst loading for basic Fe/AC ([BA]=50 ppm, P=1 bar, T=60℃,pH=4, v_{air}=0.92 ml/min) 73

6.23 Effect of temperature for basic Fe/AC ([BA]=50 ppm, [Catalyst]=1 g/L, P=1 bar, pH=4, v_{air}=0.92 ml/min)..... 74

6.24 Effect of pressure for basic Fe/AC ([BA]=50 ppm, [Catalyst]=1 g/L, T=50^{o}C, pH=4, v_{air}=0.92 ml/min)..... 75

6.25 Effect of air flowrate for basic Fe/AC ([BA]=50 ppm, [Catalyst]=1 g/L, P=1 bar, T=50^{o}C, pH=4)..... 76

6.26 Degradation efficiencies obtained by physical Fe/AC ([BA]=50 ppm, T=25°C, pH=4)..... 77

6.27 Degradation efficiencies obtained by acidic Fe/AC ([BA]=50 ppm, T=25°C, pH=4)..... 78

6.28 Degradation efficiencies obtained by neutral Fe/AC ([BA]=50 ppm, T=25°C, pH=4)..... 78

LIST OF FIGURES (Continued)

Figure Page

6.29 Degradation efficiencies obtained by basic Fe/AC ([BA]=50 ppm, T=25°C, pH=4 79

6.30 Degradation efficiencies obtained by physical Fe-TiO_2/AC ([BA]==50 ppm, T=25°C, pH=4) 80

6.31 Degradation efficiencies obtained by acidic Fe-TiO_2/AC ([BA]=50 ppm, T=25°C, pH=4) 80

6.32 Degradation efficiencies obtained by neutral Fe-TiO_2/AC ([BA]=50 ppm, T=25°C, pH=4) 81

6.33 Effect of catalyst loading for neutral Fe-TiO_2/AC ([BA]=50 ppm, UV light intensity=6 watt, T=25°C, pH=4) 83

6.34 Effect of UV light intensity for neutral Fe-TiO_2/AC ([BA]=50 ppm, [Catalyst]=0.5 g/L, T=25°C, pH=4) 84

6.35 Effect of initial pH for neutral Fe-TiO_2/AC ([BA]=50 ppm, [Catalyst]=0.5 g/L, UV light intensity =8 watt, T=25°C) 85

6.36 Effect of H_2O_2 concentration for neutral Fe-TiO_2/AC ([BA]=50 ppm, [Catalyst]=0.5 g/L, UV light intensity =8 watt, T=25°C, pH=4) 86

6.37 Effect of initial pH for neutral Fe-TiO_2/AC ([BA]=50 ppm, [Catalyst] = 0.5 g/L, UV light intensity =8 watt, [H_2O_2]= 2 mM, T=25°C) 87

6.38 Degradation efficiencies obtained by different conditions ([BA]=50 ppm, T=25°C) 88

6.39 Effect of biocatalyst loading for ([BA]=50 ppm, T=25°C) 90

6.40 Effect of glucose concentration ([BA]=50 ppm, [Biocatalyst]=0.25 g/50 ml, T=25°C) 91

6.41 Degradation efficiencies obtained by physical Fe/AC ([TPA]=50 ppm, T=25°C, pH=4) 92

LIST OF FIGURES (Continued)

Figure — Page

6.42 Degradation efficiencies obtained by acidic Fe/AC ([TPA]=50 ppm, T=25°C, pH=4) 93

6.43 Degradation efficiencies obtained by neutral Fe/AC ([TPA]=50 ppm, T=25°C, pH=4) 93

6.44 Degradation efficiencies obtained by basic Fe/AC ([TPA]=50 ppm, T=25°C, pH=4 94

6.45 Degradation efficiencies obtained by physical Fe-TiO_2/AC ([TPA]=50 ppm, T=25°C, pH=4) 95

6.46 Degradation efficiencies obtained by acidic Fe-TiO_2/AC ([TPA]=50 ppm, T=25°C, pH=4) 95

6.47 Degradation efficiencies obtained by neutral Fe-TiO_2/AC ([TPA]=50 ppm, T=25°C, pH=4) 96

6.48 Effect of catalyst loading for neutral Fe-TiO_2/AC ([TPA]=50 ppm, UV light intensity=6 watt, T=25°C, pH=4) ... 98

6.49 Effect of UV light intensity for neutral Fe-TiO_2/AC ([TPA]=50 ppm, [Catalyst]=1 g/L, T=25°C, pH=4) 99

6.50 Effect of initial pH for neutral Fe-TiO_2/AC ([TPA]=50 ppm, [Catalyst]=1 g/L, UV light intensity=6 watt, T=25°C) 100

6.51 Effect of H_2O_2 concentration for neutral Fe-TiO_2/AC ([TPA]=50 ppm, [Catalyst]=1 g/L, UV light intensity =6 watt, T=25°C, pH=4) 101

6.52 Effect of initial pH for neutral Fe-TiO_2/AC ([TPA]=50 ppm, [Catalyst] = 1 g/L, UV light intensity =6 watt, [H_2O_2]= 1 mM, T=25°C) 102

6.53 Degradation efficiencies obtained by physical Fe/AC ([p-TOL]=50 ppm, T=25°C, pH=4) 104

6.54 Degradation efficiencies obtained by acidic Fe/AC ([p-TOL]=50 ppm, T=25°C, pH=4) 105

LIST OF FIGURES (Continued)

Figure		Page
6.55	Degradation efficiencies obtained by neutral Fe/AC ([p-TOL]=50 ppm, T=25°C, pH=4)	105
6.56	Degradation efficiencies obtained by basic Fe/AC ([p-TOL]=50 ppm, T=25°C, pH=4	106
6.57	Degradation efficiencies obtained by physical Fe-TiO_2/AC ([p-TOL]=50 ppm, T=25°C, pH=4)	107
6.58	Degradation efficiencies obtained by acidic Fe-TiO_2/AC ([p-TOL]=50 ppm, T=25°C, pH=4)	108
6.59	Degradation efficiencies obtained by neutral Fe-TiO_2/AC ([p-TOL]=50 ppm, T=25°C, pH=4)	109
6.60	Effect of catalyst loading for neutral Fe-TiO_2/AC ([p-TOL]=50 ppm, UV light intensity=6 watt, T=25°C, pH=4)	110
6.61	Effect of UV light intensity for neutral Fe-TiO_2/AC ([p-TOL]=50 ppm, [Catalyst]=0.5 g/L, T=25°C, pH=4)	111
6.62	Effect of initial pH for neutral Fe-TiO_2/AC ([p-TOL]=50 ppm, [Catalyst]=0.5 g/L, UV light intensity=6 watt, T=25°C)	112
6.63	Effect of H_2O_2 concentration for neutral Fe-TiO_2/AC ([p-TOL]=50 ppm, [Catalyst]=0.5 g/L, UV light intensity =6 watt, T=25°C, pH=4)	113
6.64	Effect of initial pH for neutral Fe-TiO_2/AC ([p-TOL]=50 ppm, [Catalyst] = 0.5 g/L, UV light intensity =6 watt, [H_2O_2]= 1 mM, T=25°C)	114

LIST OF TABLES

Table		Page
3.1	Summary of literature survey	20
5.1	Catalyst screening experiments for Fenton-like oxidation	43
5.2	Catalyst screening experiments for catalytic wet air oxidation	44
5.3	Catalyst screening experiments for photocatalytic oxidation	44
5.4	Catalyst screening experiments for biological oxidation	45
5.5	Operating parameters of Fenton-like oxidation for BA and their ranges	46
5.6	Operating parameters of catalytic wet air oxidation for BA and their ranges	47
5.7	Operating parameters of photocatalytic oxidation for BA and their ranges	47
5.8	Operating parameters of photo-Fenton-like oxidation for BA and their ranges	48
5.9	Operating parameters of biological oxidation and their ranges	49
5.10	Operating parameters of photocatalytic oxidation for TPA and their ranges	49
5.11	Operating parameters of photo-Fenton-like oxidation for TPA and their ranges	50
5.12	Operating parameters of photocatalytic oxidation for p-Tol and their ranges	50
5.13	Operating parameters of photo-Fenton-like oxidation for p-Tol and their ranges	51
6.1	BET surface area results of basic activated carbon and corresponding Fe/AC catalyst	60
6.2	BET surface area results of neutrally activated carbon and corresponding Fe-TiO_2/AC catalyst	61
7.1	Maximum degradation efficiencies for each target compound	...…...117

1.0 INTRODUCTION

Terephthalic acid (1,4-benzenecarboxylic acid) (TPA) and its derivatives are the most important starting materials for making synthetic products, especially polyester fiber and plastics. For each ton of TPA manufactured, approximately 3 - 10 m^3 wastewater is produced with very high amount of organic content (5-20 kg/ m^3 COD) (Zhang et al., 2010). It has been indicated that exposure to TPA wastewater and the aromatic components can cause harm to liver, bladder, testis and kidney as well as DNA damage (Zhang, et al., 2011).

The three kind of conventional methods to treat industrial organic wastewaters including biological degradation, chemical oxidation, and adsorption have some major limitations. One of most popular biological methods, activated sludge, is often the most economically, suitably and widely used method to treat some industrial wastewaters. However, this method can be applied up wastewaters with a maximum concentration of 50 ppm Biochemical Oxygen Demand (BOD) or Chemical Oxygen Demand (COD). On the other hand, another common application, chemical oxidation is also not very efficient for wastewaters containing refractive organic pollutants due to their low oxidizing capacity and considered as insufficient to satisfy the discharge standards. Most of the conventional treatments techniques also generate large amounts of sludge which need a further treatment. These limitations of the conventional treatment methods can be overcome by other methods that have been developed to treat industrial wastewaters containing chemically strong organics (Abo Farha, 2010). Advanced Oxidation Process (AOPs) is one of these methods and can be defined as a powerful chemical oxidation process. They are considered as a feasible option for such biologically persistent wastewater and widely recognized as highly efficient treatments for recalcitrant wastewater such as contaminated ground waters, surface waters, and wastewaters containing non -biodegradable organic pollutants (Andreozzi et al., 1999, Ricciardi, 2006, Oller et al., 2011).

Advanced oxidation processes (AOPs) are based on the chemical oxidation of these refractive organics by forming hydroxyl radicals as strong oxidants in

the presence of catalysts. Common AOPs involve Fenton, Fenton-like, photo-Fenton-like oxidation, wet air oxidation, ozonation, photochemical and electrochemical oxidation, photocatalytic oxidation, photolysis with H_2O_2 and O_3, high voltage electrical discharge process, radiolysis, and various combinations of these methods (Abo-Farha, 2010, Oller et al., 2011).

Homogeneous catalysts used in AOPs have several drawbacks such as leaching of the catalyst to the treated wastewater and generation of secondary waste. Heterogeneous catalysis becomes forward by using a catalyst support which increase the stability and ease the recovery of the catalyst (Ramirez et al., 2007).

The use of activated carbon as a catalyst support has some advantages due its high surface area (Munter 2001, Puma et al., 2008). Nowadays activated carbon prepared from organic sources as a raw material gained a big interest. The use of organic waste as a raw material for activated carbon is recently preferred because agricultural wastes are cheap, renewable and available at high quantities. This leads to reuse of organic wastes such as walnut shells which have no other use in any field (Ekpete and Horsfall, 2011, Ahmed and Dhedan, 2012).

The main objective of this study is investigation the treatment of TPA wastewater major components which are terephthalic acid, benzoic acid and p-toluic acid. It was aimed to develop an innovative degradation method for these major components efficiently by using an organic waste as a catalyst support. In this context, several AOP methods such as Fenton-like oxidation, catalytic wet air oxidation, photocatalytic oxidation and photo-Fenton-like oxidation and biological oxidation were applied in the presence of the catalysts prepared from walnut shells. Different activation methods such as physical and chemical activation methods namely acidic, neutral and basic activation were applied and the effect of activation method of the catalyst support on degradation was to be searched for. Different methods in the presence of different catalysts prepared were compared in terms of degradation efficiency and optimum values of operating parameters were determined. The main contribution of this study to

literature is to improve low degradation efficiencies of these target compounds by biological oxidation methods and to apply AOPs in the presence of organic waste catalyst. Furthermore it is aimed to search for the most suitable catalysts prepared by different activation methods by comparing the catalytic performances of them.

2.0 THEORETICAL BACKGROUND

2.1. Terephthalic Acid Wastewater

Terephthalic acid (TPA) is a key component in many industries especially in petrochemical industry. It is widely used in the production of polyester fiber, non-fiber field, PET-bottle, PET-film, poultry feed additives, dyes, medicines, synthetic perfumes, pesticides and other chemical compounds. It is among the top 50 chemicals manufactured in the world with an annual production of 50 million tons in 2009 (Zhang et al., 2010). Its only manufacturer in Turkey is Petkim Petrochemical Company with an annual production of 60,000 tons in 2011 (PETKİM Petrokimya Holding A.Ş. Website (Access date: 21.07.2014)).

It is produced via catalytic oxidation of para-xylene in the presence of cobalt-manganese-bromine catalyst and acetic acid solvent (Huang et al., 2009). During the production of one ton TPA, approximately 3∼4 m^3 wastewater with 4∼10 kg COD m^{-3} is produced in which TPA is identified as a major contaminant (Shafaei et al., 2010). Other major aromatic compounds found in TPA wastewater are p-toluic acid/o-toluic acid (p-Tol), benzoic acid (BA), 4-carboxybenzaldehyde (4-CBA), and acetic acid which are shown in Table 2.1 (Raj et al., 1997, Zhang et al., 2006). The contribution of the five aromatics towards COD can be more than 75% in the wastewater (Karthik et al., 2008). The composition of TPA manufacturing process wastewater is shown in Table 2.1 (Thiruvenkatachari et al., 2007).

Table 2.1 Major aromatic compounds found in TPA wastewater and their COD contributions. (Zhang et al., 2006, Thiruvenkatachari et al., 2007)

Substance	Structural Formula
p-Toluic acid	
4-Carboxybenzaldehyde	
Benzoic acid	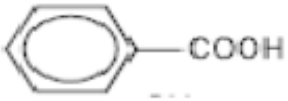

Compound	Concentration (mg/L)	Contribution to COD (mg/L)
Major Pollutants		
Terepthalic acid	100 -1600	145 – 2320
Benzoic acid	400 – 600	590 – 1180
p - Toluic acid	0 – 900	0 – 1910
o - Toluic acid	0 – 900	0 – 1910
Acetic acid	0 – 900	0 – 960

Studies showed that TPA can cause bladder stones and bladder cancer, impairment of liver, kidney, and testicular functions and DNA damage (Zhang et al., 2010, Zhang et al., 2010). Furthermore TPA wastewater components are considered as suspected mutagens and carcinogens and potential disrupting character for the endocrine system (Huff et al., 1984, Escher et al., 2011). They have been in the list of priority pollutants by the US Environmental Protection Agency (Saillenfait et al., 2005, US EPA 1992). Because of its potential threat to ecosystem and human health, wastewaters containing these compounds must be treated before discharging to receiving water bodies (Chai et al, 2012).

There have been many physical, chemical and biological methods developed for the treatment of wastewaters including TPA and its derivatives (Thiruvenkatachari et al., 2007). Today, the method widely used for the treatment of these wastewaters is activated sludge process which is also known as conventional biological method. But these wastewaters are not suitable to be treated by activated sludge. The Water Pollution Control Regulations published in 2004 on the Official Newspaper allows wastewaters to be discharged which have Chemical Oxygen Demand (COD) below 300 ppm for all industries. However, the studies in the literature show that the COD concentration of the TPA wastewater treated with activated sludge process is 500 ppm with maximum removal capacity due to the limitations of activated sludge process (Pophali et al., 2006).

The limitations of activated sludge process for TPA wastewater occurs because of their high toxicity and the biorecalcitrant compounds which causes slow biodegradation, loss of activity of the biomass during degradation, strongly rate limiting and inhibition of microorganisms of these target organic materials in the presence of certain compounds (Zhang et al., 2006). Studies show that, biodegradation of the aromatic compounds follow the order BA > 4-CBA > TPA > p-Tol which revealed that one of the major COD contributor, p-toluic acid is the most difficult compound degraded in wastewater and cannot be degraded completely (Raj et al., 1997, Yang eand Lua, 2003).

2.2 Advanced Oxidation Processes

Oxidation processes commonly employed in water treatment can be investigated in two categories: conventional oxidation and advanced oxidation methods. Conventional oxidation involves the addition of an oxidant to the water that then reacts directly with the target contaminant. Conventional oxidants are selective, specific oxidants that must be used to remove specific contaminants. The conventional chemical oxidants used in water treatment include chlorine, chlorine dioxide, ozone, potassium permanganate, and hydrogen peroxide. Several of these oxidants are also disinfectants (Crittenden et al., 2012).

Advanced oxidation processes (AOPs) were defined by as near ambient temperature and pressure water treatment processes which involve the generation of highly reactive radicals (especially hydroxyl radicals) in sufficient quantity to effect water purification. Hydroxyl radicals are extraordinarily reactive species that attack most organic molecules. The kinetics of reaction are generally first order with respect to the concentration of hydroxyl radicals and to the concentration of the species to be oxidized (Ricciardi, 2006). AOPs through which highly oxidizing species like hydroxyl radicals are produced, can provide innovative methods for efficient treatment of water and wastewater, and these processes are considered a highly competitive water treatment technology for the removal of those organic pollutants not treatable by conventional oxidation due to their high chemical stability and/or low biodegradability (Zhou and He, 2007, Oller et al., 2011).

Common AOPs involve Fenton and Fenton-like oxidation, photo-Fenton-like oxidation, wet air oxidation, ozonation, photochemical and electrochemical oxidation, photocatalytic oxidation, , photolysis with H_2O_2 and O_3, high voltage electrical discharge process, radiolysis, wet oxidation, treatment by electronic beams or γ-beams and various combinations of these methods (Abo-Farha, 2010).

AOPs can be categorized in main groups such as AOPs based on ozone (O_3), AOPs based on H_2O_2, AOPs based on photocatalysis, hot AOPs, and others which are mostly combination main AOPs. The main groups and subgroups are shown in Figure 2.1 schematically (Andreozzi et al., 1999).

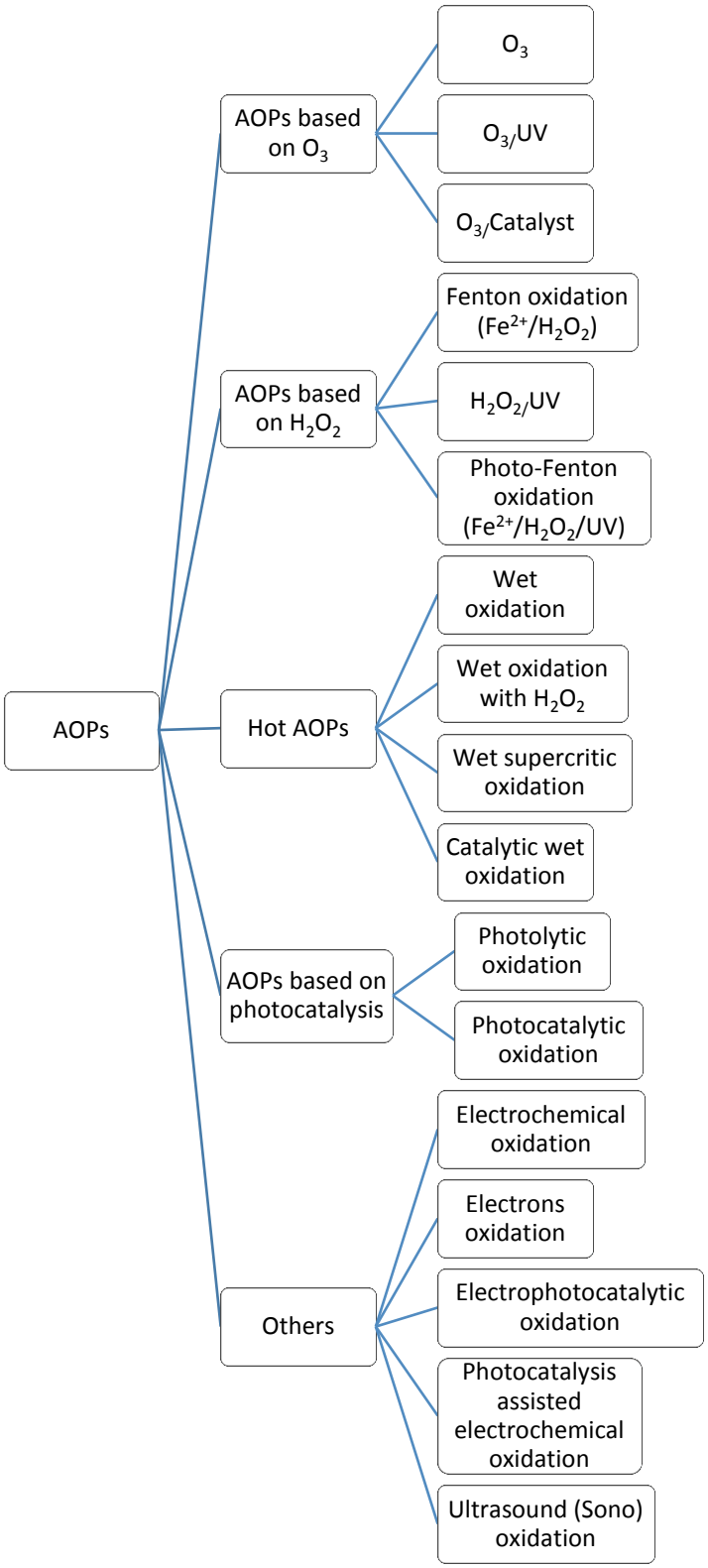

Figure 2.1 Advanced oxidation processes based on oxidant type and/or catalyst

2.2.1 Fenton-like oxidation

Fenton oxidation is one of the most common advanced oxidation processes and basically defined as the chemical oxidation of organic compounds by hydrogen peroxide (H_2O_2) using Fe ions as a catalyst. It has been particularly attractive because of the advantages it provides such as low costs, the lack of toxicity of the reagents, the absence of mass transfer limitation due to its homogeneous catalytic nature, and the simplicity of the technology (Daud and Hameed, 2010).

The Fenton reaction is chemically very efficient for the removal of organic pollutants. The overall reaction is a simple redox reaction in which Fe(II) is oxidized to Fe(III) and H_2O_2 is reduced to the hydroxide ion and the hydroxyl radical.

$$Fe^{2+} + H_2O_2 \rightarrow Fe^{3+} + \bullet OH + OH^-$$

But this reaction is also of biological relevance because for most living organisms, the alteration of the intracellular concentration of Fe^{2+} and H_2O_2 can increase the intracellular formation of •OH, leading to DNA and cell damage. Hence reduction of the ferric ion (Fe^{3+}) produced to ferrous ion (Fe^{2+}) by a second molecule of hydrogen peroxide,

$$Fe^{3+} + H_2O_2 \rightarrow Fe^{2+} + HO_2\bullet + H^+$$

can be used as a regeneration of ferrous ions and it is called Fenton-like reactions (Spuhler et al., 2010).

2.2.2 Catalytic wet air oxidation

Wet air oxidation (WAO) is an attractive technique for industrial wastewater treatment. WAO involves the combustion of pressurized organic matter at relatively high temperatures. The main drawback of this technique is its high energetic requirements. In order to be able to employ milder operating conditions and reduce the operating costs, catalytic wet air oxidation processes

(CWAO) have been developed. The presence of catalyst may improve the overall reaction rate and enhances the removal of reaction intermediates compounds, which are refractory to the WAO process, improving the formation of hydroxyl radicals, well-known promoters of the oxidation (Ovejero et al., 2013).

Wet air oxidation (WAO) and catalytic wet air oxidation processes (CWAO) using air or pure oxygen as oxidant have been used to treat industrial wastewaters and these methods are very preferable due to its their effectiveness on high concentrations of contaminants and being eco-friendly (Kim and Ihm, 2011).

2.2.3 Photocatalytic oxidation

Photocatalytic processes make use of a semiconductor metal oxide as catalyst and of oxygen as oxidizing agent. Many semiconductor catalysts have been so far tested, although only TiO_2 in the anatase form seems to have the most interesting attributes such as high stability, good performance and low cost. The initiating event in the photocatalytic process is the absorption of the radiation with the formation of electron-hole pairs:

$$TiO_2 \rightarrow e^- + h^+$$

The considerable reducing power of formed electrons allows them to reduce some metals and dissolved oxygen with the formation of the superoxide radical ion $O_2\bullet^-$ whereas remaining holes are capable of oxidizing adsorbed H_2O or HO^- to reactive •OH radicals:

$$TiO_2\,(h^+) + H_2O_{ad} \rightarrow TiO_2 + HO_{ad}{}^- + H^+$$

$$TiO_2\,(h^+) + HO_{ad}{}^- \rightarrow TiO_2 + HO_{ad}$$

These reactions are of great importance in oxidative degradation processes due to the high concentration of H_2O and HO^- adsorbed on the particle surface which attackes the organic contaminant to degrade. Most of the contaminants are oxidized by hydroxyl radicals but some adsorbed contaminant can also be directly oxidized by electron transfer:

$$TiO_2\,(h^+) + RX_{ad} \rightarrow TiO_2 + RX_{ad}^{\cdot +}$$

Unfortunately a significant part of electron-hole pairs recombine thus reducing the quantum yield. Intensive researches are carried out worldwide to obtain modified (doped) TiO_2 with broader absorption spectrum and characterized by higher quantum yield. Despite the great efforts devoted to the study of photocatalytic processes no indications have been found in the literature of their application on industrial scale (Andreozzi et al.,1999).

2.3 Biological Oxidation

Industrial effluent usually contains non-biodegradable pollutants with a high value of COD/BOD_5 (Biological Oxygen Demand) ratio. In addition, the existence of toxic chemicals makes the biological treatment more difficult. Anaerobic sludge systems have various limitations, such as sensitivity to low temperatures and toxic compounds, the loss of activity due to poor separability of biomass, and additional equipment requirement for accumulating sludge. Therefore, there has been a continuous search for other alternatives. A number of investigations have reported that biofilm systems immobilized on some carriers also known as packed bed bioreactors are more advantageous due to accumulation of high concentration of active biomass via microorganism immobilization (Chen et al., 2007).

Biological oxidation also known as biofiltration, a potential biological treatment technique is based on the ability of microorganisms (generally bacteria) to convert, under aerobic conditions, organic pollutants to water, carbon dioxide and biomass. Biofiltration is considered as a cost-effective treatment process. Furthermore, in most of the cases no undesirable byproducts

or secondary emissions are formed which make the process preferred than conventional activated sludge process (Agarwal et al., 2008).

2.3.1 Cell immobilization

Cell immobilization is a general term that describes many different forms of cell attachment or entrapment. The technology of immobilized cells can be applied in biological treatment to enhance the efficiency and effectiveness of biodegradation. The carrier provides a high specific surface area for microbial growth and also provides a shelter for bacteria that encountered chemicals toxicities. The main advantages in the use of immobilized cells in comparison with suspended ones include the retention in the reactor of higher concentration of microorganisms, protection of cells against toxic substances, and eliminate the cost processes of cell recovery and cell recycle (Chen et al., 2008).

2.4 Heterogeneous Catalysis

The common catalysts used in AOPs are metals, metal oxides, photons (from UV light) and ultrasound. Catalysts can be homogeneous, for which the catalysts and the reactants are in the same phase; or heterogeneous, for which the catalysts are in different phases than the reactants. There are wide range of combinations of oxidants and catalyst that can generates •OH radicals the AOPs are widely categorized (Umar et al, 2010).

Homogeneous catalysts used in AOPs have several drawbacks such as leaching of the catalyst to the treated waste and generation of secondary waste. As an example homogeneously catalyzed reactions in homogeneous Fenton-like process need up to 50–80 ppm of Fe ions in solution, which is well above the European Union directives that allow only 2 ppm of Fe ions in treated water to be dumped directly into the environment. But the removal/treatment of the of the generated secondary waste at the end of the wastewater treatment is expensive and needs large amount of chemicals and manpower (Ramirez et al., 2007). In photocatalytic oxidation applications in which TiO_2 used as photocatalyst, TiO_2 suspensions or agglomerations cannot be removed from the reaction medium

(Foo and Hameed, 2010). To overcome the disadvantages of the homogeneous catalysis processes, the immobilization of the catalyst on inert support surfaces known as heterogeneous catalysis becomes forward. It prevents the drawbacks of high amount of metals in treated water and secondary waste generation. In this manner, a catalyst support is used which bonds to the metal ion and that provides an efficient separation of the catalyst at the end of operation (Pariente et al., 2008, Duarte et al., 2011).

2.4.1 Activated carbon as catalyst support

Activated carbon materials have been extensively used as adsorbents, catalysts and catalyst supports for removal of pollutant species from gases or liquids, and for purification or recovery of chemicals. Pore structure is an important factor for physical adsorption, while surface chemistry plays a key role in specific adsorption and surface reactions (Liu et al., 2010).

Recently, activated carbon (AC) has proven to be an excellent catalytic support in the oxidation of aromatic compounds which have high chemical resistance to breakage and attrition and easy to recover that increases reusability of the catalyst. Among their excellent properties, it can be emphasized that their high surface area, well developed and different porous structure which leads homogeneous distribution of catalyst and variable surface composition which determine important differences in their reactivity allows to study the effects of these features on the catalytic behavior. Specifically in environmental applications related to wastewater treatments, the structure of activated carbon plays an important role because the adsorption capacity is determined by both the porous structure and the chemical nature of the surface. So, it is very important to understand the role of the activated carbon surface in the preparation of optimized catalysts in terms of activity and stability. It is well known that some transition metallic elements like iron promote hydrogen peroxide decomposition to hydroxyl radicals capable to efficiently oxidize organic matter (Puma et al., 2008, Rey et al., 2009).

2.4.2 Activated carbon production

Activated carbon can be produced from any solid precursor either natural or synthetic. Nowadays activated carbon prepared from agricultural waste gained big interest. Agricultural wastes are cheap, renewable, safe, available at large quantities, easily accessible sources and have high carbon and low ash content (Ahmed and Dhedan, 2012). This leads to reuse of organic wastes such as walnut shells which have almost no other use in any field for production of more valuable products like activated carbon (Aworn et al.,2008).

Generally, the activated carbons are manufactured in two stages that is, carbonization and activation processes. The carbonization process, which includes drying and then heating, is performed to eliminate byproducts such as tars and other hydrocarbons (including volatile organic compounds) from the raw material. The carbonized material is then activated in the second stage by exposing them to an activating agent. These two carbonization and activation processes can be combined and the activated carbon can be prepared by thermally treating the chemical reagent impregnated carbonaceous material which results a less time and energy consuming process (Yang and Lua, 2003 Ekpete and Horsfall, 2011).

The carbonization process is performed by exposure of heat to the material in an inert atmosphere to remove volatile organic impurities and obtain pure carbon structure. Activation is applied to the pure carbon mass by various chemical reactions resulting the porous structure of the activated carbon (Nowicki et al., 2010). The activation process can be applied by two different methods: Physical activation and chemical activation. For physical activation, heat treatment is applied in CO_2, water vapour, air or various gas atmospheres. These atmospheres react with some of the carbon atoms on the surface by producing gas and pores are formed. On the other hand chemical activation is performed by heating the carbon mass in an inert atmosphere after impregnation of chemical reagents to the carbon mass. The impregnated reagents have the same role of the gas atmospheres in physical activation and they react with the carbon structure to create porous structure and retard the formation of tars during

the carbonization process and increase the carbon yield. The most important and commonly used chemical activating agents are zinc chloride, potassium hydroxide and alkaline metals (Kim et al., 2001).

The chemical and physical activation of carbon determine the adsorption behaviour of activated carbon. The chemical activation usually takes place at a temperature lower than that used in physical activation, therefore it can improve the pore development in the carbon structure because the effect of chemicals. The carbon yields of chemical activation are higher than physical one (Ahmadpour and Do, 1997).

Oxidized activated carbon is another common application of activated carbon as catalyst support especially for treatment of organic pollutants. Activated carbon as an efficient adsorbent both for metal catalysts and the contaminants present in wastewater, inhibit the efficiency of the catalyst because of the strong adsorption of the contaminants instead of catalyst. Oxidation of the activated carbon causes formation of the surface functional groups which increase the adsorption of catalysts, selectively. For this purpose, carbonized material is treated with HNO_3 solution to oxidized surface groups (El-Sheikh et al., 2007).

3.0 LITERATURE SURVEY

The studies found in literature survey were categorized according to target compounds, methods, and catalysts.

3.1 Studies About TPA and Derivatives by Biological Methods

In 1997, Raj et al., studied biodegradation of acetic, benzoic, isophthalic, toluic and terephthalic acids using a mixed culture. They examined the biodegradation of TPA and its derivatives with traditional active sludge method. As a result of experiments, p-toluic acid is found as the most difficult compound degraded in wastewater and only almost 50 % degradation achieved with 48 hours residence time (Raj et al., 1997).

In 2005, Kleerebezem et al. examined the treatment of terephthalic acid production process wastewater including benzoate, acetate and terephthalate in a two-stage anaerobic bioreactor. Only acetate and benzoate were degraded at the first stage in 300 days while no terephthalate degradation was observed during this time at the same conditions. After 300 days, terephthalate degradation could be observed. They concluded that using two-stage anaerobic bioreactor for treatment of terephthalate had many drawbacks which were not easy to overcome (Kleerebezem et al., 2005).

In 2006, Pophali et al., studied the treatment of purified terephtalic acid (PTA) effluent using anareobic and aerobic process. An activated sludge process and upflow anaerobic film fixed bed reactor were used. They concluded that the treatment of PTA effluent using two stage activated sludge process alone doesn’t meet treated effluent quality within predescribed standards. They also revealed that pretreatment of PTA effluents using AFFBR ensured substantial reduction in BOD (63%) and COD (62%) (Pophali et al.,2006).

In 2006, Zhang et al., investigated the degradability five aromatic compounds in a pilot wastewater treatment system. Purified terephthalic acid-manufacturing wastewater was treated aerobically with the microbial fusant in

the carrier activated sludge process at a pilot wastewater treatment plant. Biodegradability of p-toluic acid (p-Tol), benzoic acid (BA), 4-carboxybenzaldehyde (4-CBA), phthalic acid (PA) and terephthalic acid (TA) was monitored. As a result of the experiments, the biodegradation of the aromatic compounds monitored followed the order: BA>PA>4- CBA>TA>p-Tol (Zhang et al., 2006).

3.2 Studies About TPA and Derivatives by AOPs

In 2004, Andreozzi and Marotta, in the study named as "The removal of benzoic acid in aqueous solution by Fe(III) homogeneous photocatalysis", investigated treatment of benzoic acid by photo-Fenton oxidation. They focused on the filtration of Fe(III) ions by the help of its colloidal structure. They determined that both Fe(II) and Fe(III) ions had the same effect on degradation efficiency with COD reduction for 60 -70 % and the optimum value for pH is 3.5 (Andreozzi and Marotta, 2004).

In 2006, Thiruvenkatachari et al. investigated degradation of phthalic acids and benzoic acid from wastewater by advanced oxidation processes. This study investigates the degradation of three major toxic target organic species, namely terephthalic acid (TPA), isophthalic acid (IPA), benzoic acid (BA), present in the TPA wastewater, by several advanced oxidation methods. The performance of three main oxidation processes such as photo-Fenton oxidation (UV-H_2O_2-Fe), photocatalytic ozonation (UV-O_3- Fe) and photo-Fenton ozonation (UV-O_3- H_2O_2-Fe) were studied. Photo-Fenton ozonation was found to be the most efficient process by almost complete destruction of target organic species in 30 min (Thiruvenkatachari et al., 2006).

In 2008, Pariente et al. studied "Heterogeneous photo-Fenton oxidation of benzoic acid in water: Effect of operating conditions, reaction byproducts and coupling with biological treatment" to investigate degradation of benzoic acid by photo-Fenton oxidation. They observed that degradation of benzoic acid increased by increasing the Fenton reagent concentration and decreased by increasing the initial benzoic acid concentration. Also they investigated the

aerobic biodegradability of benzoic acid and they found that chemical oxidation of benzoic acid improved biodegradability of benzoic acid. TiO_2- mediated photocatalysis were used with photo-Fenton-like oxidation method. The results were obtained as 72% and 16% COD reduction at 150 and 450 mg/L benzoic acid concentration and also coombining photo-Fenton oxidation with aerobic post-oxidation led to 77% and 69% overall COD removal at 150 and 450 mg/L (Pariente et al., 2008).

In 2008, Velegraki et al. published their study "Conversion of benzoic acid during TiO_2- mediated photocatalytic degradation in water" which focused on photocatalytic oxidation of benzoic acid. It has been concluded that the aromatic structure had been completely mineralized to CO_2 and water (Velegraki et al., 2008).

In 2010, Shafaei et al., investigated the photocatalytic degradation of terephthalic acid (TPA) using titania and zinc oxide nanoparticles. The effect of initial pH, catalyst loading, initial TPA concentration and H_2O_2 were studied. TPA degraded in the presence of only UV light but its rate was very slow while addition of TiO_2 and ZnO accelerated the photodegradation of TPA. The photocatalytic oxidation efficiency increased with increasing light intensity, irradiation time, catalyst loading up to 2.5 g/L and also by addition of small amounts of H_2O_2. The results showed that the pH 6.0 and 9.0 were the optimal pH for TiO_2 and ZnO, respectively. It was determined that the photocatalytic degradation of TPA obeyed the pseudo- first order kinetic reaction in the presence of both photocatalysts. The experiments show that TiO_2 and ZnO photocatalysts can be used as an effective catalyst for the elimination of TPA from wastewater but in optimized conditions zinc oxide was more efficient catalyst than TiO_2. (Shafaei et al., 2010).

In 2011, Velegraki et al. have another study also focused on degradation of benzoic acid named as "Wet oxidation of benzoic acid catalyzed by cupric ions: Key parameters affecting induction period and conversion". They observed that the CWO of BA is strongly affected by the reaction temperature and to a lesser extent by the initial BA concentration, the oxygen partial pressure, as well as by

the second order interaction between initial BA concentration and oxygen partial pressure and hydroxylation of the aromatic ring is an important pathway during the CWO of BA. They achieved complete conversion is achieved within 90–120 min at relatively mild conditions, e.g. <30 bar oxygen partial pressure, <180 °C reaction temperature and <40 mg/L metal concentration. (Velgraki et al., 2011).

In 2007, Yang et al. studied the activities for the CWAO of phenol, benzoic acid and sulfonic salicylic acid have been investigated in the study named by ‘‘Removal of salicylic acid on perovskite-type oxide $LaFeO_3$ catalyst in catalytic wet air oxidation process’’. They concluded that, with compared to the very poor activities for phenol and benzoic acid, the activities for salicylic acid and sulfonic salicylic acid were very high, which are attributed to their same intramolecular H-bonding structures (Yang et al., 2007).

3.3 Studies About Fe Supported on Activated Carbon Catalysts

In 2006, Quintanilla et al. studied CWAO of phenol with molecular oxygen using a Fe/Activated Carbon catalyst at mild operation conditions (100-127^{o}C; 8 atm) in a trickle-bed reactor in their study named by ‘‘Reaction pathway of the catalytic wet air oxidation of phenol with a Fe/Activated carbon’’. They found that only acetic acid, one of the reaction intermediates, showed to be refractory to CWAO under the operating conditions (Quintanilla et al., 2006).

In 2006, Zazo et al. performed a study on ‘‘Catalytic wet peroxide oxidation of phenol with a Fe/active carbon catalyst’’. They found that oxidation of phenol gives rise to highly toxic aromatic intermediates which finally disappear completely evolving to short-chain organic acids. Some of these last showed to be fairly resistant to oxidation being responsible for the residual TOC (Zazo et al, 2006).

The summary of the studies in the literature is given in Table 3.1.

Table 3.1 Summary of literature survey.

TARGET COMPOUND	METHOD/CATALYST	RESULT	REFERENCE
• Acetic acid • Benzoic acid • Isophthalic acid • Toluic acid • Terephthalic acid	Traditional active sludge method	p-Toluic acid is found as the most difficult compound to for biodegradation with almost 50 % degradation for 48 hours residence time.	Raj et al.,1997
Purified terephtalic acid effluent	Activated sludge	Reduction in BOD (63%) and COD (62%)	Pophali et al.,2006
• Benzoic acid • p-toluic acid • 4-carboxybenaldehyde • Phthalic acid • Terephthalic acid	Aerobical degradation with microbial fusant	• Order of biodegradation was determined as BA>PA>4-CBA>TA>p-Tol. • p-toluic acid was the poorest biodegradable compound which cannot be degraded completely.	Zhang et al.,2006

Table 3.1 Continued

Benzoic acid	Homogeneous photocatalysis by Fe(III) ions	• Both Fe(II) and Fe(III) ions had the same effect on degradation efficiency with COD reduction for 60 -70 % • The optimum value for pH is 3.5	Andreozzi and Marotta, 2004
Phthalic acid and benzoic acid from wastewater	Advanced oxidation methods	The most efficient method was Photo-fenton ozonation which resulted almost complete destruction in 30 minutes	Thiruvenkatachari et al., 2006
Benzoic acid	Heterogeneous photo-Fenton oxidation and biological treatment	• 72% and 16% COD reduction at 150 and 450 mg/L benzoic acid concentration by only Fenton oxidation • combining photo-Fenton oxidation with aerobic post-oxidation led to 77% and 69% overall COD removal at 150 and 450 mg/L	Pariente et al., 2008
Benzoic acid	Photocatalytic degradation in the presence of TiO_2	Complete mineralization of benzoic acid to CO_2 and H_2O	Velegraki et al., 2008

Table 3.1 Continued

Terephthalic acid	Activated sludge	• TiO_2 and ZnO photocatalysts can be used as an effective catalyst • At optimized conditions ZnO was more efficient than TiO_2	Shafaei et al., 2010
Benzoic acid	Photocatalytic wet air oxidation in the presence of TiO_2	Complete conversion is achieved within 90–120 min at relatively mild conditions, e.g. <30 bar oxygen partial pressure, <180 °C reaction temperature and <40 mg/L metal concentration.	Velegraki et al., 2011
• Phenol • Benzoic acid • Salicylic acid • Sulfonic salicylic acid	Catalytic wet air oxidation in the presence of perovskite $LaFeO_3$	Very poor activities for phenol and benzoic acid due to their aromatic structure, where almost complete degradation was observed for salicylic and sulfonic salicylic acid	Yang et al., 2007
Phenol	Catalytic wet air oxidation in the presence of Fe/AC	Only one of the reaction intermediates, acetic acid was refractory and cannot be degraded efficiently	Quintanilla et al., 2006
Phenol	Catalytic wet peroxide oxidation in the presence of Fe/AC	Oxidation of phenol caused formation of highly toxic aromatic intermediates	Zazo et al., 2006

4.0 FOREWORD TO STUDY

Many industries recently deal with huge water supply and water purification problems. Industrial wastewaters contain organic biorecalcitrant pollutants even being highly dangerous both for humans and environment, cannot be treated efficiently yet and remain as threat. TPA plant wastewater is one of them and its treatment has been a great challenge for scientists.

Recent advances in research areas focusing on the treatment of TPA wastewater have been reviewed. This review revealed that there are very few studies about treatment of TPA wastewater by AOPs and those studies mostly involve biological oxidation could not accomplish promising results in terms of degradation.

The conclusions extracted from literature review assisted and guided in developing the outline of the study. Main reasons for selection of pollutants, methods and catalysts according to these conclusions are explained in detail below.

4.1 The Choice of Pollutants

TPA is being widely used as an important key chemical for many industrial fields both in Turkey and in world and the amount wastewater generated during its production is huge. But unfortunately, there is no successful attempt for degradation of major contaminants in TPA wastewater except for few studies. These major contaminants are namely terephthalic acid, benzoic acid, and p-toluic acid. p-Toluic acid is determined as the most refractive compound present in TPA wastewater in many studies and around 50 % degradation efficiencies' were obtained in 48 hours or even longer time periods. These studies about treatment of TPA and its derivatives are very few as it can be observed from Literature Survey part and in these studies mostly biological methods were applied for almost non-biodegradable major contaminants present in the wastewater. Only promising studies were the ones that applied AOPs to actual TPA wastewater or synthetic terephthalic acid and benzoic acid

contacting wastewater. The results with high degradation efficiencies obtained in these studies were the motivation for this study. However there was almost no study on application AOPs to p-toluic acid and there is almost no information about its efficient degradation. Also there wasn't any study about applying different AOPs to TPA and its derivatives to compare methods for each compound.

Since the studies were missing in literature about application of AOPs for TPA wastewater in detail and there are many open ends in this field, it has been selected as the thesis topic.

4.2 The Choice of Methods and Catalyst

4.2.1 The choice of AOPs and biological oxidation

Advanced oxidation processes are known to be highly effective on especially refractive organic pollutants due to high oxidizing potentials of •OH radicals which is the basis of AOPs (Zhou and He, 2007). But main limitation of AOPs is that it is considered as high cost technology because of high energy consumption and using expensive chemicals. This is why there isn't any AOP applied to industry efficiently and widely (Andreozzi et al., 1999). Conventional methods currently being used such as biological oxidation or incineration are not sufficient to satisfy discharge standards and/or they may create secondary waste. AOPs eliminate these drawbacks in theory and this has been proven by many studies in literature (Oller et al., 2011). Unfortunately from the economical point of view, application of AOPs have been only in lab-scale in academic researches and they couldn't have been adapted in industrial level. One of the main goals of this study is to reduce cost by achieving high degradation efficiencies in short time to minimize energy consumption and by using catalysts derived from organic wastes to minimize use of expensive chemicals.

AOPs namely Fenton-like oxidation, catalytic wet air oxidation and photocatalytic oxidation were chosen to be applied. The reason of selecting these methods is they have wide application in recent studies due to some advantages

they provide such as easy application for Fenton-like oxidation, using non-toxic chemicals for catalytic wet air oxidation and being effective on highly recalcitrant organic compounds for photocatalytic oxidation.

There are very few studies with biological methods except for activated sludge process (Pellegrini et al., 2011). Hence, more effective, ecofriendly, and economical methods were planned to be developed for the treatment of TPA wastewater with this study. Furthermore the application of advanced oxidation techniques and new biological methods were thought to be stimulated for the treatment of TPA and other aromatic pollutants in industry which leads to contributions to environmental protection.

4.2.2 The choice of catalyst

Literature survey also showed that recent studies focused on using heterogeneous catalysis since it eliminates many drawbacks of homogeneous catalysis such as metal leaching and generation of secondary waste (Ramirez et al., 2007). Activated carbon has been widely used as catalyst support in many studies due to the several advantages it provides (Liu et al., 2010). The activation method is highly essential for distribution of metal catalysts since it affects specific surface are, pore size and structure. Homogeneous distribution of catalyst on catalyst support directly affects catalytic activity and reproducibility of the results. Several activation methods were planned to be applied to compare the effect of activation methods on catalytic performance. Walnut shells as an organic precursor were being used for this study as agricultural wastes that have almost no industrial use and easy to find especially in Turkey. This study aimed both reuse of an organic waste and to develop and eco-friendly catalyst for environmental applications.

5.0 EXPERIMENTAL STUDY

The experimental study has been carried out for selected target compounds to represent TPA wastewater as terephthalic acid (TPA), benzoic acid (BA) and p-toluic acid (p-Tol) by chemical and biological oxidation. The study was performed in four main steps:

- Catalyst Preparation
- Catalyst Characterization
- Catalyst Screening Experiments
- Parametric Study Experiments

In catalyst preparation for chemical oxidation, Fe doped activated carbon (Fe/AC) catalysts and Fe-TiO_2 doped activated carbon (Fe-TiO_2/AC) catalysts were prepared by using different physically or chemically activated carbons.

In catalyst characterization for chemical oxidation, all Fe/AC and Fe-TiO_2/AC catalysts prepared were characterized by several analyses.

In catalyst screening experiments for chemical oxidation, all Fe/AC and Fe-TiO_2/AC catalysts prepared were tested in terms of degradation efficiencies for all target compounds presence in TPA wastewater by different advanced oxidation methods.

In parametric study experiments for chemical oxidation, the selected catalysts from catalyst screening experiments were used to determine the operating conditions of efficient methods for each target compound.

In catalyst preparation for biological oxidation, selected microorganisms were grown, incubated and immobilized on walnut shells.

In catalyst screening for biological oxidation, immobilized microorganisms were used as biocatalyst and effects of biocatalyst type, glucose presence and hydrogen peroxide presence were to be searched for.

In parametric study for biological oxidation, the optimum values for operating conditions such as biocatalyst loading, glucose concentration and hydrogen peroxide concentration.

The schematic representation of the experimental study is given in Figure 5.1.

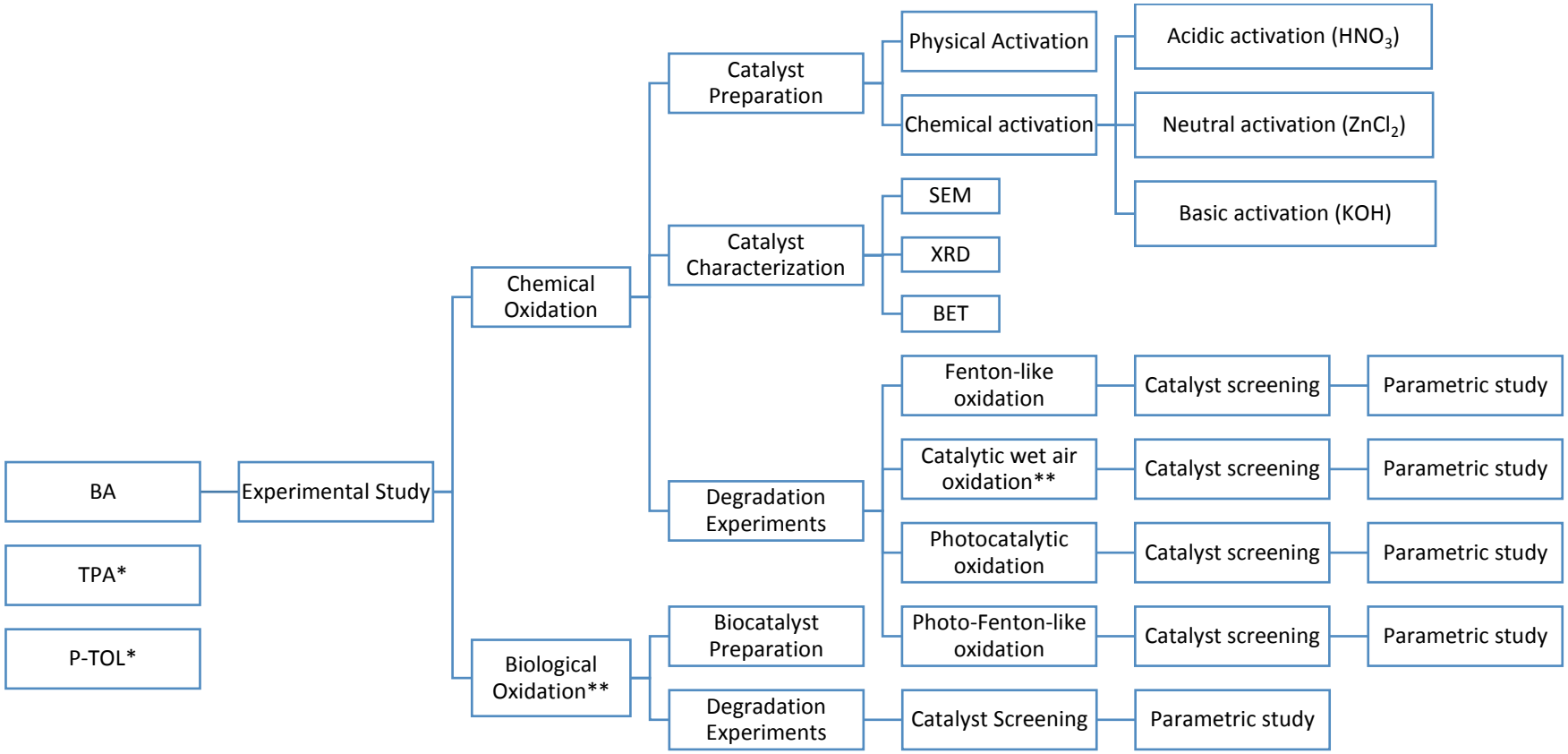

*Same experimental study were also carried out for this compounds.
** This method weren't applied for TPA and p-TOL.

Figure 5.1 Schematic representation of experimental study

5.1 Catalyst Preparation

5.1.1 Catalyst preparation for chemical oxidation

Firstly, activated carbon were prepared from walnut shells by physical and chemical activation methods and used as a catalyst support. Fe/AC catalysts were prepared by impregnation of iron ions to the prepared activated carbons and Fe-TiO_2/AC photocatalysts were prepared by Sol-gel method.

The preparation of the catalysts was carried out in two steps. In the first step, the production of activated carbon was accomplished and in the second step, the Fe or Fe/TiO_2 were doped to the prepared activated carbon.

5.1.1.1 Activated carbon preparation

The production of activated carbon involves two main steps: the pre-treatment and carbonization-activation. Pre-treated walnut shells were activated by physical activation method and chemical activation methods using different chemical reagents such as HNO_3 (acidic), $ZnCl_2$ (neutral) and KOH (basic) activation.

All the preparation procedures are explained in detail, below and also shown in Figure 5.2 (Choi et al., 2012, Kalderis et al., 2008, Nowicki et al., 2010, Rambabu et al., 2013, Rey et al., 2011, Tseng, 2007).

Pre-treatment:

The walnut shells were obtained from a local Turkish bazaar and used as they were obtained without any modifications. In pre-treatment step, walnut shells were first crushed into smaller particles and ground to increase surface area. Then they were washed with distilled water to remove impurities and dried at 110^{o}C for 6 h to remove moisture.

Carbonization-activation:

For physical activation method, the pre-treated walnut shells were carbonized at 400 °C for 2 hours under N_2 flow. Then the carbonized shells were activated at 800 °C for 2 hours under CO_2 flow.

For acidic activation method, the pre-treated walnut shells were carbonized and a pure carbon mass was obtained. Then the carbonized shells were impregnated with HNO_3 for a weight ratio of 1:1 (walnut shells: HNO_3).

For basic and neutral activation methods, the pre-treated walnut shells were impregnated with the chemical reagents KOH or $ZnCl_2$ for a weight ratio of 1:1 (walnut shells (WS): KOH/$ZnCl_2$). Then impregnated walnut shells were carbonized and activated at 800^oC for 3 hours under N_2 flow separately.

The activated carbons obtained by different activation methods except for acidic activation were washed with 1 M HCl to remove inorganic impurities and then washed with distilled water for neutralization. The activated carbon obtained by acidic activation was only washed with distilled water for neutralization because of the previous acid treatment which had already completed the removal of inorganic impurities.

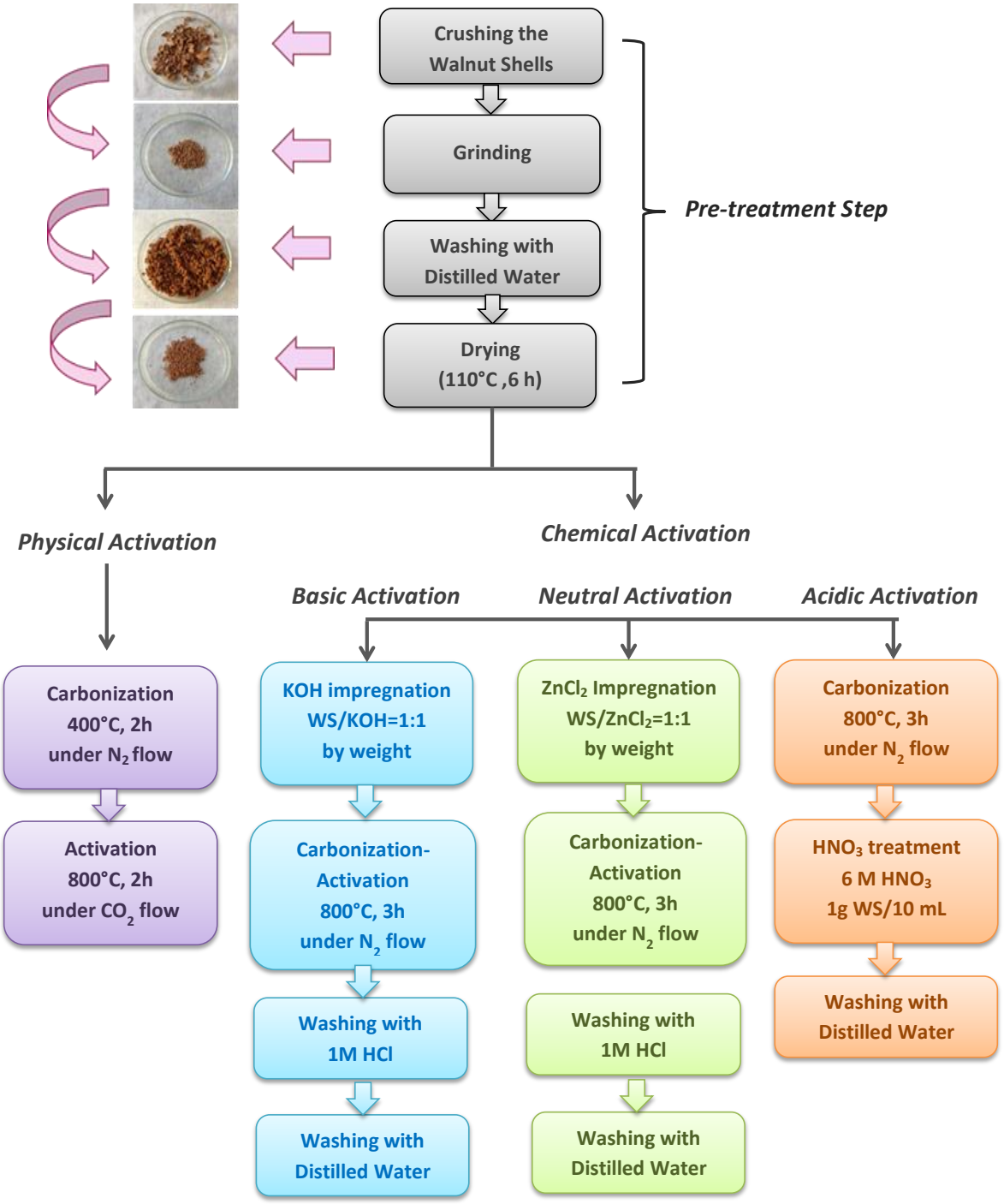

Figure 5.2 Schematic representation of activated carbon preparation

5.1.1.2 Metal doping

The Fe/AC and Fe-TiO_2/AC catalysts used in this study were prepared by doping Fe or Fe-TiO_2 by using impregnation or Sol-gel methods, respectively. The procedures applied for all activated carbons obtained by all activation methods are given in detail below.

Fe/AC catalyst preparation:

Ferric ion (Fe^{3+}) was attached to the activated carbon by impregnation method which is widely applied in previous studies (Duarte et al., 2011, Ling et al., 2011). $Fe(NO_3)_3.9H_2O$ was used as Fe^{3+} ion source and impregnated to the prepared activated carbon at a weight ratio of 1:10 (Fe:catalyst). After impregnation, the activated carbon was dried at 110^{o}C for 6 h. Finally, it was calcinated at 200^{o}C for 4 h. Preparation steps are shown in the Figure 5.3.

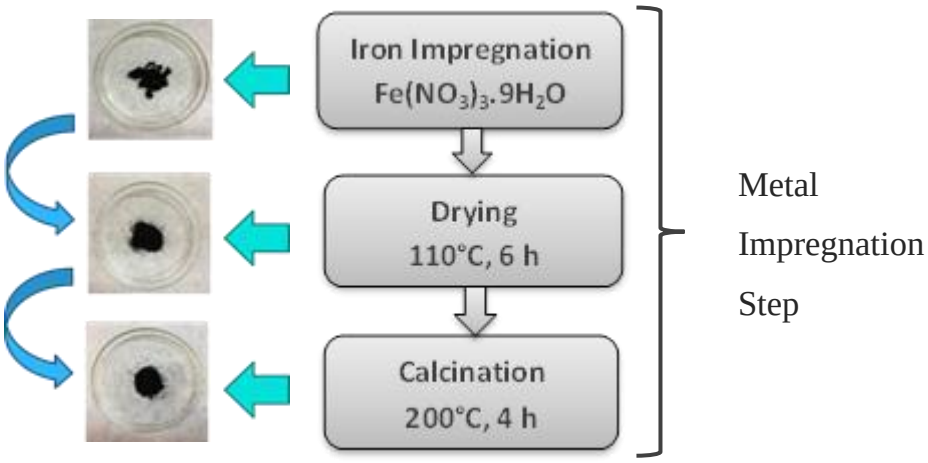

Figure 5.3 Schematic representation of Fe/AC preperation

Fe-TiO_2/AC photocatalyst preparation:

The catalyst used in photocatalytic experiments so called as photocatalyst and consisted of trace amount of iron containing titanium dioxide supported on activated carbons prepared by different activation methods. Fe ions were used for improving the photocatalytic activity of TiO_2 which has been proven in previous studies (Banic et al., 2011, Teh et al., 2011).

The photocatalyst (Fe-TiO_2/AC) is prepared by Sol-gel method which is widely used in many studies. It is a convenient low temperature method for preparation of homogeneous materials, especially inorganic materials which provides great homogeneous structure in atomic level (Asiltürk and Şener, 2012, Huang et al., 2011, Tang et al., 2011).

The preparation of the catalyst was performed in two steps. First, Fe-TiO_2 sol (1% Fe, w/w) was prepared which included the use of $Fe(NO_3)_3.9H_2O$ and $Ti(OBu)_4$ as metal precursors. Then, prepared Fe-TiO_2 sol was mixed with activated carbon at a weight ratio of 1:10 (Fe-TiO_2: photocatalyst). The mixture was kept under stirring until homogeneous mixture was observed. Photocatalytic oxidation parameters are shown in Figure 5.4.

The photocatalyst was prepared by following procedure:

Fe-TiO_2 Sol preparation

- $Ti(OBu)_4$ and $Fe(NO_3)_3.9H_2O$ were dissolved in methanol and mixed.
- pH of the mixture was adjusted with NaOH solution for neutral pH (pH=7) and Fe-TiO_2 sol was obtained.

Fe-TiO_2/AC preparation

- The desired amount of activated carbon is then added to the Fe-TiO_2 sol.
- Fe-TiO_2 Sol and activated carbon mixture was kept under stirring until homogeneous mixture was observed.
- Fe-TiO_2 Sol coated activated carbon was kept at room temperature for gelation.
- The catalyst in gel form is vacuum dried to remove methanol and butyl content.
- The obtained particles are treated at 500^oC for 2 h under N_2 flow for calcination.

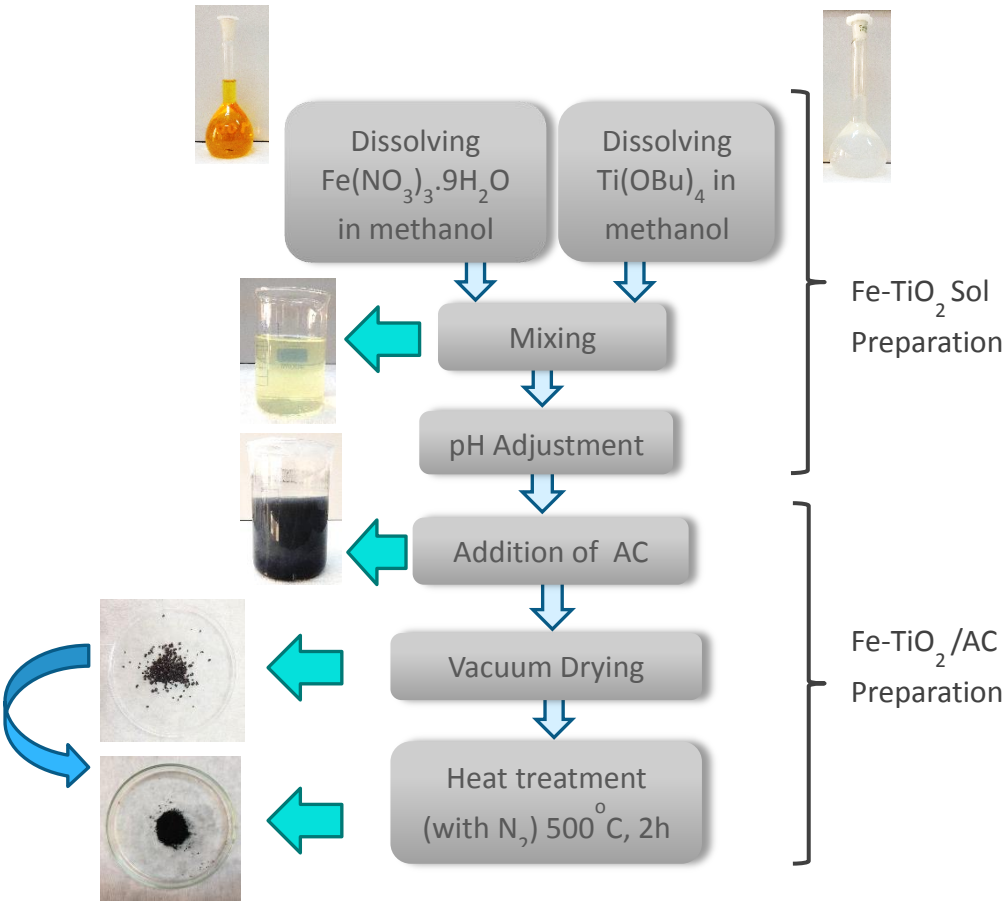

Figure 5.4 Schematic representation of Fe-TiO_2/AC preparation

5.1.2 Catalyst preparation for biolocigal oxidation

Microorganism for biological oxidation were selected as *Phanerochaete chrysosporium* (*P. chrysosporium*) and *Trametes versicolor* (*T. versicolor*) and purchased as active growing cultures from culture collection of Germany (DSMZ-Deutsche Sammlung von Mikroorganismen und Zellkulturen). Active growing cultures were cultivated on potato dextrose agar (PDA) and malt extract agar plates in darkness for 3 days at 37°C and 26°C, respectively. Agar plates and broth were prepared by dissolving required amount of potato dextrose/malt extract agar and malt extract broth in distilled water and sterilized at 121°C for 15 minutes. Cultivated cultures were transferred to malt extract broth in a round bottom

flask and incubated for 7 days at 37°C and 26°C, respectively. Malt extract broth was previously sterilized at 121°C for 2 hours.

After incubation, required amount of walnut shell powder were added to the broth medium and grown whole cells were immobilized to the walnut shells. Walnut shell powder was previously sterilized at 121°C for 2 hours. After immobilization was complete, the immobilized whole cells were filtered and stored in laboratory jar at 4°C. Schematic overview of biocatalyst preparation for *P. chyrsosporium* is given in Figure 5.5. Same procedure was applied for *T. versicolor*, too.

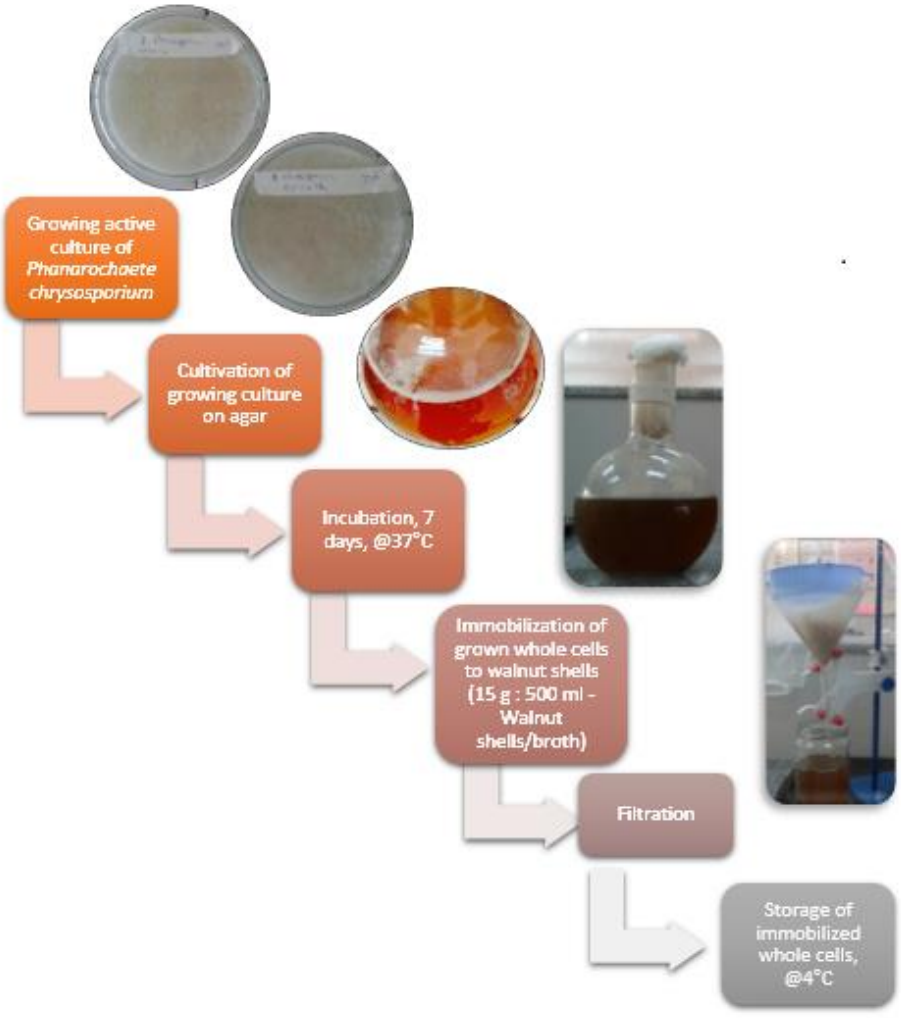

Figure 5.5 Schematic overview of catalyst preparation for biological oxidation

5.2 Catalyst Characterization

The catalyst characterization was performed for the activated carbons, Fe/AC and Fe-TiO_2/AC catalysts. The surface morphology of the activated carbons and the catalysts was observed by scanning electron microscopy (SEM) (Phillips XL-30S FEG). The crystallinity and metal content were investigated by the help of powder X-ray diffraction (XRD) (Phillips X'Pert Pro X-ray diffraction). Additionally, specific surface area by Brunauer, Emmett and Teller (BET) surface and corresponding area method was performed for the catalyst, determined as most successful activated carbon and considered as most successful analysis. All of the analyses were performed in Material Research Center of İzmir Institute of Technology (İYTE-MAM).

5.3 Experimental Setups and Procedures

5.3.1 Experimental setups

Three different experimental setups were used for Fenton-like oxidation, catalytic wet air oxidation and photocatalytic/photo-Fenton-like oxidation.

5.3.1.1 Fenton-like oxidation setup

The experimental setup used for Fenton like oxidation experiments which is given in Figure 5.6, consists of a three necked flask, a magnetic stirrer and a thermocouple.

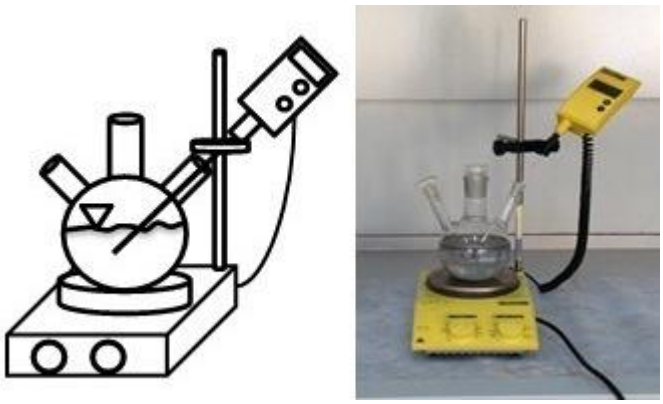

(a) **(b)**

Figure 5.6 The schematic view (a) and picture of experimental setup (b) of catalytic wet air oxidation

5.3.1.2 Catalytic wet air oxidation setup

The experimental setup for catalytic wet air oxidation which is given in Figure 5.7 consists of:

- A bubble column stainless steel reactor of 500 mL volume which is insulated using glasswool
- Electrical wires wrapped around the reactor to provide heating to the desired temperature and the reaction temperature controlled by a PID controller
- A condenser at the top of the reactor which is used to condense the vapours formed during the reaction and send the condensate back to the reactor.

Air is fed continuously and distributed in the reactor and a rotameter is used to adjust the flow rate of the air stream.

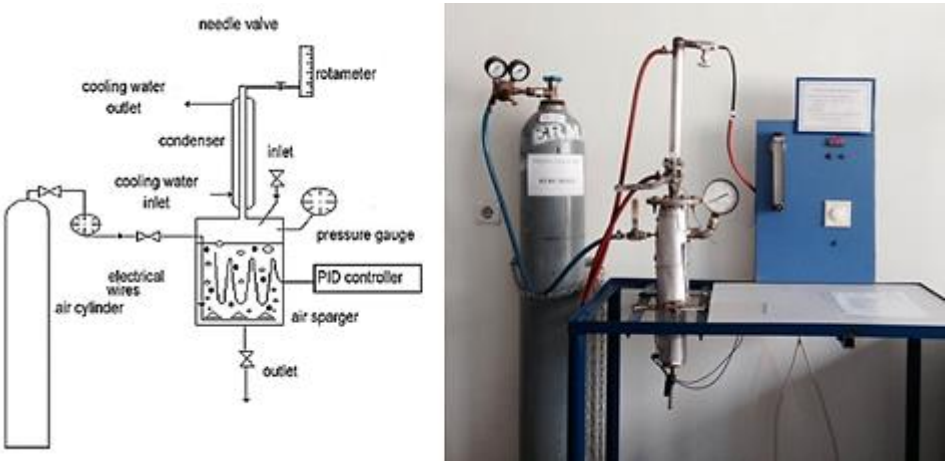

(a) **(b)**

Figure 5.7 The schematic view (a) and picture of experimental setup (b) of catalytic wet air oxidation

5.3.1.3 Photocatalytic oxidation setup

The experimental set up mainly consists of a photo reactor (1), a magnetic stirrer (2) and a cooler (3). Water is circulated through the jacket (4) to keep the reaction temperature constant. The reactor is in a cabinet (5) to avoid release of radiation. The UV lamp (6) is placed in a quartz tube (7). The samples are taken from the sample spout (8) during the reaction. The schematic representation of experimental set up is given in Figure 5.8.

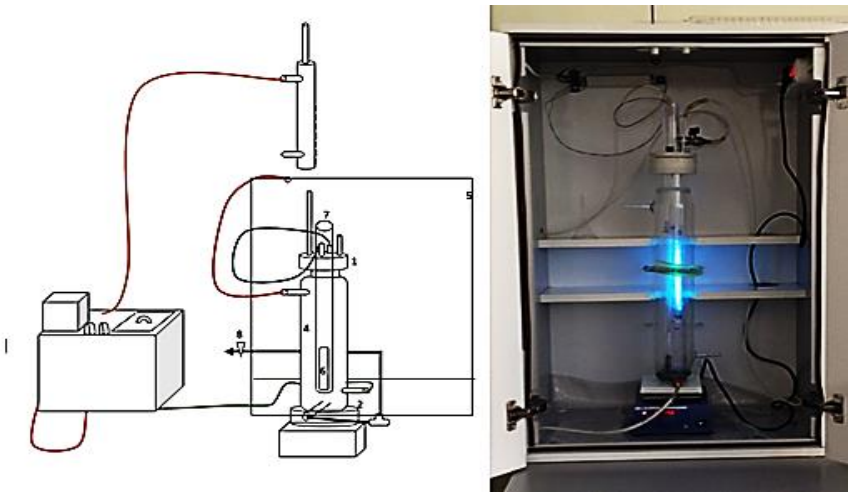

(a) **(b)**

Figure 5.8 The schematic view (a) and picture of experimental setup (b) of photocatalytic oxidation

5.3.1.4 Experimental setup for biological oxidation

Batch experiments were carried out in 50 mL beakers in an orbital shaker with a shaking speed of 200 rpm. The experimental setup is shown in Figure 5.9.

Figure 5.9 Experimental setup for biological oxidation experiments

5.3.2 Experimental procedures

5.3.2.1 Fenton-like oxidation experimental procedure

For a typical run the following procedure is as follows:

- Synthetic aqueous target compound solution with an initial concentration of 50 mg/L was prepared with distilled water for BA or 30% Tetrahydrofuran (THF)-water solution for TPA nd p-TOL in a 250 ml flask.
- Required amount of hydrogen peroxide was added.
- Catalyst was added to the wastewater and a sample as an initial sample was taken.
- During the experiments, samples from reaction medium were taken at 10, 20, 30, 40, 60, 80,100 and 120 minutes.
- Experiment was ended at 120 min. pH and volume of the reaction medium were measured.

- Samples were diluted with 1:25 ratio of distilled water or with 2:25 ratio of 30% THF-water solution, respectively.
- The samples were analyzed by using UV/VIS Spectrophotometer.

5.3.2.2 Catalytic wet air oxidation experimental procedure

For a typical run the following procedure is as follows:

- Synthetic aqueous target compound solution with an initial concentration of 50 mg/L was prepared with distilled water in a 250 ml flask.
- Catalyst was added to the wastewater and a sample as an initial sample was taken.
- The prepared wastewater was charged to the reactor.
- The reaction temperature and pressure were set to the desired values.
- Experiment was ended at 120 min and the gas flow was stopped and the heater was turned off.
- The reactor was allowed to cool and the final sample was taken. pH and the volume of the reaction medium were measured.
- Samples were diluted with 1:25 ratio of distilled water.
- The samples were analyzed by using UV/VIS Spectrophotometer.

5.3.2.3 Photocatalytic oxidation experimental procedure

For a typical run the following procedure is as follows:

- Synthetic aqueous target compound solution with an initial concentration of 50 mg/L was prepared with distilled water for BA or 30% Tetrahydrofuran (THF)-water solution for TPA and p-TOL in a 250 ml flask.
- Catalyst was added to the wastewater and a sample as an initial sample was taken.
- The prepared wastewater was charged to the reactor.
- The UV lamp was turned on.
- During the experiments, samples from reaction medium were taken at 10, 20, 30, 40, 60, 80,100 and 120 minutes.

- Experiment was ended at 120 min and the UV lamp is turned off, pH and volume of the reaction medium were measured.
- Samples were diluted 1:25 ratio of distilled water or 2:25 ratio with 30% THF-water solution, respectively.
- The samples were analysed by using UV/VIS Spectrophotometer.

5.3.2.4 Biological oxidation experimental procedure

For a typical run the following procedure is as follows:

- Synthetic aqueous target compound solution with a initial concentration of 50 mg/L was prepared with distilled water in a 50 ml flask.
- Biocatalyst was added to the wastewater and a sample as an initial sample was taken.
- Required amounts of glucose and/or hyrodgen peroxide were added.
- The prepared wastewater was placed in the orbital shaker.
- The speed of shaking was set.
- During the experiments, samples from reaction medium were taken every day.
- Experiment was ended in 5 days, pH and volume of the reaction medium were measured.
- Samples were diluted 1:25 ratio of distilled water.
- The samples were analyzed by using UV/VIS Spectrophotometer.

5.3.3 Analysis

The analysis for all experiments were performed by measuring the absorbance of the samples at the maximum absorbance wavelength of each compound in a UV/VIS Spectrophotometer (Thermo Genesys 10S UV-VIS). The wavelengths for maximum absorbance were determined as 242 nm, 193 nm, and 236 nm for terephthalic acid, benzoic acid and p-toluic acid, respectively.

The target compound removal efficiency was calculated by the formula given below:

$$x(\%) = \frac{m_0 - m_f}{m_0} \times 100$$

where m_0 and m_f were initial and final amount of target compound, respectively.

5.4 Catalyst Screening Experiments

The catalyst screening experiments were performed for all target compounds to determine the most efficient catalyst which were used in further parametric studies. Fe/AC catalysts were used for Fenton like oxidation and catalytic wet air oxidation and both Fe/AC and Fe-TiO_2/AC catalysts were used for photocatalytic oxidation. All of the experiments were performed two or three times and average values of degradation efficiencies were used. The data for change in degradation efficiencies with respect to time is available, but only final degradation efficiencies at the end of 120 minutes were shown. Concentration of target compound was kept constant as 50 mg/L for all experiments.

5.4.1 Catalyst screening experiments for Fenton-like oxidation

Experiments were carried out using Fe/AC catalysts obtained by physical and chemical (acidic, neutral, basic) activation for Fenton-like oxidation experiments. For each Fe/AC catalyst, two different catalyst loadings ([Catalyst]) 0.1 and 0.2 g/L, and H_2O_2 concentrations ([H_2O_2]) 3 and 4 mM were studied. Four conditions studied for each catalyst are shown in Table 5.1.

Table 5.1 Catalyst screening experiments for Fenton-like oxidation.

		Catalyst Loading (g/L)	**H_2O_2 Concentration (mM)**
Fenton-like Oxidation	Condition 1	0.1	3
	Condition 2		4
	Condition 3	0.2	3
	Condition 4		4

5.4.2 Catalyst screening experiments for catalytic wet air oxidation

Experiments were carried out using Fe/AC catalysts obtained by physical and chemical (acidic, neutral, basic activation) for catalytic wet air oxidation of BA. No catalyst screening and further parametric study were carried out for TPA and p-TOL since solvent for these compounds were 30% THF-water solution and THF is very flammable beyond 40°C. For each catalyst, two different catalyst loadings (0.25 and 0.5 g/L), pressures (1 and 3 bar), and temperatures (60 and 80°C). Eight conditions studied for each catalyst are shown in Table 5.2.

Table 5.2 Catalyst screening experiments for catalytic wet air oxidation.

		Catalyst Loading (g/L)	**Pressure (bar)**	**Tempeature (°C)**
Catalytic Wet Air Oxidation	Condition 1	0.25	1	60
	Condition 2			80
	Condition 3		3	60
	Condition 4			80
	Condition 5	0.5	1	60
	Condition 6			80
	Condition 7		3	60
	Condition 8			80

5.4.3 Catalyst screening experiments for photocatalytic oxidation

Experiments were carried out using Fe/AC and Fe-TiO_2/AC catalysts obtained by physical and chemical (acidic, neutral, basic) activation for photocatalytic oxidation experiments. For each catalyst, two different catalyst loadings (0.25 and 0.5 g/L) and UV intensities (6 and 8 watt) were studied. Four conditions studied for each catalyst are shown in Table 5.3.

Table 5.3 Catalyst screening experiments for photocatalytic oxidation.

		Catalyst Loading (g/L)	**UV light intensity (watt)**
Photocatalytic Oxidation	Condition 1	0.25	6
	Condition 2		8
	Condition 3	0.5	6
	Condition 4		8

5.4.4 Catalyst screening experiments for biological oxidation

Experiments were carried out for two different microorganisms (*P. chyrsosporium* and *T.versicolor*) in the presence of biocatalyst only, biocatalyst and glucose, biocatalyst and hydrogen peroxide and in the presence of biocatalyst, glucose and hydrogen peroxide. Catalyst screening experiments carried out for biological oxidation of BA for both microorganisms are shown in Table 5.4. No catalyst screening and further parametric study were carried out for TPA and p-TOL since solvent for these compounds were 30% THF-water solution and THF is very toxic for microorganisms.

Table 5.4 Catalyst screening experiments for biological oxidation.

		Biocatalyst loading (g/50 ml)	**Glucose (g/L)**	**H_2O_2 Concentration (mM)**
Biological Oxidation	Condition 1	0.25	0	0
	Condition 2		1	0
	Condition 3		0	5
	Condition 4		1	5

5.5 Parametric Study Experiments

Parametric studies were carried out for each target compound and for each method to improve degradation efficiencies and determine the optimum values of operating conditions. The most efficient catalysts determined from catalyst screening experiments for each compound and method were used for this purpose. The operating parameters and their range varied for different methods. They are explained for each target compound and each method in detail below. Concentration of target compound was kept constant as 50 mg/L for all experiments. All of the experiments were performed two or three times and average values of degradation efficiencies were used.

5.5.1 Parametric study for benzoic acid

5.5.1.1 Fenton-like oxidation

The main operating parameters of Fenton-like oxidation can be considered as catalyst loading, H_2O_2 concentration, temperature and pH. The ranges of these parameters studied for BA are given in detail in Table 5.5.

Table 5.5 Operating parameters of Fenton-like oxidation for BA and their ranges.

Fenton-like oxidation of BA [BA]=50 mg/L	**Catalyst Loading (g/L)** ([H_2O_2]=3 mM, T=25°C, pH=4)	0
		0.1
		0.2
		0.3
		0.4
	H_2O_2 Concentration (mM) ([Catalyst]=0.3 g/L, T=25°C , pH=4)	0
		1
		2
		3
		4
		5
	Temperature (°C) ([Catalyst = 0.3 g/L, [H_2O_2] = 2 mM, pH=4)	25
		50
	pH ([Catalyst = 0.3 g/L, [H_2O_2] = 2 mM, T=25°C)	3
		4
		6

5.5.1.2 Catalytic wet air oxidation

The main operating parameters of catalytic wet air oxidation can be considered as catalyst loading, pressure, temperature, and air flowrate. The ranges of these parameters studied for BA are given in detail in Table 5.6.

Table 5.6 Operating parameters of catalytic wet air oxidation for BA and their ranges.

Catalytic wet air oxidation of BA [BA]=50 mg/L	**Catalyst Loading (g/L)** (P=1 bar, T=60°C, v_{air}=0.92 ml/min)	0
		0.25
		0.5
		1
		2
	Temperature (°C) ([Catalyst]=1 g/L, P=1 bar, v_{air}=0.92 ml/min)	40
		50
		60
		70
		80
		90
	Pressure (bar) ([Catalyst]=1 g/L, T=50°C, v_{air}=0.92 ml/min)	1
		2
		3
	Air flow rate (ml/min) ([Catalyst]=1 g/L, P=1 bar, T=60°C)	0.61
		0.92
		1.36
		1.72

5.5.1.3 Photocatalytic oxidation

The main operating parameters of photocatalytic oxidation can be considered as catalyst loading, UV light intensity, and pH. The ranges of these parameters studied for BA are given in detail in Table 5.7.

Table 5.7 Operating parameters of photocatalytic oxidation for BA and their ranges.

Photocatalytic oxidation of BA [BA]=50 mg/L	**Catalyst Loading (g/L)** (UV light intensity=6 watt, pH=4)	0
		0.25
		0.5
		1
		2
	UV light intensity (watt) ([Catalyst]=0.5 g/L, pH=4)	6
		8
	pH ([Catalyst]=0.5 g/L, UV light intensity=8 watt)	3
		4
		6

5.5.1.4 Photo-Fenton-like oxidation

The optimum values of main operation parameters such as catalyst loading ([Catalyst]) and UV light intensity were determined previously for photocatalytic oxidation since same catalyst screening was used both for photocatalytic and photo-Fenton-like oxidation. Additionally, effect of H_2O_2 concentration and initial pH were investigated to search for the effect of initial pH in the presence of H_2O_2. The ranges of these parameters studied for BA are given in detail in Table 5.8.

Table 5.8 Operating parameters of photo-Fenton-like oxidation for BA and their ranges.

Photo-Fenton-like oxidation of BA [BA]=50 mg/L	**H_2O_2 Concentration (mM)** ([Catalyst]=0.5 g/L, UV light intensity=8 watt, pH=4)	0
		1
		2
		3
		4
		5
	pH ([Catalyst]=0.5 g/L, UV light intensity=8 watt, [H_2O_2]=2 mM)	3
		4
		6

5.5.1.5 Biological oxidation

The main operating parameters of biological oxidation can be considered as biocatalyst loading, glucose and H_2O_2 concentration which was previously mentioned in catalyst screening experiments for biological oxidation section. The optimum values of these parameters were to be searched for in parametric study for biological oxidation. The ranges of these parameters studied are given in detail in Table 5.9.

Table 5.9 Operating parameters of biological oxidation and their ranges.

Biological oxidation of BA [BA]=50 mg/L	**Biocatalyst Loading (g/50 ml)**	0.125
		0.25
		0.5
	Glucose (g/L)	0
		0.25
		0.5
		1
		1.5

5.5.2 Parametric study for terephthalic acid

5.5.2.1 Parametric study for photocatalytic oxidation

The main operating parameters of photocatalytic oxidation can be considered as catalyst loading, UV light intensity, and pH. The ranges of these parameters studied for TPA are given in detail in Table 5.10.

Table 5.10 Operating parameters of photocatalytic oxidation for TPA and their ranges.

Photocatalytic oxidation of TPA [TPA]=50 mg/L	**Catalyst Loading (g/L)** (UV light intensity=6 watt, pH=4)	0
		0.25
		0.5
		1
		2
	UV light intensity (watt) ([Catalyst]=1 g/L, pH=4)	6
		8
	pH ([Catalyst]=1 g/L, UV light intensity=6 watt)	3
		4
		6

5.5.2.2 Parametric study for photo-Fenton-like oxidation

The optimum values of main operation parameters such as catalyst loading ([Catalyst]) and UV light intensity were determined previously for photocatalytic oxidation since same catalyst screening was used both for photocatalytic and photo-Fenton-like oxidation. Additionally, effect of H_2O_2

concentration and initial pH were investigated to search for the effect of initial pH in the presence of H_2O_2. The ranges of these parameters studied for TPA are given in detail in Table 5.11.

Table 5.11 Operating parameters of photo-Fenton-like oxidation for TPA and their ranges.

Photo-Fenton-like oxidation of TPA [TPA]=50 mg/L	**H_2O_2 Concentration (mM)** ([Catalyst]=1 g/L, UV light intensity=6 watt, pH=4)	0
		1
		2
		3
		4
	pH ([Catalyst]=1 g/L, UV light intensity=6 watt, [H_2O_2]=1 mM)	3
		4
		6

5.5.3 Parametric study for p-toluic acid

5.5.3.1 Parametric study for photocatalytic oxidation

The main operating parameters of photocatalytic oxidation can be considered as catalyst loading, UV light intensity, and pH. The ranges of these parameters studied for p-Tol are given in detail in Table 5.12.

Table 5.12 Operating parameters of photocatalytic oxidation for p-Tol and their ranges.

Photocatalytic oxidation of p-Tol [TPA]=50 mg/L	**Catalyst Loading (g/L)** (UV light intensity=6 watt, pH=4)	0
		0.25
		0.5
		1
		2
	UV light intensity (watt) ([Catalyst]=0.5 g/L, pH=4)	6
		8
	pH ([Catalyst]=0.5 g/L, UV light intensity=6 watt)	3
		4
		6

5.5.3.2 Parametric study for photo-Fenton-like oxidation

The optimum values of main operation parameters such as catalyst loading ([Catalyst]) and UV light intensity were determined previously for photocatalytic oxidation since same catalyst screening was used both for photocatalytic and photo-Fenton-like oxidation. Additionally, effect of H_2O_2 concentration and initial pH were investigated to search for the effect of initial pH in the presence of H_2O_2. The ranges of these parameters studied for p-Tol are given in detail in Table 5.13.

Table 5.13 Operating parameters of photo-Fenton-like oxidation for p-Tol and their ranges.

Photo-Fenton-like oxidation of p-Tol [TPA]=50 mg/L	**H_2O_2 Concentration (mM)** ([Catalyst]=1 g/L, UV light intensity=6 watt, pH=4)	0
		1
		2
		3
		4
	pH ([Catalyst]=0.5 g/L, UV light intensity=6 watt, [H2O2]=2 mM)	3
		4
		6

6.0 RESULTS AND DISCUSSION

6.1 Catalyst Characterization

The results obtained by SEM, XRD, and BET analyses are shown in Figure 6.1 through Figure 6.14 and Table 6.1 through Table 6.3.

6.1.1 SEM analysis

SEM analysis was performed by using Everhart-Thornley detector (ETD). The SEM images of activated carbon, Fe/AC catalysts and Fe-TiO_2/AC catalysts prepared by different activation methods at 20000 times magnification are shown in Figure 6.1, 6.2, and 6.3 respectively.

SEM images of activated carbons show that all activated carbons consist of pores which provide high specific surface area. That leads higher adsorption capacity to attach metal catalyst successfully.

For physical AC, porous structure was obtained in some parts but unfortunately not homogeneously (Figure 6.1-a). This was due to the characteristic of the reaction that forms pores during activation process. Carbon dioxide was used as the activation atmosphere to react carbon structure but using activation in gas form as atmosphere reduces contact with the carbon structure which causes decrease in reaction and consequently porous structure (Ahmadpour and Do, 1997, Nowicki et al.2010).

For acidic AC, oxidizing process was applied to create smaller pores by creating thinner walls and modify surface chemistry by creating surface functional groups. Those surface functional groups look different than regular porous structure (El-Sheikh et al., 2007). Successful porous structure was observed for acidic AC. Lighter colored areas indicating surface functional groups were also observed (Figure 6.1-b).

For neutral AC, porous structure was accomplished less successful than other activated carbons with smaller pores and more complex pore networks

were observed. Lighter colored areas indicate Zn ions remained from activation process due to the reaction between zinc chloride as activation agent and carbon atoms (Figure 6.1-c).

The most porous structure was obtained by basic activation. Basic AC images revealed highly porous structure and homogeneous distribution of pores. Almost no lighter area was observed which indicates pure carbon structure without any activation reagent remaining, KOH in this case (Figure 6.1-d).

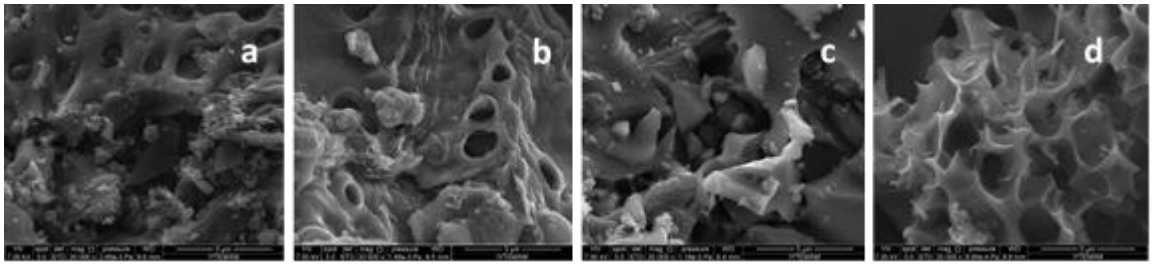

Figure 6.1 SEM images of activated carbons at 20000x times magnifications: (a) physical activation, (b) acidic activation, (c) neutral activation, (d) basic activation

SEM images of Fe/AC catalysts show that metal impregnation to the porous structure of activated carbons were performed successfully.

For physical Fe/AC, catalyst lighter spots indicate Fe ions that have higher atomic number as the darker areas represent carbon atoms with lower atomic number. Porous structure observed for physical AC disappeared mostly as an indicator of most of the pores filled with Fe ions which was observed as white spots (Figure 6.2-a).

For acidic Fe/AC catalyst, lighter areas were less than acidic AC and homogeneously distributed. This indicates surface functional groups of acidic AC were preserved and additionally Fe ions were doped successfully which can be observed from white spots (Figure 6.2-b).

For neutral Fe/AC catalyst, heterogeneous porous structure was observed as remaining Zn ions from activation step and Fe ions from impregnation step were filled the pores. Larger and brighter light colored areas were observed

because of the increase in the amount of high atomic numbered atoms (Fe ions) (figure 6.2-c).

For basic Fe/AC catalyst, as the porous structure was preserved mostly and almost no lighter area was detected, it has been concluded that the Fe ions were attached inside the pores instead of surface (Figure 6.2-d).

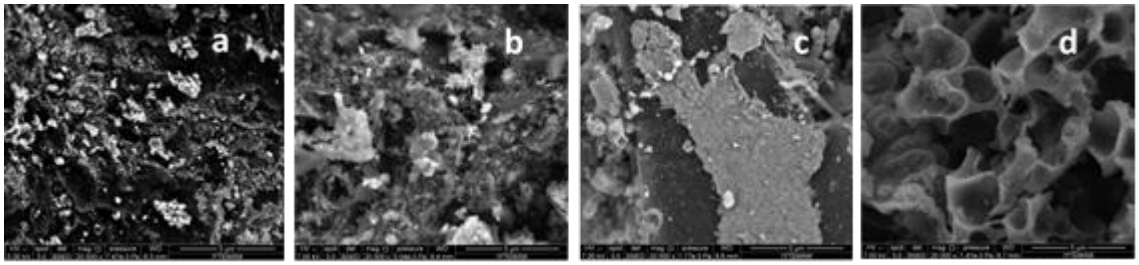

Figure 6.2 SEM images of Fe/AC at 20000x times magnifications: (a) physical activation, (b) acidic activation, (c) neutral activation, (d) basic activation.

For physical Fe-TiO_2/AC catalyst, very bright spots were observed which indicate Fe-TiO_2 complex structure. However the distribution wasn't perfectly homogeneous. This was probably caused by heterogeneous structure of physical AC which did not allow attachment of Fe-TiO_2. The difference between physical Fe/AC and physical Fe-TiO_2/AC catalyst was because Fe-TiO_2 structure is much larger than Fe atom (Figure 6.3-a).

For acidic Fe-TiO_2/AC catalyst, light areas were homogeneously distributed and covered most of the surface. Very bright spots represent Fe-TiO_2 structure and less light colored areas indicate Fe ions. The difference between acidic Fe/AC and acidic Fe-TiO_2/AC catalyst was because of larger Fe-TiO_2 structure as in physical Fe-TiO_2/AC catalyst (Figure 6.3-b).

For neutral Fe-TiO_2/AC catalyst, light colored areas weren't observed as well as the porous structure. The possible reason for that all the pores and cavities filled by Fe-TiO_2 structure and this was not visible on the surface (Figure 6.3-c).

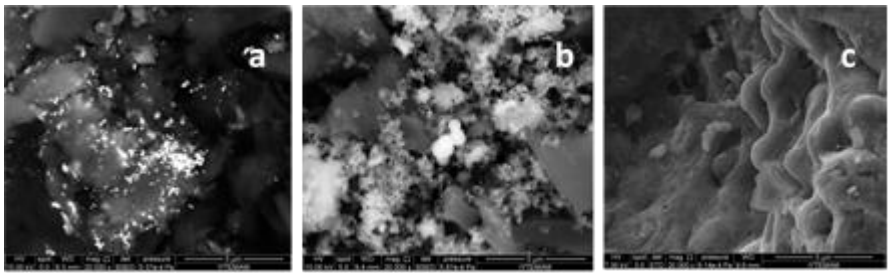

Figure 6.3 SEM images of Fe-TiO_2/AC at 20000x times magnifications: (a) physical activation, (b) neutral activation, (c) acidic activation.

As a conclusion, images belong to ACs and Fe/AC or Fe-TiO_2/AC catalysts reveal that expected porous structure were obtained and metal content of the catalyst (Fe^{3+} ions or Fe-TiO_2) were doped on activated carbons successfully and mostly homogenously. The results for Fe/AC and Fe-TiO_2/AC are consistent with similar studies in literature (Zazo et al., 2006, Li et al., 2010).

6.1.2 XRD analysis

The XRD patterns of activated carbons, Fe/AC, and Fe-TiO_2/AC catalysts are shown in Figure 6.4 through Figure 6.10.

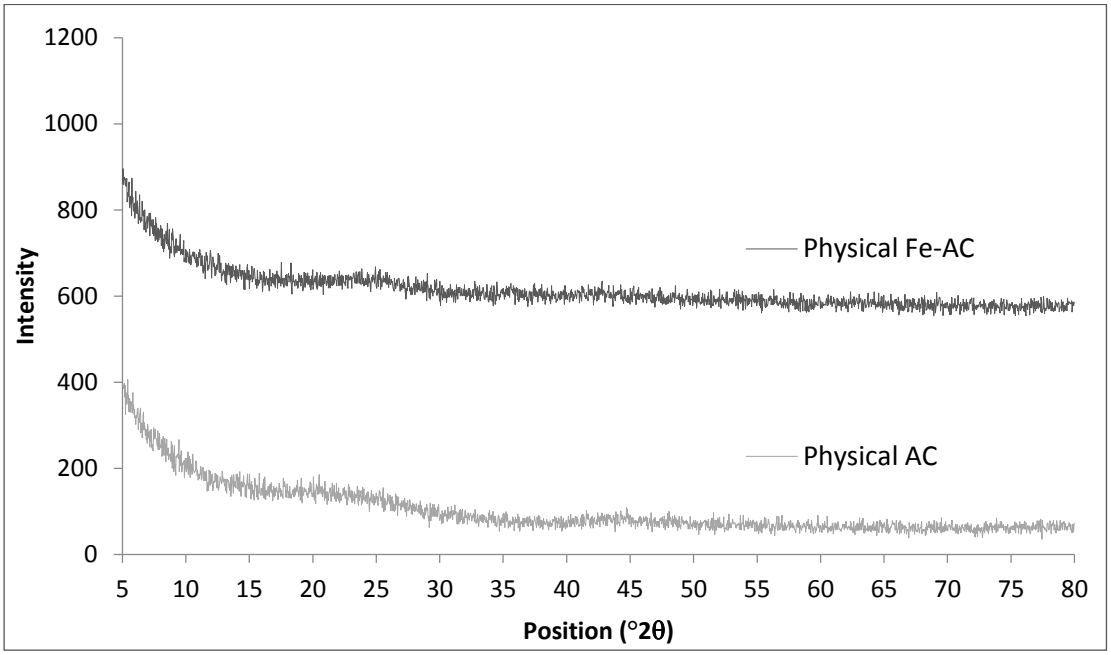

Figure 6.4 XRD patterns of physically activated carbon and Fe/AC catalyst

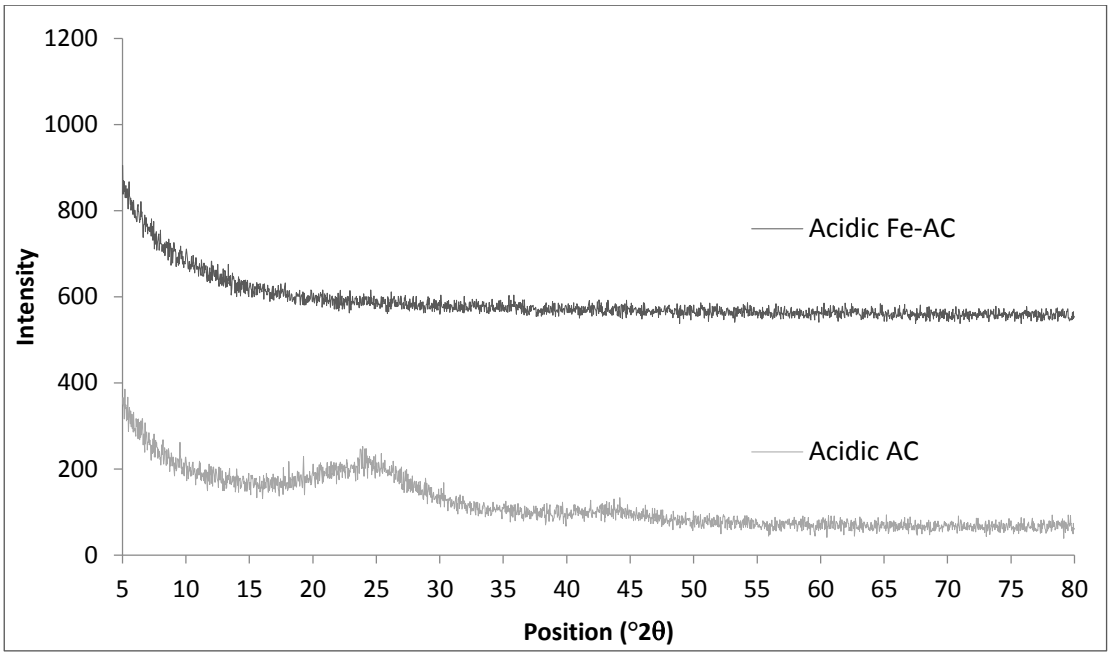

Figure 6.5 XRD patterns of acidic activated carbon and Fe/AC catalyst

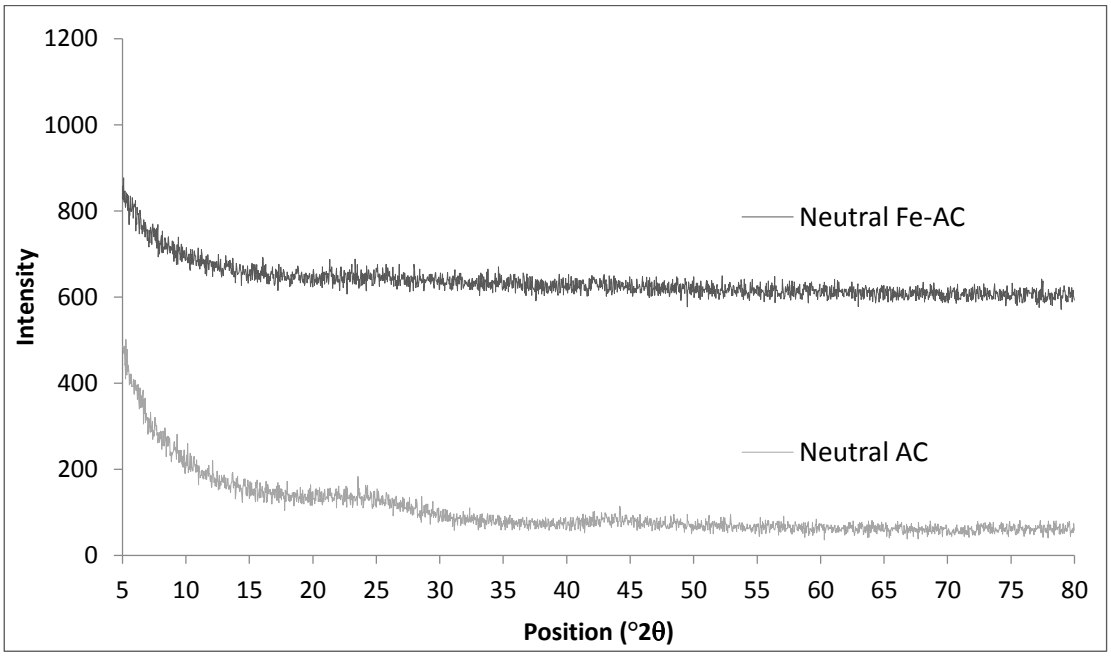

Figure 6.6 XRD patterns of neutrally activated carbon and Fe/AC catalyst

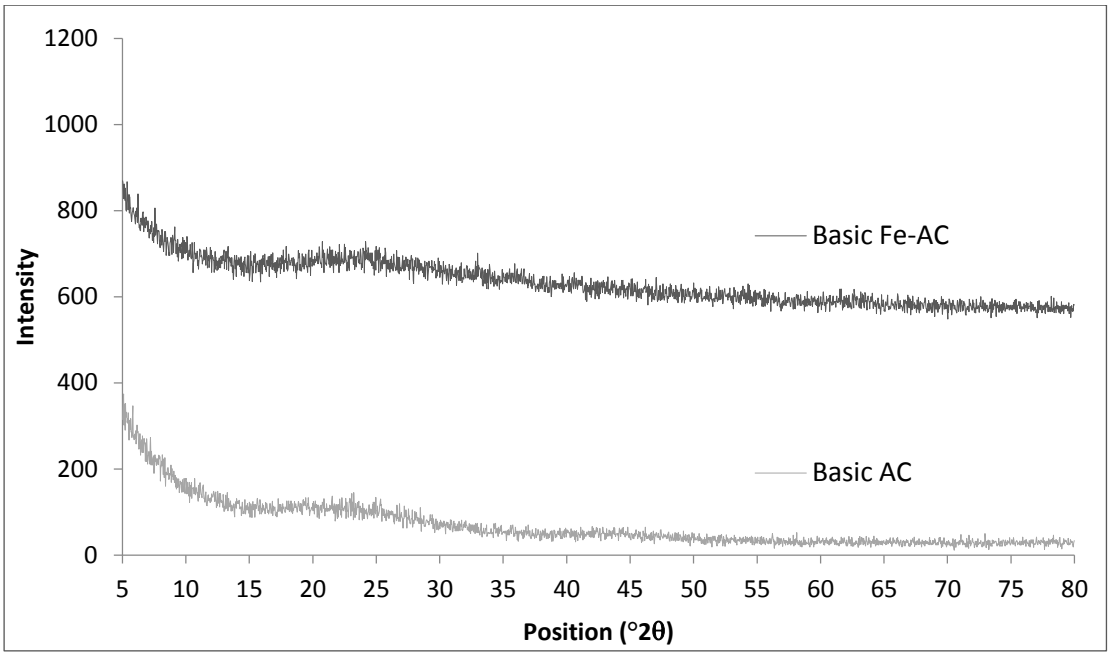

Figure 6.7 XRD patterns of basic activated carbon and Fe/AC catalyst

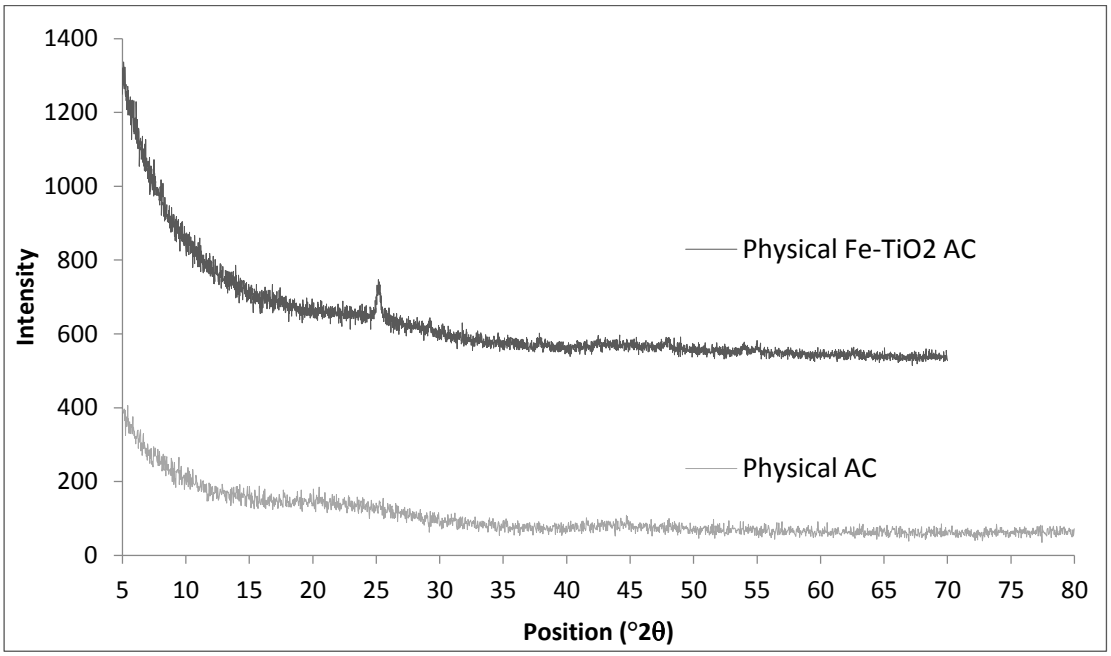

Figure 6.8 XRD patterns of physically activated carbon and Fe-TiO_2/AC catalyst

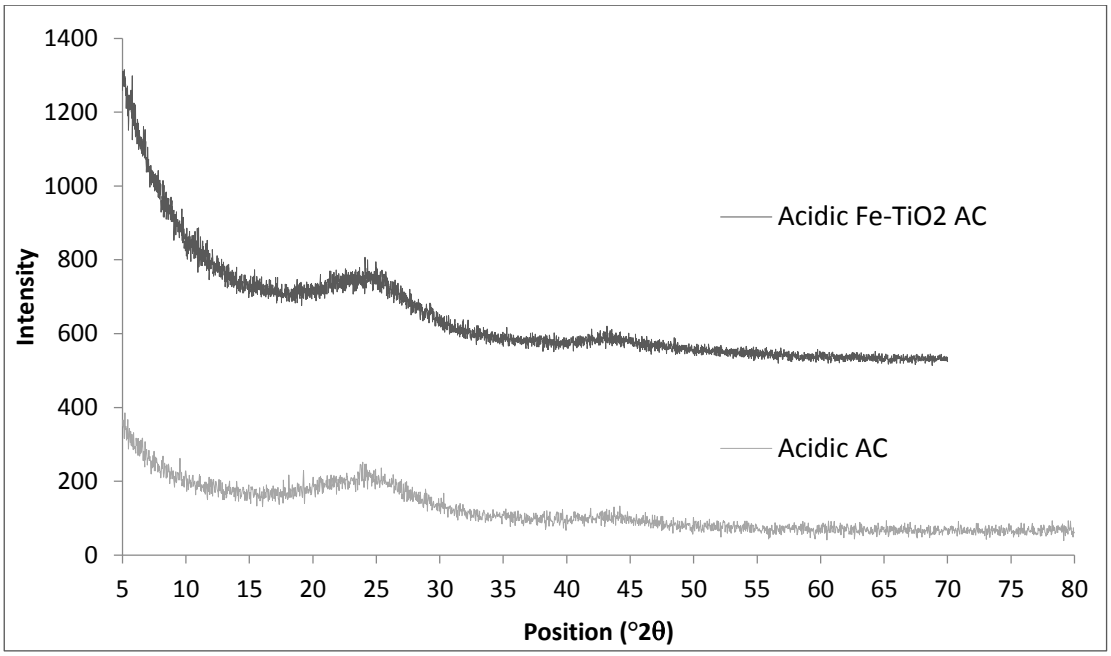

Figure 6.9 XRD patterns of acidic activated carbon and Fe-TiO_2/AC catalyst

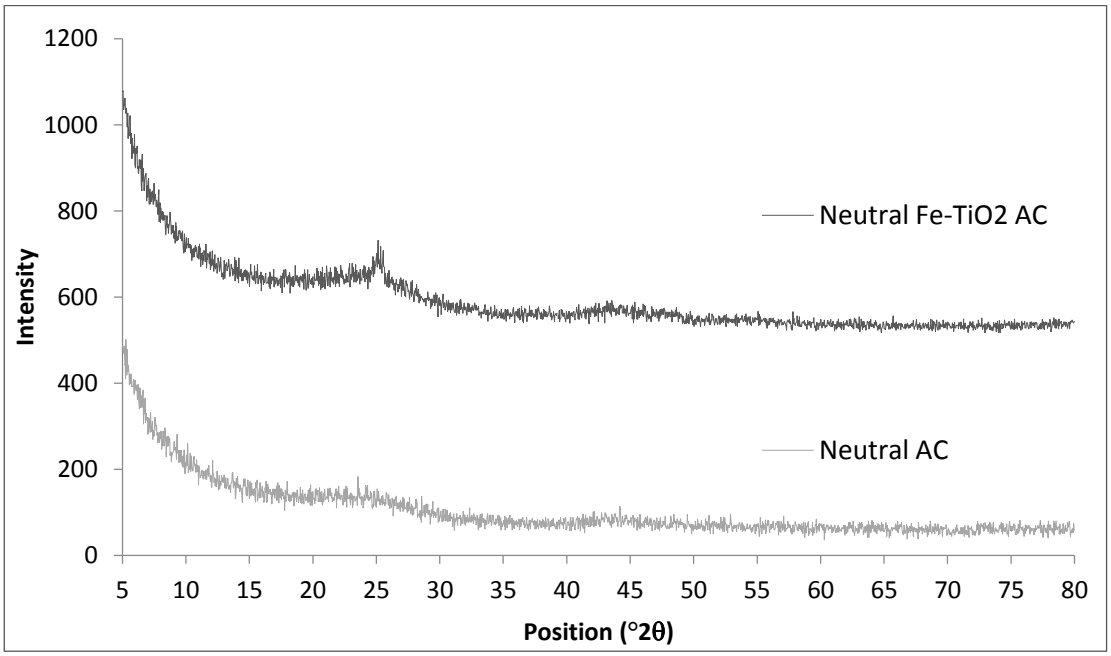

Figure 6.10 XRD patterns of neutrally activated carbon and Fe-TiO_2/AC catalyst

No sharp peak could be seen in XRD patterns of all activated carbons which indicates low crystallinity. The small peaks observed in 2θ=24° indicate low graphitization and it is consistent with the amorphous structure of activated carbon (Djilani et al., 2012, Senthilkumar et al., 2011). Same amorphous

patterns were also observed for Fe/AC and Fe-TiO_2/AC catalysts due to their high activated carbon content.

The absence of metal peaks in Fe/AC catalyst patterns can be explained by very low content of metal in the Fe/AC catalysts. Only XRD pattern belongs to neutrally activated Fe/AC catalyst resulted a small peak in 2θ=25° as an indicator of Zn ions remained from activation step of preparation (Figure 6.6). The tiny peak observed in pattern of physically activated Fe/AC catalyst shows that impregnation of Fe^{3+} ions to activated carbon was the least successful among others (Figure 6.4). Same results were also obtained in similar studies (Duarte et al. 2011, Ramirez et al., 2011).

The peaks around in 2θ=25° indicates the anatase phase of TiO_2 which colud be clearly observed in patterns of Fe-TiO_2/AC catalysts prepared by physical and neutral activation in Figure 6.8 and 6.10 (Carpio et al., 2005, Asiltürk and Şener, 2012). The pattern of Fe-TiO_2 catalyst prepared by acidic activation revealed that its TiO_2 content is lower among the others. Fe^{3+} ion couldn't be observed since its content in the catalysts are very low (Figure 6.9).

6.1.3 BET analysis

The BET surface area analysis was only carried out for the catalysts determined as the most efficient which are basic Fe/AC catalyst for Fenton-like oxidation and catalytic wet air oxidation of BA, and neutral Fe-TiO_2/AC catalyst for photocatalytic oxidation of TPA and p-Tol. Both activated carbons and Fe or Fe-TiO_2 doped activated carbon catalysts are shown in Table 6.1and 6.2.

Table 6.1 BET surface area results of basic activated carbon and corresponding Fe/AC catalyst.

	Basic AC	**Basic Fe/AC Catalyst**
Single Surface Area (m^2/mg)	(p/p°=0.1603) 997.17	(p/p°=0.1601) 749.23
BET Surface Area (m^2/mg)	961.06	724.86
Langmuir Surface Area (m^2/mg)	911.91	1207.36
t-Plot Micropore Area (m^2/mg)	593.74	828.34
t-Plot External Surface Area (m^2/mg)	131.12	132.73
Pore Size (Å)	18.62	20.48
Pore Volume (cm^3/g)	(p/p°= 0.9850) 0.4474	(p/p°= 0.9844) 0.3711

BET Surface Area analysis showed that the surface area of the basic activated Fe/AC catalyst is less than basic activated carbon due to the successful metal impregnation which caused some of the pores get filled by Fe^{3+} ions. This also led to a decrease in pore volume. The pore size almost remained constant which revealed that the porous structure of the activated carbon has been kept after metal impregnation. The results are consistent with other studies that applied same conditions (Tay et al., 2009, Gao et al., 2013)

Table 6.2 BET surface area results of neutrally activated carbon and corresponding Fe-TiO_2/AC catalyst.

	Neutral AC	**Neutral Fe-TiO_2/AC Catalyst**
Single Surface Area (m^2/mg)	(p/p°=0.1600) 1333.76	(p/p°=0.2000) 1209.43
BET Surface Area (m^2/mg)	1370.30	1229.54
Langmuir Surface Area (m^2/mg)	1771.36	1668.83
t-Plot Micropore Area (m^2/mg)	321.77	342.26
t-Plot External Surface Area (m^2/mg)	1048.53	887.28
Pore Size (Å)	18.76	19.55
Pore Volume (cm^3/g)	(p/p°=0.9843) 0.6427	(p/p°=0.9844) 0.6010

BET Surface Area analysis showed that the surface area of the neutrally activated Fe-TiO_2/AC catalyst is less than neutrally activated carbon due to the successful metal impregnation which caused some of the pores get filled by Fe-TiO_2. This also led to a decrease in pore volume. The pore size almost remained constant which revealed that the porous structure of the activated carbon has been preserved after metal impregnation step. The results are consistent with other studies in which the same conditions were applied (Yorgun et al., 2009, Oliveira et al., 2009).

6.2 Benzoic Acid Degradation

6.2.1 Fenton-like oxidation

6.2.1.1 Catalyst screening

Experiments were carried out using Fe/AC catalysts obtained by physical and chemical (acidic, neutral, basic) activation for Fenton-like oxidation. For each Fe/AC catalyst, two different catalyst loadings (0.1 and 0.2 g/L) and hydrogen peroxide (H_2O_2) concentrations (3 and 4 mM) were tested. The results for the effect of those different catalyst loadings and H_2O_2 concentrations for each catalyst are shown in Figure 6.11, 6.12, 6.13 and 6.14.

Final degradation efficiencies for physical Fe/AC catalyst experiments were almost same and rather low around 10–15 % for each condition tested (Figure 6.11). Increasing catalyst loading from 0.1 to 0.2 g/L or H_2O_2 concentration from 3 to 4 mM didn't cause considerable increase in degradation. Only increase in both catalyst loading and H_2O_2 concentration, increased degradation slightly which is only 3 % and can be considered as very insignificant. Hence it can be concluded that physical Fe/AC catalyst was not successful for Fenton-like oxidation of BA because of low degradation efficiencies.

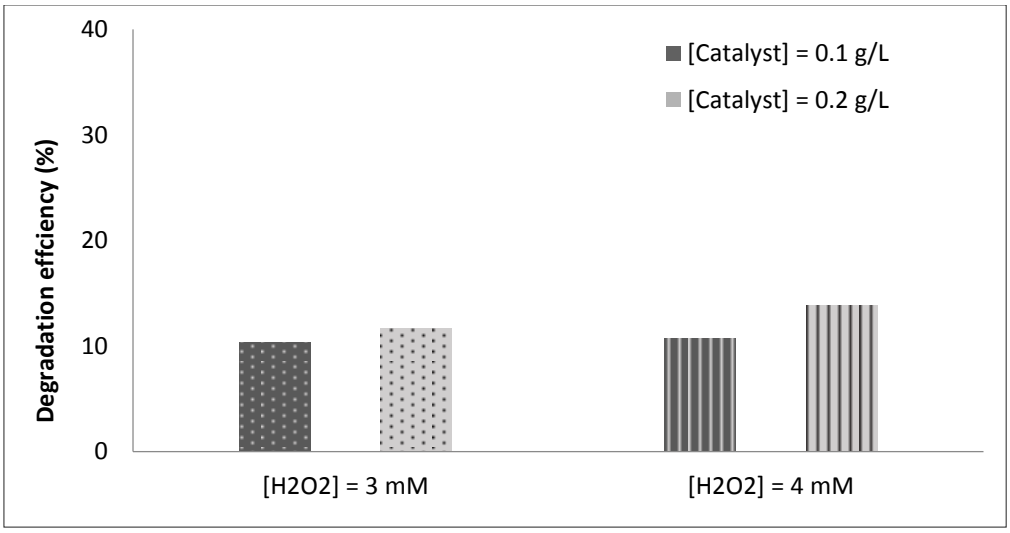

Figure 6.11 Degradation efficiencies obtained by physical Fe/AC ([BA]=50 ppm, T=25°C, pH=4)

Final degradation efficiencies for acidic Fe/AC were around 5 to 10 % which were very low. Catalyst loading was effective and increased degradation efficiencies for both peroxide concentrations. But for 4 mM H_2O_2 concentration a sharp decrease were observed for both catalyst loadings. Also the increase in degradation was very low even the catalyst loading was doubled. So it was concluded that 4 mM H_2O_2 concentration as excess H_2O_2. For 3 mM however, increase in catalyst loading had more considerable effect on degradation as an additional indicator that 4 mM was excess concentration. Nevertheless, all degradation efficiencies obtained were very low and this catalyst was not promising for parametric study, too (Figure 6.12).

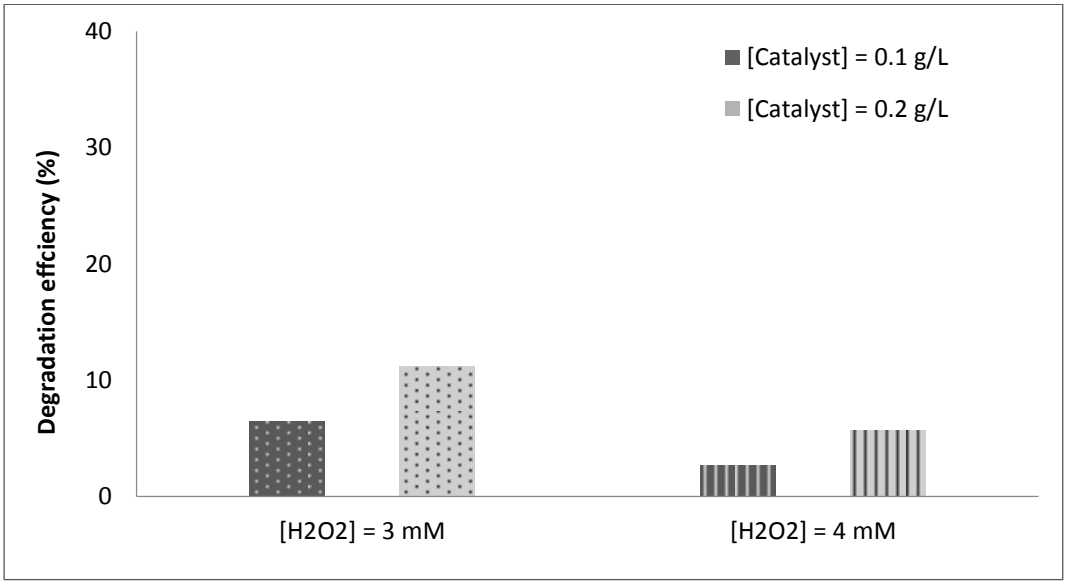

Figure 6.12 Degradation efficiencies obtained by acidic Fe/AC ([BA]=50 ppm, T=25°C, pH=4)

Final degradation efficiencies obtained by neutral Fe/AC catalyst was around 10 to 30 %. The degradation efficiency observed at 0.1 g/L catalyst loading was 15 % and it was doubled up to 30 % when catalyst loading was also doubled to 0.2 g/L for both H_2O_2 concentrations. However according to the change in degradation with respect to time which are not shown here, degradation was much slower for 4 mM than 3 mM H_2O_2 concentration although the final degradation efficiencies were the same. There is no considerable change in final degradation in the change H_2O_2 concentration. In contrast, increase in catalyst loading had almost doubled the degradation efficiency (Figure 6.13).

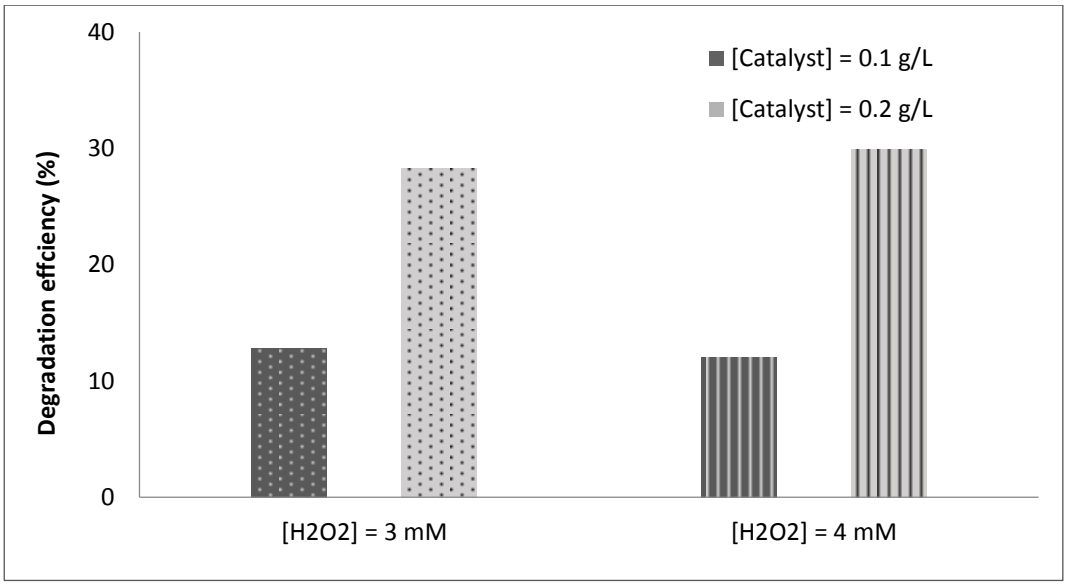

Figure 6.13 Degradation efficiencies obtained by neutral Fe/AC ([BA]=50 ppm, T=25°C, pH=4)

Final degradation efficiencies obtained by basic Fe/AC catalyst were around 15 % for low catalyst loadings for both H_2O_2 concentrations. For high catalyst loading, increase in H_2O_2 concentration from 3 to 4 mM slightly increased degradation from 20 to 30 %. The effect of H_2O_2 concentration was not observed at low catalyst loadings due to the lack of enough amount of catalyst in reaction medium (Figure 6.14).

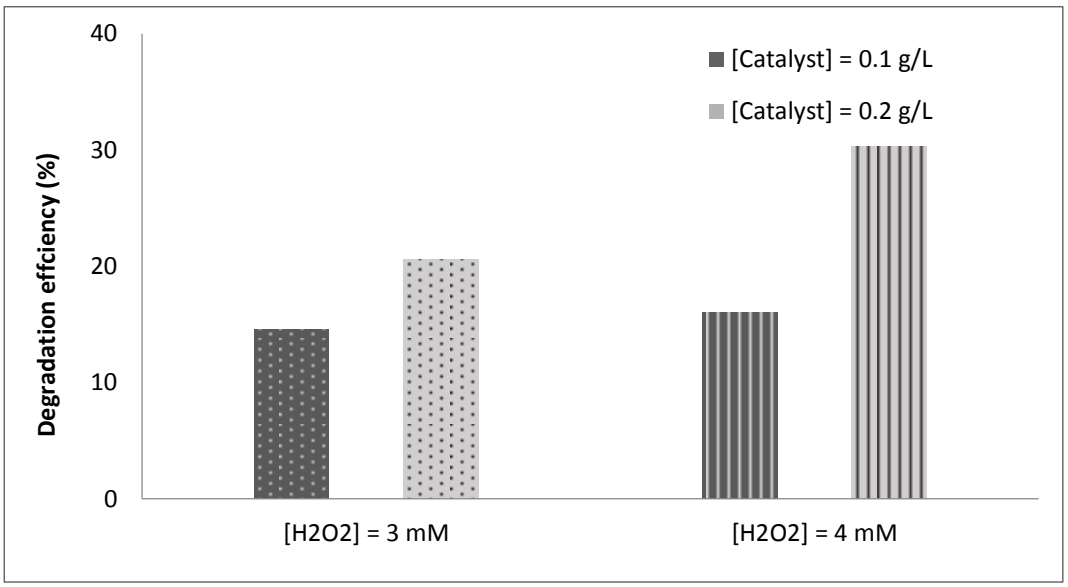

Figure 6.14 Degradation efficiencies obtained by basic Fe/AC ([BA]=50 ppm, T=25°C, pH=4)

Considering final degradation efficiencies; both neutral and basic Fe/AC catalysts were more successful than acidic and physical Fe/AC catalyst. However, although the final degradation efficiencies achieved were approximately same for neutral and basic Fe/AC, basic Fe/AC catalyst achieved same degradation efficiency in 30–40 minutes where neutral Fe/AC achieved it in 60–80 minutes.

Hence, further parametric study was performed in the presence of basic Fe/AC catalyst for Fenton-like oxidation by considering final degradation efficiencies.

6.2.1.2 Parametric study

Fenton-like oxidation screening experiment results showed that the highest and fastest degradation efficiency was achieved by Fe/AC catalyst prepared by one of the chemical activation method, basic activation. So the parametric study to determine the optimum values of operation conditions was carried out with basic Fe/AC. In this context, the effects of operational parameters such as catalyst loading ([Catalyst]), hydrogen peroxide concentration ($[H_2O_2]$) and initial pH on degradation efficiency were investigated.

Effect of catalyst loading:

The experiments investigating the effect of catalyst loading showed a significant increase in degradation efficiency due to the increase in catalyst loading and mostly degradation efficiencies remained constant around 20–40 minutes. When no catalyst was present in reaction medium, degradation efficiency remained almost constant during the experiment and it was very low around 5 %. 0.1 g/L catalyst loading achieved almost 20 % degradation in 20 minutes and degradation remained constant beyond that time. The increase in catalyst loading from 0.1 to 0.2 g/L caused faster and higher degradation efficiency but the great increase in both degradation efficiency and degradation rate was accomplished at 0.3 catalyst loading (45 %). Despite further increase in catalyst loading from 0.3 to 0.4 g/L, degradation efficiencies almost remained

same with almost same degradation rate where degradation reached its maximum in 20 minutes for both loadings. Hence the optimum catalyst loading was determined as [Catalyst]=0.3 g/L with a degradation efficiency of 45 % (Figure 6.15).

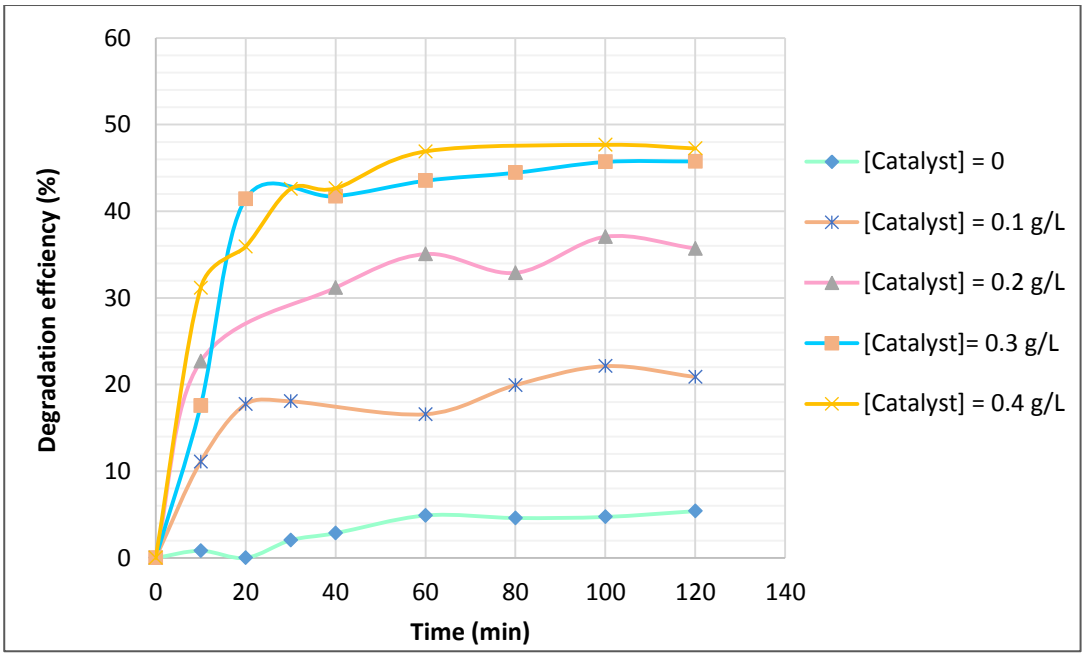

Figure 6.15 Effect of catalyst loading for basic Fe/AC ([BA]=50 ppm, [H_2O_2]=3 mM, T=25°C, pH=4)

Effect of hydrogen peroxide concentration:

The results obtained from the experiments investigating the effect of hydrogen peroxide concentration showed that it did not have a great influence on degradation efficiency. When H_2O_2 was absent in reaction medium, around 40 % degradation efficiency was achieved. Even though slight increase was observed in degradation by increasing H_2O_2 concentrations from 1 to 2 mM, approximately same final degradation efficiencies were achieved around 45 % for both H_2O_2 concentrations. However degradation was faster for 2 mM, and additionally degradation behavior observed for 1 mM wasn't stable as many oscillations in degradation efficiencies were observed. The increase in degradation from 2 to 4 mM was also insignificant, so 2 mM was considered as sufficient enough and no further increase was necessary. Generally, increasing the concentration until 4 mM increased degradation efficiency approximately to

the no H_2O_2 in reaction medium (Figure 6.16). It has been also observed in previous studies and the reason was thought that the formation of hydroxyperoxyl radicals (HO_2•) in the presence of local excess H_2O_2 which are less reactive and has almost no role in oxidation reactions (Ji et al., 2011). A further increase from 4 to 5 mM even caused a decrease in degradation due to the scavenging effect of excess hydrogen peroxide which was also observed in many studies about AOPs in the presence of H_2O_2 (Anotai et al. 2010, Chen et al. 2009, Duarte et al., 2011). So any concentration beyond 4 mM can be considered as excess hydrogen peroxide in reaction medium. Since the increase in degradation from 2 to 4 mM was insignificant, the optimum hydrogen peroxide concentration was determined as around 2 mM with a degradation efficiency of around 45 % in order to prevent oscillations and observe the synergic effect of H_2O_2 with other parameters.

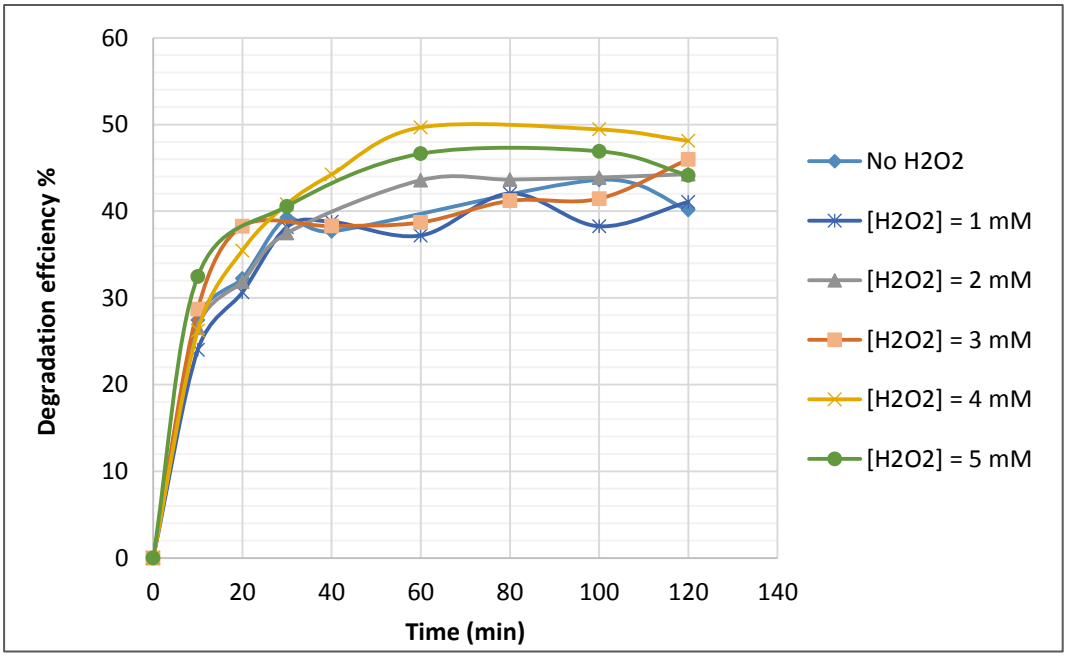

Figure 6.16 Effect of hydrogen peroxide concentration for basic Fe/AC ([BA]=50 ppm, [Catalyst]=0.3 g/L, T=25°C, pH=4)

Effect of initial pH:

pH had a negative effect on degradation since the target compound, benzoic acid, is a weak acid and highly sensitive to change in pH. The results from the initial pH experiments showed that the highest degradation efficiency

was observed with the lowest pH (pH=3) with a degradation efficiency of nearly 60 % and the degradation reached its maximum in 30 minutes and remained constant after that which can be considered as very fast. Fenton or Fenton-like reactions are known to be more effective in acidic reaction medium due to the Fe^{2+}/Fe^{3+} ions' higher catalytic activity when pH is in acidic range (pH=2–5) (Chen et al., 2009, Ramirez et al., 2010). However, Fe leaching from heterogeneous catalysts is very high when pH is 2 and below (Ramirez et al., 2010) Additionally, H_3O_2 is formed when pH is 2 which enhances the stability of H_2O_2 that causes a decrease in formation of •OH radicals. Therefore, many previous studies focused on avoiding initial pH below 3. This was also followed in this study and initial pH below 3 wasn't investigated. For the experiment for initial pH=4 showed that the degradation was not as high as when initial pH=3 which can be explained by decrease in precipitation of Fe^{3+} catalyst as FeOOH which slows down the formation •OH radicals (Ramirez et al. 2010). Increasing pH from 4 to 6 caused a drastic decrease in degradation. It was very low and almost remained constant during the experiment due to the formation and precipitation of the catalyst as $Fe(OH)_3$ which has less catalytic activity (Chen et al., 2009, Ramirez et al., 2010). Hence the optimum pH was determined as pH=3 with a degradation efficiency of 60 % which also confirmed the theory for Fenton-like reactions (Figure 6.17). In the case when degradation rate and final degradation efficiency are very important, optimum initial pH can be taken as pH=3. However in such a case that corrosion is essential and additional chemicals for pH adjustment are not desired, optimum initial pH can be taken as pH=4 which also achieved considerable degradation efficiency.

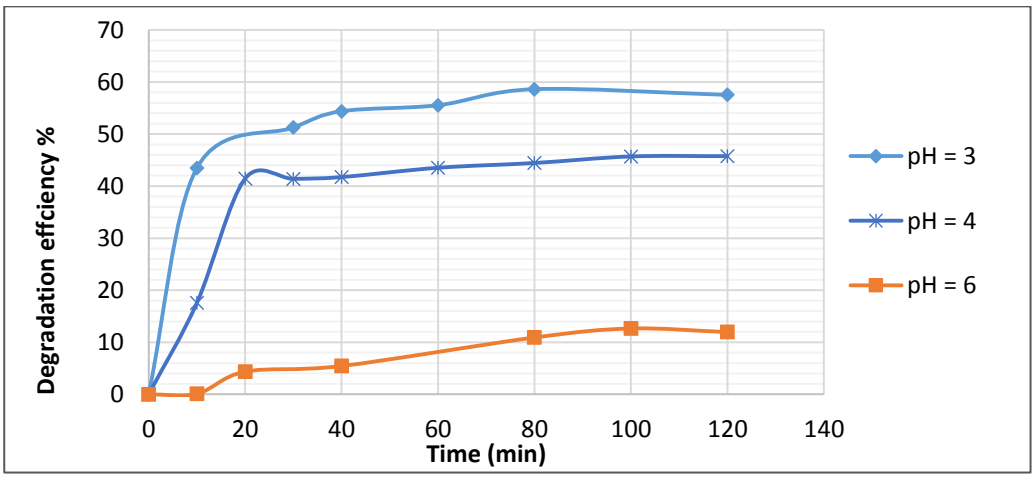

Figure 6.17 Effect of initial pH for basic Fe/AC ([BA]=50 ppm, [Catalyst]=0.3 g/L, [H_2O_2]=2 mM, T=25°C)

Effect of temperature:

Effect of temperature was also investigated by increasing operating temperature from 25°C (room temperature) to 50°C after determining optimum values of other parameters. Since there was almost no change in degradation with temperature, the results have not been presented.

The optimum values of operating parameters for Fenton-like oxidation of BA with an initial concentration of 50 mg/L in the presence of basic Fe/AC catalyst were determined as 0.3 g/L for catalyst loading, 2 mM for hydrogen peroxide concentration, 3 or 4 for initial pH, and 25°C (room temperature) for temperature with a final degradation efficiency of approximately 60 % in 40 minutes.

6.2.2 Catalytic wet air oxidation

6.2.2.1 Catalyst screening

Experiments were carried out using Fe/AC catalysts obtained by physical and chemical (acidic, neutral, basic) activation for catalytic wet air oxidation. For each catalyst, two different catalyst loadings (0.25 and 0.5 g/L) temperatures (60 and 80°C), and pressures (1 and 3 bar). The results for the effect of those different catalyst loadings, temperatures, and pressures for each catalyst are shown in Figure 6.18 to 6.21.

Increasing catalyst loading for physical Fe/AC catalyst decreased degradation at low pressure whereas increased degradation at high pressures. At low pressures, the decrease in degradation because of the increase in temperature was remarkable for both catalyst loadings. On the other hand at high pressure, temperature change did not have a great effect since the decrease in degradation was insignificant for low catalyst loadings and almost no change in degradation at all for high catalyst loadings. Additionally catalyst loading had positive effect

on degradation due to the increase in loading only at high pressures. The highest degradation achieved by this catalyst was around 30 % with low catalyst loading, temperature and pressure which were considered as not successful for catalytic wet air oxidation of BA (Figure 6.18).

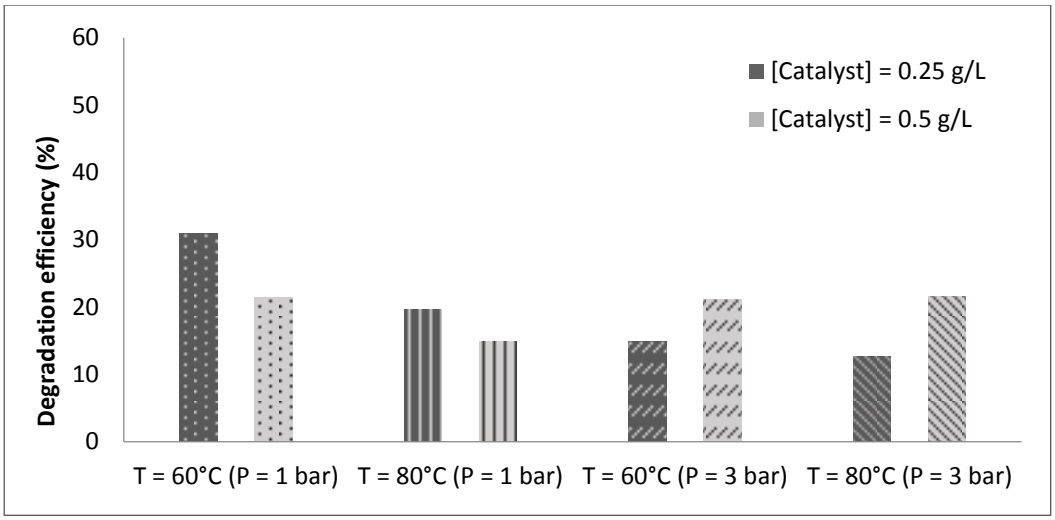

Figure 6.18 Degradation efficiencies obtained by physical Fe/AC for different temperature and pressure ([BA]=50ppm, [Catalyst]=0.25-0.5 g/L, pH=4, v_{air}=0.92 mL/min)

Increasing catalyst loading for acidic Fe/AC catalyst increased degradation for almost all conditions except in the experiment in which high temperature and high pressure were applied. This was because of the possible formation of reaction intermediates or byproducts. For the both catalyst loadings, the effect of temperature was insignificant because of degradation was almost constant or slightly decreased. Since there was no degradation efficiency exceeded 20 %, this catalyst was also considered as not successful (Figure 6.19).

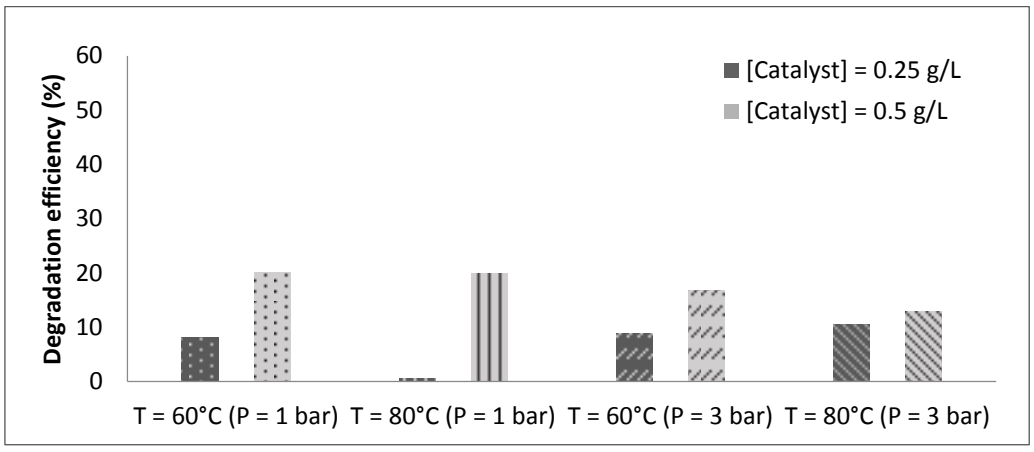

Figure 6.19 Degradation efficiencies obtained by acidic Fe/AC for different temperature and pressure ([BA]=50ppm, [Catalyst]=0.25-0.5 g/L, pH=4, v_{air}=0.92 mL/min)

For neutral Fe/AC, increasing temperature caused significant increase in degradation. This observation was valid for both catalyst loadings at high pressure. However at low pressure for catalyst loading was an exception as degradation efficiency slightly decreased from approximately 21 to 16 %. due to the increase in temperature. Increasing catalyst loading didn't have the expected effect on degradation efficiency, mostly. The final degradation efficiencies obtained by this catalyst can be considered as successful with degradation efficiencies around 30–40 % (Figure 6.20).

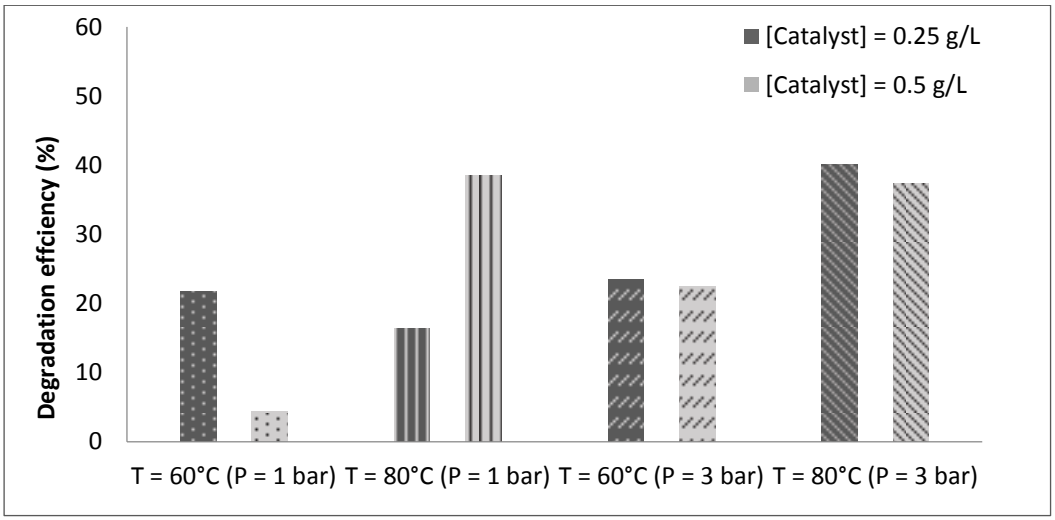

Figure 6.20 Degradation efficiencies obtained by neutral Fe/AC for different temperature and pressure ([BA]=50ppm, [Catalyst]=0.25-0.5g/L, pH=4, v_{air}=0.92 mL/min)

The increase in catalyst loading for basic Fe/AC catalyst affected degradation positively only when temperature and pressure were both high. In other experiments catalyst loading didn't affect degradation. Temperature was also insignificant since the degradation efficiencies mostly remained same due to the temperature changes. Increasing pressure slightly decreased degradation mostly because of the possible formation of byproducts. Generally, the degradation efficiencies were around 40–50 % which can also be considered as successful (Figure 6.21).

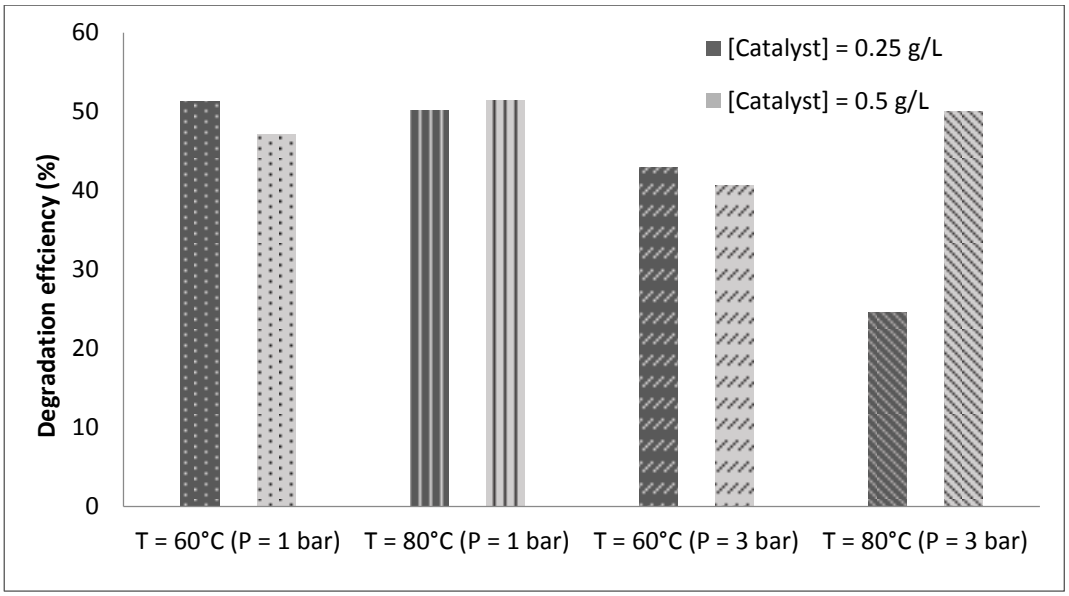

Figure 6.21 Degradation efficiencies obtained by basic Fe/AC for different temperature and pressure ([BA]=50ppm, [Catalyst]=0.25-0.5 g/L, pH=4, v_{air}=0.92 mL/min)

The results showed that since catalysts such as physical and acidic Fe/AC achieved very low degradation efficiencies, they were eliminated for parametric study in the first place. When neutral and basic Fe/AC catalysts were compared, basic Fe/AC was much more promising (40–50 %) and as a result it was selected for parametric study.

6.2.2.2 Parametric study

Catalytic wet air oxidation screening experiments showed that the highest degradation efficiency achieved by Fe/AC catalyst prepared by basic activation. Since up to 50 % degradation efficiency was observed, the parametric study to determine the optimum values of operation conditions was carried out with this catalyst. In this context, the effects of operational parameters such as catalyst loading, temperature, and pressure and air flowrate on degradation efficiency were investigated. Because of the implementation of CWAO system, there was no possibility to take samples during the experiment. Consequently, results of parametric study for CWAO experiments are given only for final degradation efficiencies without changes in degradation with respect to time.

Effect of catalyst loading:

The experiments investigating the effect of catalyst loading showed a significant increase in degradation efficiency due to the increase in catalyst loading. Very low degradation observed with no catalyst present and it was probably achieved by thermal decomposition of BA which is around only 4 %. Addition of catalyst with a loading of 0.25 g/L increased degradation efficiency up to 50 %. A slight decrease observed in degradation from 0.25 to 0.5 g/L. These experiments were repeated and same results were observed. Hence degradation was considered as almost constant for both catalyst loadings 0.25 and 0.5 g/L. Highest increase rate was observed where loading was increased from 0.5 to 1 g/L for 20 % increase in the degradation efficiency. However the effect of increase from 1 to 2 g/L on degradation efficiency can be considered as insignificant which was only 10 % even the catalyst loading was doubled. Hence the optimum catalyst loading was determined as [Catalyst]=1 g/L with a degradation efficiency of 70 % (Figure 6.22).

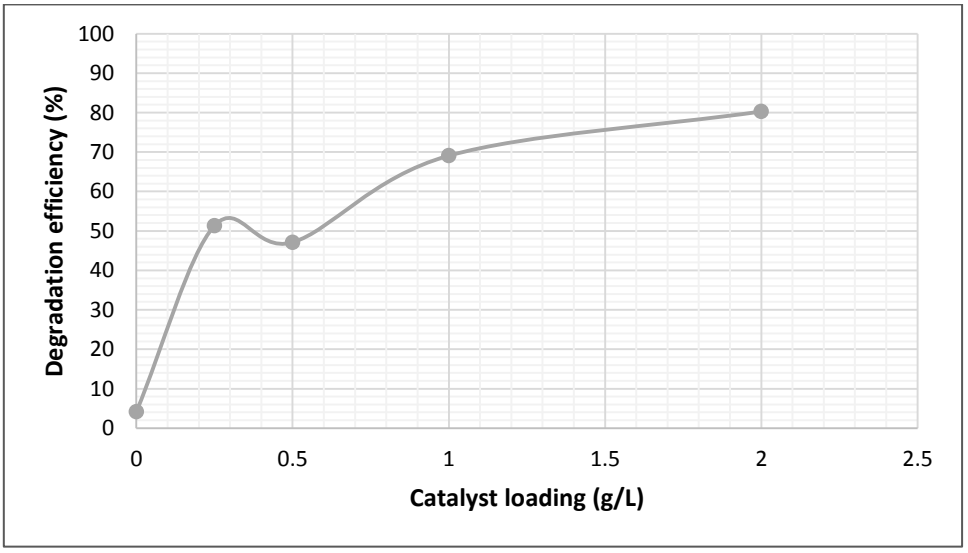

Figure 6.22 Effect of catalyst loading for basic Fe/AC ([BA]=50 ppm, P=1 bar, T=60°C,pH=4, v_{air}=0.92 ml/min)

Effect of temperature:

The experiments investigating the effect of temperature showed almost no change in degradation efficiency with respect to increase in temperature from 50

to 80°C. The only increase observed was from 50 to 60 % when temperature was increased from 40 to 50°C. The reason that there was no change in degradation beyond that temperature was compensation between increase in rate constant and decrease in dissolved O_2 in reaction medium. The decrease in degradation efficiency observed at 90°C could be due to the very low amounts of dissolved air which was so low for oxidizing BA or other reaction intermediates. Hence since there is no remarkable change in degradation, the optimum temperature was determined as 50°C with a degradation efficiency of 70 % (Figure 6.23).

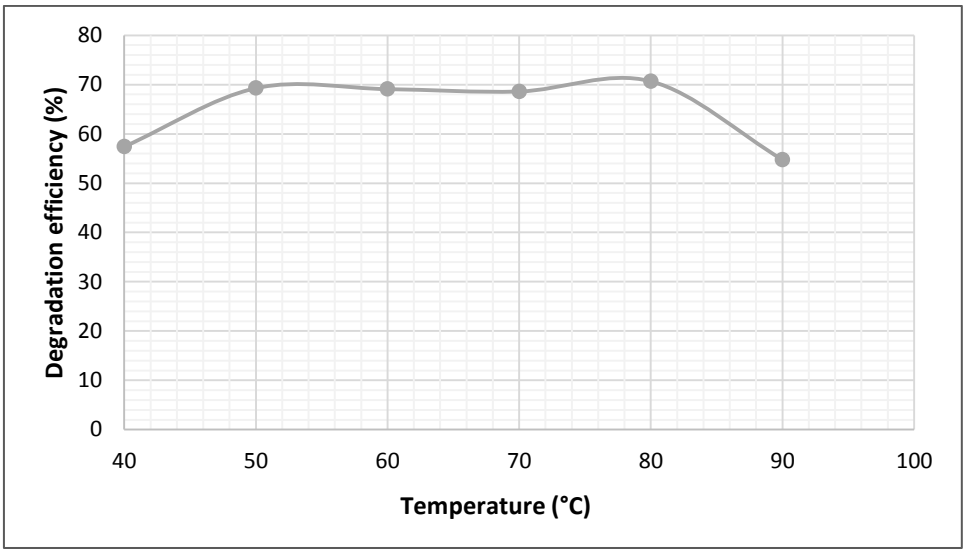

Figure 6.23 Effect of temperature for basic Fe/AC ([BA]=50 ppm, [Catalyst]=1 g/L, P=1 bar, pH=4, v_{air}=0.92 ml/min)

Effect of pressure:

The experiments investigating the effect of pressure showed a dramatic decrease in degradation efficiency due to the increase in pressure from 1 bar to 2 bars. This might be explained by formation of byproducts and reaction intermediates. Further increase from 2 to 3 bars did not affect degradation. Since there was no chance to take samples from reaction medium in certain time intervals, only final degradation efficiencies were measured at the end of 120 minutes. Therefore it wasn't possible to observe if there was any increase in degradation before 120 minutes and even increase in pressure would increase degradation rate due to the higher dissolved air in reaction medium, this couldn't

be observed. Hence the optimum pressure was determined as 1 bar with a degradation efficiency of 70 % (Figure 6.24).

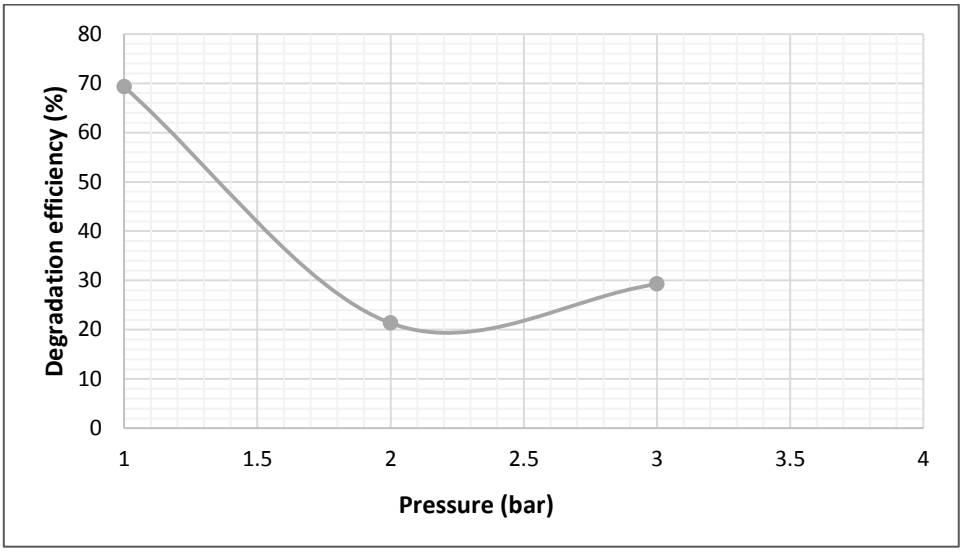

Figure 6.24 Effect of pressure for basic Fe/AC ([BA]=50 ppm, [Catalyst]=1 g/L, T=50^{o}C, pH=4, v_{air}=0.92 ml/min)

Effect of air flowrate:

The experiments investigating the effect of air flowrate showed that the degradation efficiency only increased from 60 to 70 % when air flowrate was increased to 0.61 to 0.92 ml/min. Then degradation was almost constant even the air flowrate was increased from 0.92 to 1.72 ml/min. Hence the optimum air flowrate was found as 0.92 ml/min with a degradation efficiency of 70 % (Figure 6.25).

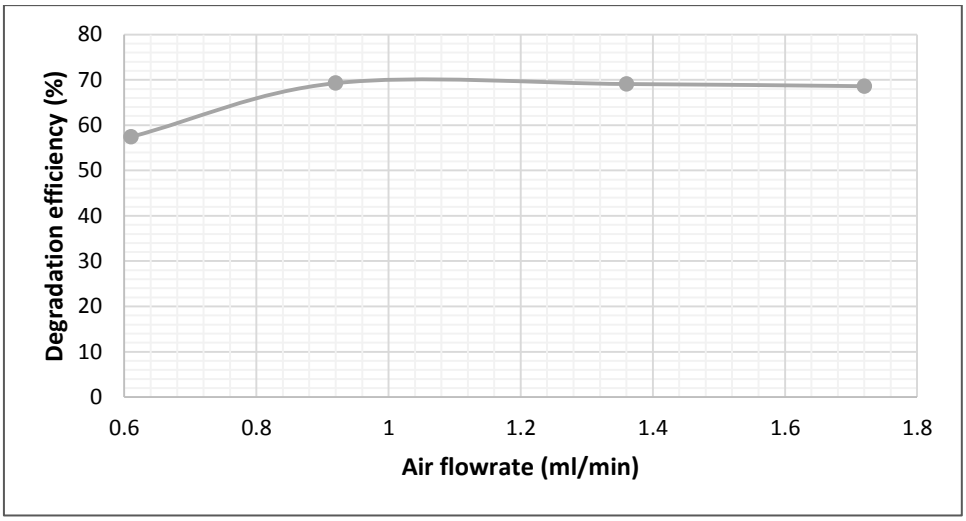

Figure 6.25 Effect of air flowrate for basic Fe/AC ([BA]=50 ppm, [Catalyst]=1 g/L, P=1 bar, T=50^{o}C, pH=4)

The optimum values of operating parameters for catalytic wet air oxidation of BA with an initial concentration of 50 mg/L were determined as 1 g/L for catalyst loading, 50°C for temperature, 1 bar for pressure, and 0.92 ml/min for air flow rate with a final degradation efficiency of approximately 70 %.

6.2.3 Photocatalytic and photo-Fenton-like oxidation

6.2.3.1 Catalyst screening

Experiments were carried out using Fe/AC and Fe-TiO_2/AC catalysts obtained by physical and chemical (acidic, neutral, basic) activation for both photocatalytic and photo-Fenton-like oxidation. For each catalyst, two different catalyst loadings (0.25 and 0.5 g/L) and UV intensities (6 and 8 watt) were studied. The results for the effect of those different catalyst loadings and UV intensities for each catalyst are shown in Figures 6.26 to 6.32.

For physical Fe/AC, degradation efficiencies achieved varied between 20 to 35 %. At low UV light intensity (6 watt), degradation efficiencies were around 30–35 % and catalyst loading wasn't effective. For high UV light intensity however, effect of catalyst loading was observed better. Since

degradation efficiencies obtained for this catalyst were quite low, it was considered as not appropriate for further parametric study (Figure 6.26).

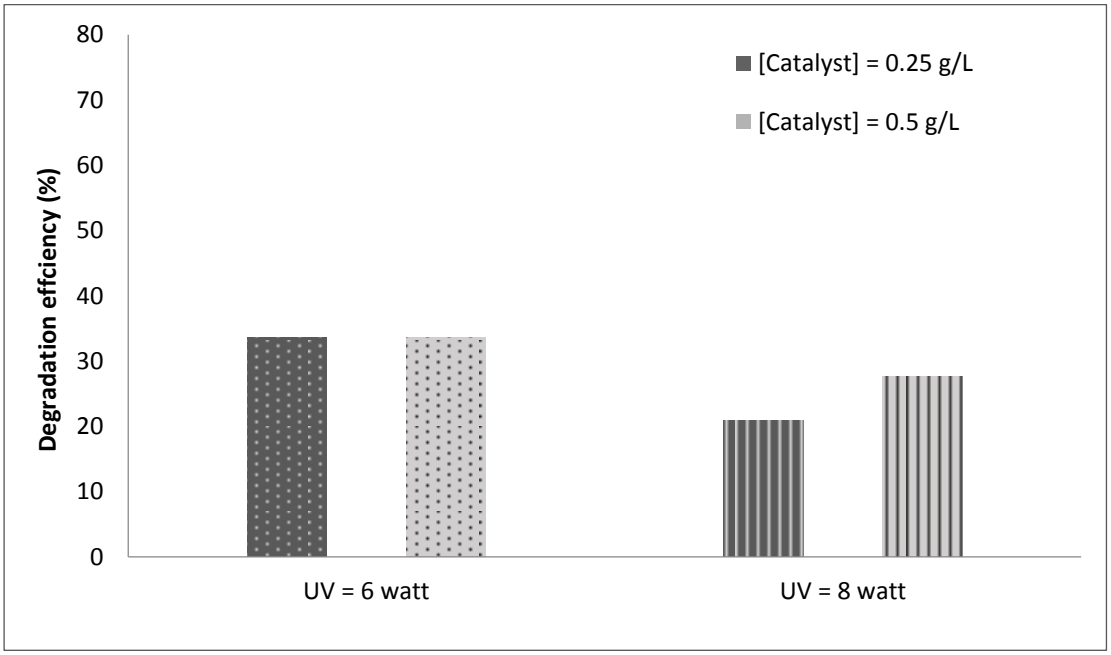

Figure 6.26 Degradation efficiencies obtained by physical Fe/AC ([BA]=50 ppm, T=25°C, pH=4)

The results obtained by acidic Fe/AC showed that increasing UV intensity increased degradation between 0–30 minutes which are not shown in Figure 6.31. But after 30 minutes although theoretical expectations suggest that higher UV intensity caused higher degradation, final degradation efficiency was lower. The reason of the decrease in degradation efficiency as 7 % for higher UV intensity was probably generation of byproducts during the reaction which made interferences in analysis. For high catalyst loading, increasing UV intensity caused higher degradation. For higher UV intensity, increase in catalyst loading had a positive effect on degradation which was also observed in a similar study (Pariente et al., 2008). However this positive effect could not be observed for low UV intensity which is due to the possible low penetration of UV light when catalyst loading was increased. This catalyst was also considered as not appropriate for further parametric study because of very low degradation efficiencies (Figure 6.27).

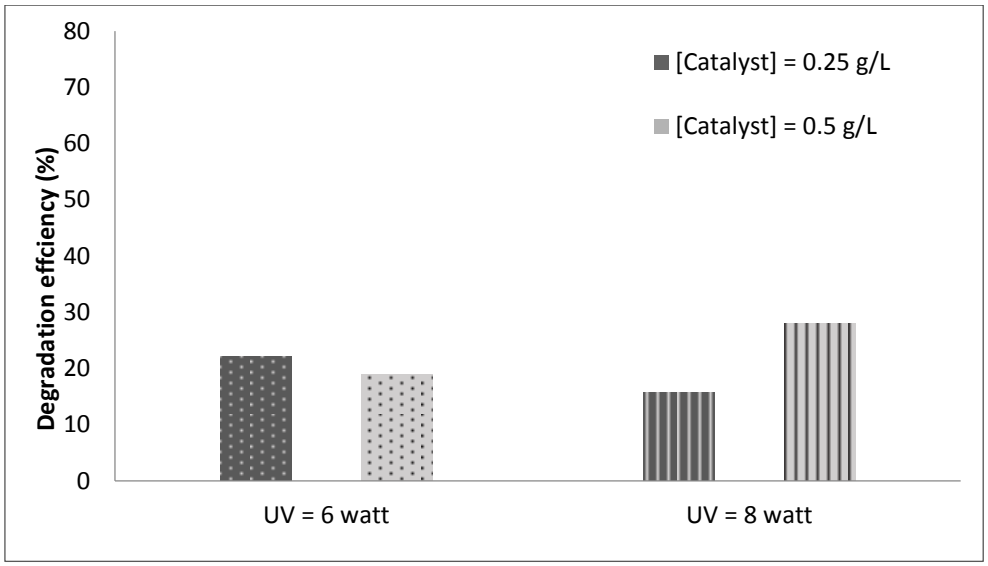

Figure 6.27 Degradation efficiencies obtained by acidic Fe/AC ([BA]=50 ppm, T=25°C, pH=4)

With neutral Fe/AC catalyst higher degradation efficiencies were observed especially at higher catalyst loadings. Very remarkable increase was observed due to the increase in catalyst loading. But for high catalyst loadings, no significant effect on degradation could be observed even increase in UV light intensity However, increasing UV intensity affected degradation more and positively at low catalyst loading than at high catalyst loading (Figure 6.28).

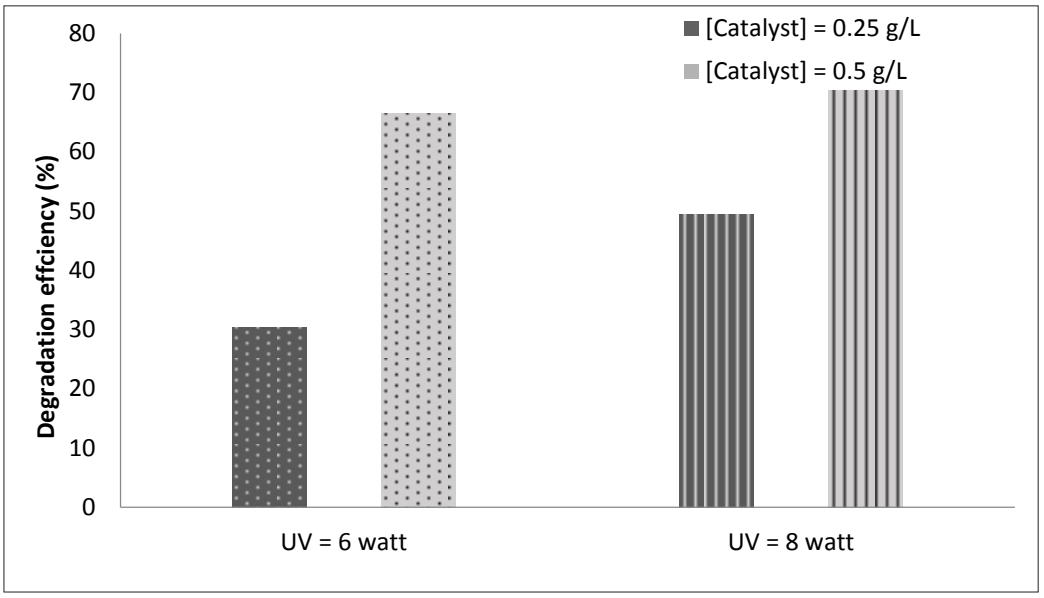

Figure 6.28 Degradation efficiencies obtained by neutral Fe/AC ([BA]=50 ppm, T=25°C, pH=4)

The final degradation efficiencies obtained by basic Fe/AC catalyst were almost same around 50–60 %. Increasing the UV intensity showed different behaviours for the two catalyst loading values. For low catalyst loading, there was an insignificant decrease in degradation by increasing UV intensity. However there was a remarkable increase at high catalyst loading and this was caused by very low UV light penetration when UV light intensity was 6 watt and catalyst concentration was high in reaction medium. Increasing UV light intensity from 6 watt to 8 watt eliminated this situation by increasing penetration (Figure 6.29).

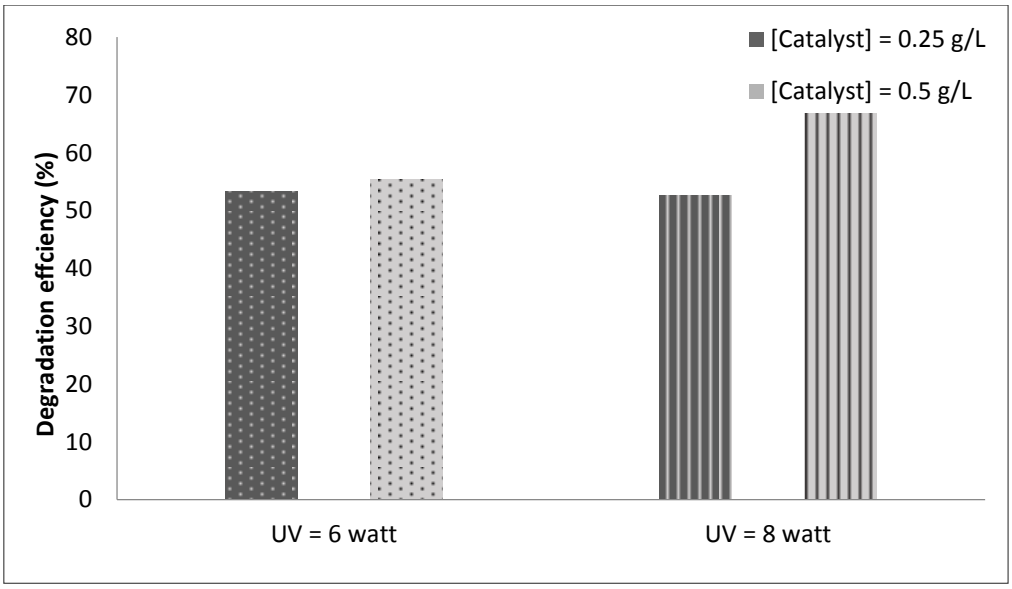

Figure 6.29 Degradation efficiencies obtained by basic Fe/AC ([BA]=50 ppm, T=25°C, pH=4

Further catalyst screening experiments were performed to investigate effect of TiO_2 doping to the catalyst on degradation efficiency.

For physical Fe-TiO_2/AC catalyst, the degradation efficiencies were around 40–50 % except for high catalyst loading at low UV light intensity experiment. There was a sharp decrease caused by increasing catalyst loading at low UV light intensity from 40 to 15 %. Up to 20 % increase was observed for high UV light intensity because of increase in catalyst loading. Degradation efficiencies obtained with this catalyst was quite low so it wasn't used in parametric study (Figure 6.30).

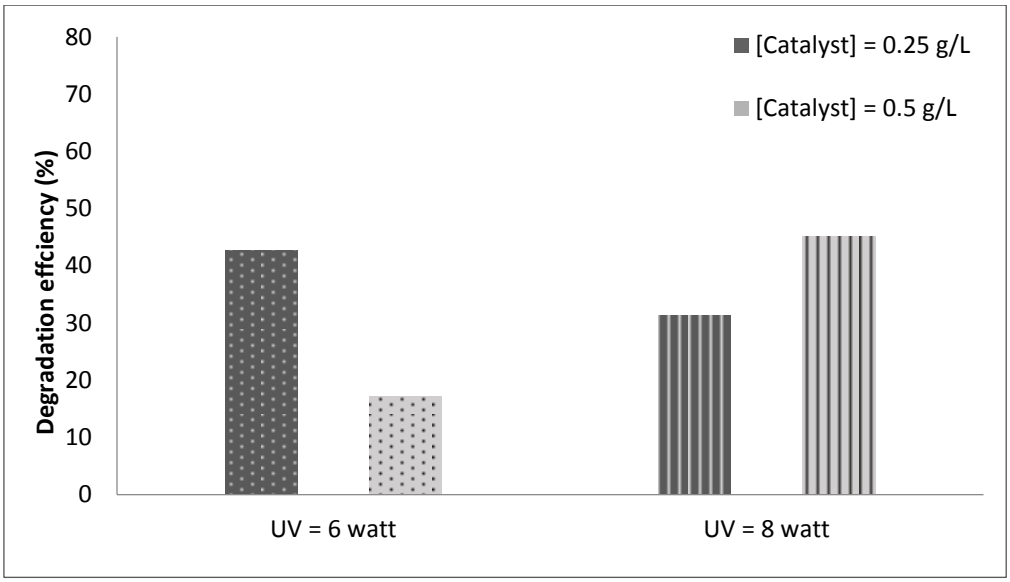

Figure 6.30 Degradation efficiencies obtained by physical Fe-TiO_2/AC ([BA]=50 ppm, T=25°C, pH=4)

For acidic Fe-TiO_2/AC catalyst, final degradation efficiencies were around 40 % for all experiments. Both increasing catalyst loading and/or UV light intensity had no significant effect on degradation since the increases were very slight due to the increase in catalyst loading and/or UV light intensity (Figure 6.31).

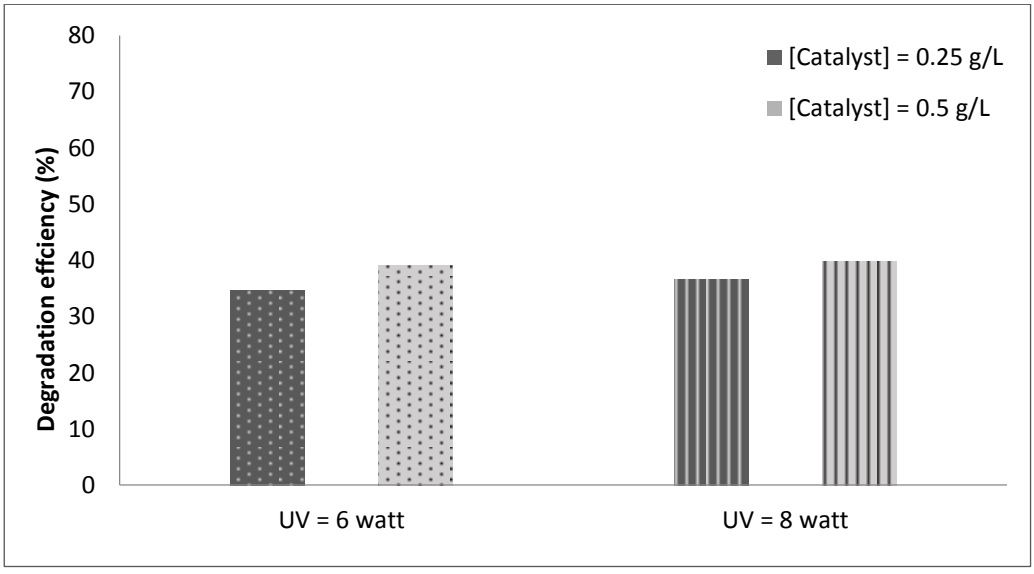

Figure 6.31 Degradation efficiencies obtained by acidic Fe-TiO_2/AC ([BA]=50 ppm, T=25°C, pH=4)

Neutral Fe-TiO_2/AC catalyst was the most promising catalyst among other because the final degradation efficiencies were the highest (60–70 %) and almost constant after 60 minutes. Also increases in catalyst loading or UV light intensity caused increase in degradation and this proves that minimum by-product formation was accomplished with this catalyst. Furthermore low penetration of UV light was not observed for this catalyst (Figure 6.32).

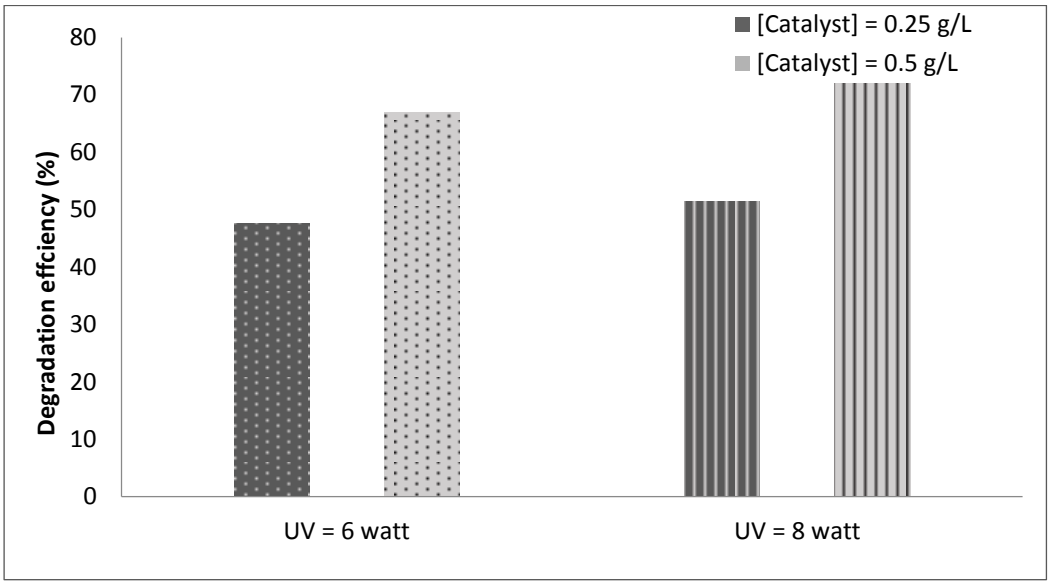

Figure 6.32 Degradation efficiencies obtained by neutral Fe-TiO_2/AC ([BA]=50 ppm, T=25°C, pH=4)

Final degradation efficiencies for neutral Fe-TiO_2/AC catalyst were higher than others. Neutral Fe/AC and basic Fe/AC catalyst also achieved almost same degradation efficiencies but there were more oscillations during the experiment and less stable degradation efficiencies with slower degradation rates were observed. For neutral Fe-TiO_2/AC catalyst however, the effects of operating conditions were much more consistent with the theory and degradation was much faster and more stable. Hence neutral Fe-TiO_2/AC catalyst was selected for parametric study for photocatalytic and photo-Fenton-like oxidation of benzoic acid.

6.2.3.2 Parametric study for photocatalytic oxidation

Photocatalytic oxidation screening experiments showed that the highest degradation efficiency (up to 70%) achieved by Fe-TiO_2/AC catalyst prepared by neutral activation. Hence the parametric study for this method to was performed in the presence of neutral Fe-TiO_2/AC. In this context, the effects of operational parameters such as catalyst loading ([Catalyst]), UV light intensity and initial pH on degradation efficiency were investigated.

Effect of catalyst loading:

The experiments investigating the effect of catalyst loading showed very significant increase in degradation. Around 20 % degradation efficiency was achieved when no catalyst was present in reaction medium but with catalyst addition at 0.25 g/L loading, degradation efficiency increased from 20 to 40 %. Degradation efficiency kept on increasing until the loading was 1 g/L. However when the catalyst loading was doubled from 0.5 to 1 g/L, the increase in degradation efficiency was only 15 %. Additionally the degradation rate was almost same for first 20 minutes and remained almost constant after 60 minutes for both catalyst loadings 0.5 and 1 g/L. Moreover at catalyst loading 1 g/L, the degradation was unstable with oscillations for first 40 minutes, especially between 20–40 minutes. Further increase in loading from 1 to 2 g/L caused faster degradation without oscillations but final degradation efficiencies achieved were approximately same. The insignificant degradation rate despite increasing the catalyst amount was due to the decrease in penetration of UV light because of turbidity of reaction solution (Chen et al., 2009, Rusevova et al., 2012). By considering degradation rate, stable degradation and final degradation efficiency, the optimum catalyst loading was determined as [Catalyst] =0.5 g/L with a degradation efficiency of 70 % (Figure 6.33).

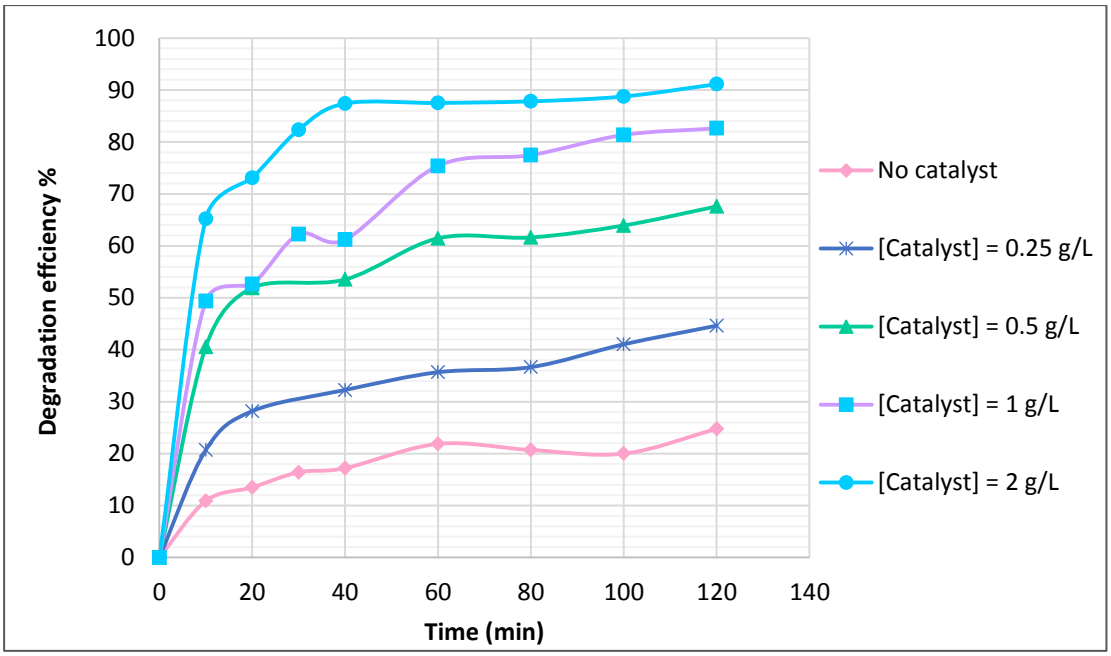

Figure 6.33 Effect of catalyst loading for neutral Fe-TiO_2/AC ([BA]=50 ppm, UV light intensity=6 watt, T=25°C, pH=4)

Effect of UV light intensity:

The experiments investigating the effect of UV light intensity revealed presence of UV light increased degradation insignificantly. However an increase in the intensity of UV light had a significant increase in degradation. But for first 80 minutes, degradation achieved with UV light intensity=6 watt was higher than UV light intensity=8 watt. After 80 minutes, degradation with UV light intensity=8 watt increases and reached higher than UV light intensity=6 watt. Since the increase was in last 40 minutes, it was thought that it would be much higher if further samples were taken after 120 minutes. Additionally when UV light intensity was 8 watt, energy consumption would be not so high since the difference between intensities of UV lights was low (6 to 8 watt). Hence the optimum UV light intensity was determined as UV light intensity=8 watt with a degradation efficiency of 70 % (Figure 6.34).

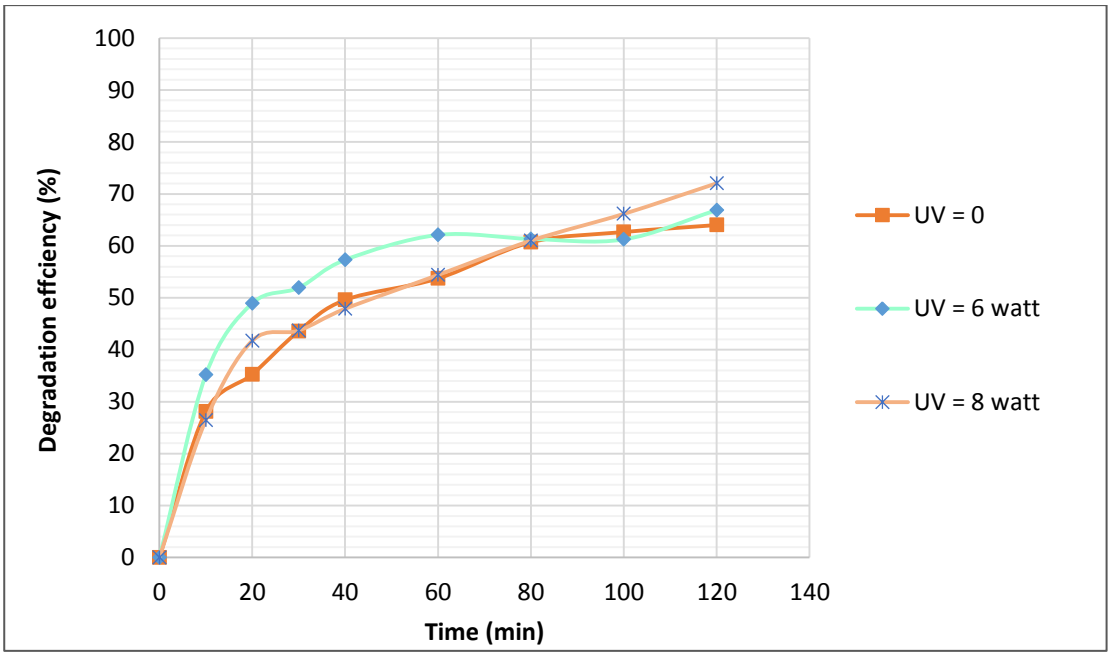

Figure 6.34 Effect of UV light intensity for neutral Fe-TiO_2/AC ([BA]=50 ppm, [Catalyst]=0.5 g/L, T=25°C, pH=4)

Effect of initial pH:

The experiments showed that highest degradation for the effect of pH was observed for pH=4 which is the natural pH of aqueous benzoic acid solution. Low degradation efficiencies were observed for pH=3 which remained constant around 20–30 % between 20 minutes and a small increase to 40 % was observed in last 20 minutes. This was caused by pH decrease below 3 during oxidation due to the formation of acidic intermediates. Previous studies concluded that when pH is below 3, the reduction in photocatalytic activity of Fe^{3+} doped TiO_2 occurs because of the acidic intermediates which highly inhibit the photocatalytic activity and this was also observed in the study (Ramirez et al., 2010). An increase in pH from 4 to 6 also caused a decrease in degradation and this might be explained by same reason that initial pH of the solution was 4. When the initial pH was 6, it decreased to almost 4–5 due to the formation of acidic intermediates during the reaction which also affected photocatalytic activity negatively. Because pH above 3 causes the activity loss of Fe^{3+} ions due to the formation of $Fe(OH)_3$ in neutral or basic reaction medium as mentioned in Fenton-like oxidation section (Chen et al., 2009, Ramirez et al., 2010). Hence the optimum initial pH was determined as pH=4 which provides reaction

medium pH=3 during reaction with a degradation efficiency of 70 %. However optimum pH can also be selected as pH=6 by considering corrosion which achieved almost same degradation efficiencies with pH=4 (Figure 6.35).

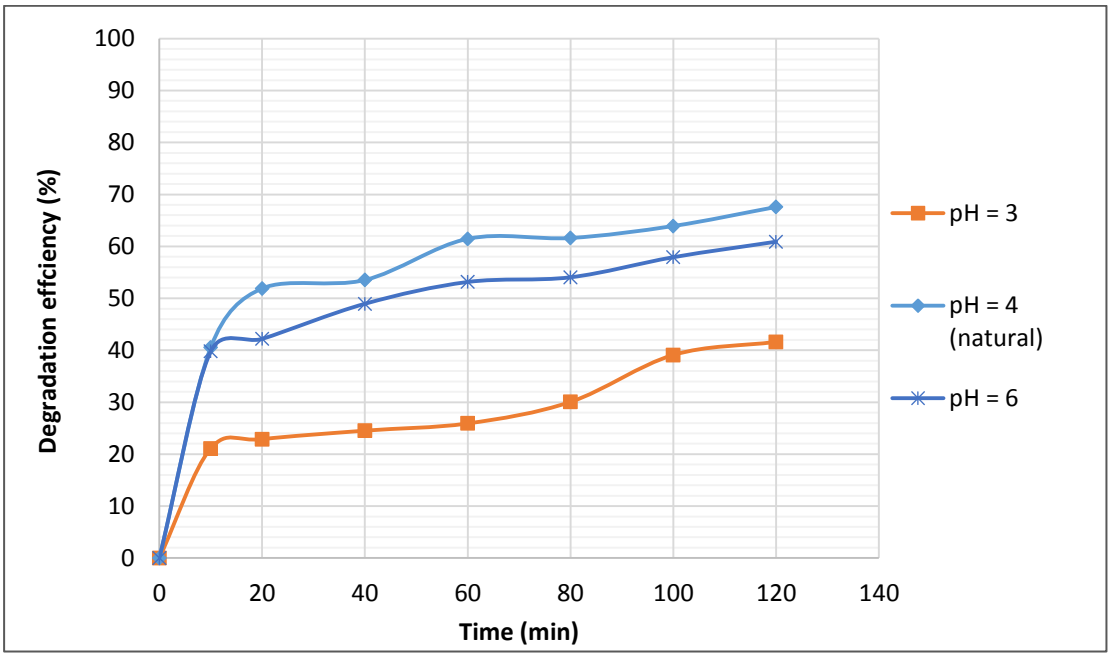

Figure 6.35 Effect of initial pH for neutral Fe-TiO_2/AC ([BA]=50 ppm, [Catalyst]=0.5 g/L, UV light intensity =8 watt, T=25°C)

The optimum values of operating parameters for photocatalytic oxidation of BA with an initial concentration of 50 mg/L were determined as 0.5 g/L for catalyst loading, 8 watt for UV light intensity, and 4 or 6 for initial pH with a final degradation efficiency of approximately 70 % in 60 minutes.

6.2.3.3 Parametric study for photo-Fenton oxidation

The parametric study for photo-Fenton like oxidation was performed by using the same catalyst (neutral Fe-TiO_2/AC) determined from photocatalytic oxidation catalyst screening experiments. Hence the optimum values of operational parameters such as catalyst loading ([Catalyst]) and UV light intensity determined previously for photocatalytic oxidation were applied for this method. Additionally, effect of H_2O_2 concentration and initial pH were investigated.

Effect of H_2O_2 concentration:

When there was no H_2O_2 present in reaction medium, around 70 % degradation efficiency was observed which can be considered as high. However addition of H_2O_2 increased the efficiencies from 70 to 90–95 % with higher degradation rates compared to the absence of H_2O_2 which caused much slower and relatively lower degradation. This was accomplished by increasing generation of •OH radicals which increases its oxidizing potential among many oxidants and proves that H_2O_2 assisted UV light and the catalyst in terms of both degradation rate and degradation efficiency (Anotai et al., 2010, Chen et al., 2009, Duarte et al., 2011). Unfortunately, the increase in concentration of H_2O_2 did not show a great increase in degradation due to the formation of hydroxyperoxyl radicals (HO_2•) because of local excees H_2O_2 which was also observed for Fenton-like oxidation of BA. Therefore it has been concluded that low concentrations of hydrogen peroxide were sufficient enough to achieve high degradation efficiencies. By considering degradation rate and final degradation efficiencies, the optimum hydrogen peroxide concentration could be determined as 1 or 2 mM. But the degradation wasn't stable for 1 mM and many oscillations were observed. Hence rest of the parametric study was performed with [H_2O_2]=2 mM with a degradation efficiency around 90 % (Figure 6.36).

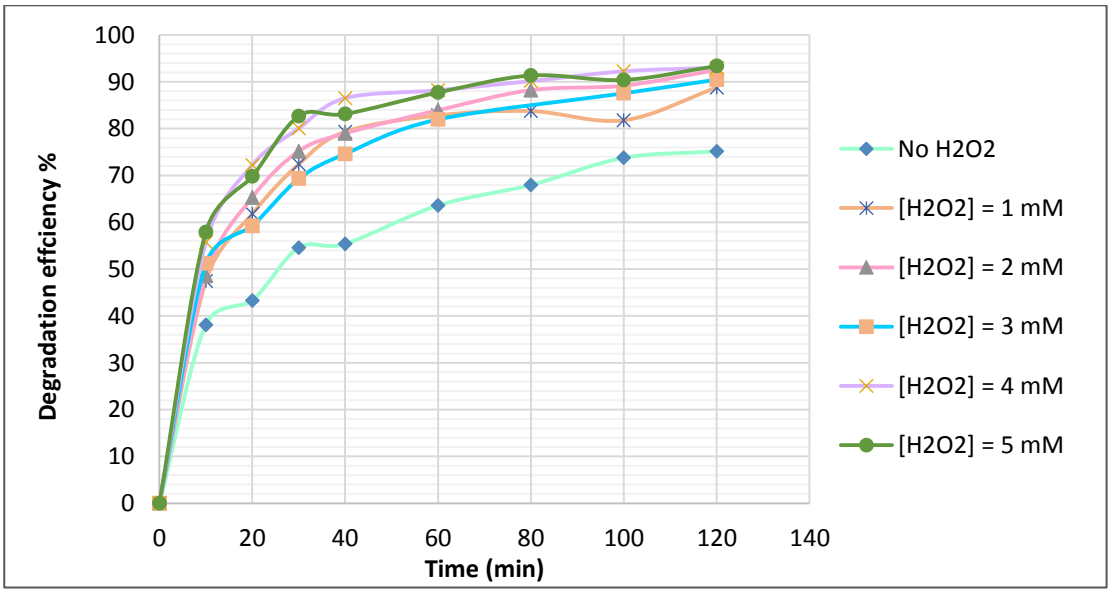

Figure 6.36 Effect of H_2O_2 concentration for neutral Fe-TiO_2/AC ([BA]=50 ppm, [Catalyst]=0.5 g/L, UV light intensity =8 watt, T=25°C, pH=4)

Effect of initial pH:

The experiments for the effect of pH for photo-Fenton oxidation showed that pH did not have very remarkable effect on degradation unlike photocatalytic oxidation. Even the degradation rate was faster when pH=3, the final degradation efficiencies were almost same around 90 %. This may be explained by the presence of hydrogen peroxide which was enough to compensate the reduction in photocatalytic activity of Fe-doped TiO_2 due to the changes in pH of reaction medium. The reason for faster degradation at pH=3 can be explained by a UV promoted basic Fenton reaction. It dominated the degradation where Fe^{3+} ions as the main catalyst and hydrogen peroxide as the strong oxidant. In this case, undesirable decomposition of H_2O_2 was the least and catalytic activity of Fe^{3+} ions was the highest when pH=3 (Chen et al., 2009, Ramirez et al., 2010). But in general the degradation rates were so close for all pHs and final degradation efficiencies were almost same around 95 %. By considering that, the optimum pH was determined as pH=4 with a degradation efficiency of 95 % which does not require additional pH adjustment using extra chemicals. If corrosion was considered as very essential for the process, optimum pH can also be taken as 6 with almost same degradation efficiencies with slightly lower degradation rates (Figure 6.37).

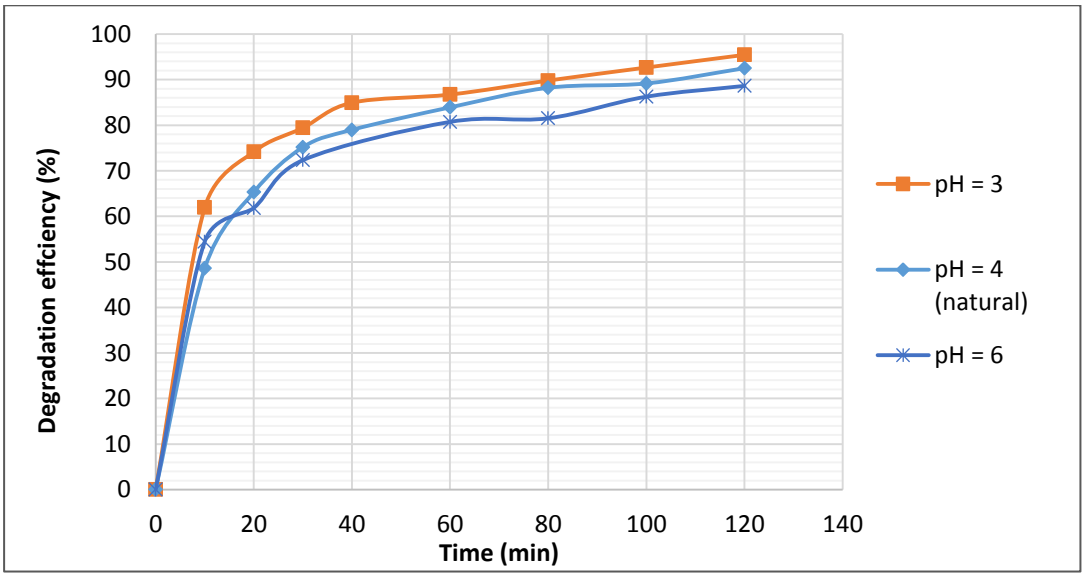

Figure 6.37 Effect of initial pH for neutral Fe-TiO_2/AC ([BA]=50 ppm, [Catalyst] = 0.5 g/L, UV light intensity =8 watt, [H_2O_2]= 2 mM, T=25°C)

The optimum values of operating parameters for photo-Fenton-like oxidation of BA with an initial concentration 50 mg/L were determined as 1 or 2 mM for hydrogen peroxide concentration, and 3 or 6 for initial pH with a final degradation efficiency of approximately 95 % in 80 minutes.

6.2.4 Biological oxidation

6.2.4.1 Catalyst screening

Experiments were carried out for two different microorganisms (*P. chyrsosporium* and *T.versicolor*) in the presence of biocatalyst only, biocatalyst and glucose, biocatalyst and hydrogen peroxide and in the presence of biocatalyst, glucose and hydrogen peroxide.

Biological oxidation screening experiments showed that for using free whole cells, *P.chrysosporium* was more successful than *T.versicolor*. Because the degradation achieved for *T.versicolor* was only around 50 % where *P.chrysosporium* achieved around 75 %. So further catalyst screening experiments were performed in the presence of immobilized *P.chrysosporium* on walnut shells referred as Biocatalyst-PC. The highest degradation efficiencies for different conditions are shown in Figure 6.38.

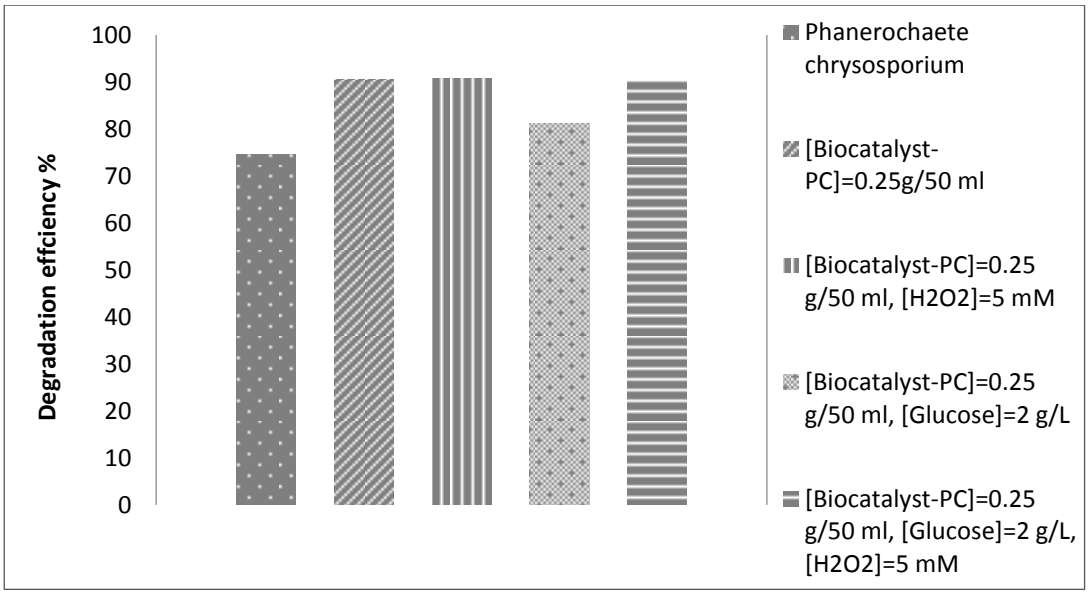

Figure 6.38 Degradation efficiencies obtained by different conditions ([BA]=50 ppm, T=25°C)

For parametric study using this biocatalyst, the effects of operational parameters such as biocatalyst loading ([Biocatalyst]) and glucose concentration ([Glucose]) on degradation efficiency were investigated. Since there was no considerable effect of H_2O_2 concentration on degradation, this parameter wasn't investigated in parametric study.

6.2.4.2 Parametric study

The parametric study for biological oxidation of BA was performed by investigating biocatalyst loading and glucose concentration.

Effect of biocatalyst loading:

The experiments investigating the effect of biocatalyst loading showed that there was no significant effect of biocatalyst loading since there was no remarkable change in degradation efficiency (≈90 %). This was probably sufficient amounts of enzymes to catalyze degradation reaction could be provided for even at the lowest biocatalyst loading. However degradation rate was doubled when biocatalyst loading was increased from 0.125 g/50 ml to 0.25 g/50ml since degradation efficiencies increased from 35 to 70 % for first day. Additionally the degradation efficiencies were around 30 % for 0.125 g/50 ml and same around 65 % for both 0.25 g/50 ml and 0.5 g/50 ml in at the end of first day. After 4 days sharp decrease in final degradation efficiencies for all biocatalyst loadings were observed because of the beginning of death phase for microorganisms. By considering beginning of death phase, degradation rate for first day and final degradation efficiencies, optimum biocatalyst loading was determined as 0.25 g/50 ml since degradation rate is very essential for biological processes for industrial applications that conventional biological processes applied recently in many industries are known to be very slow (Figure 6.39).

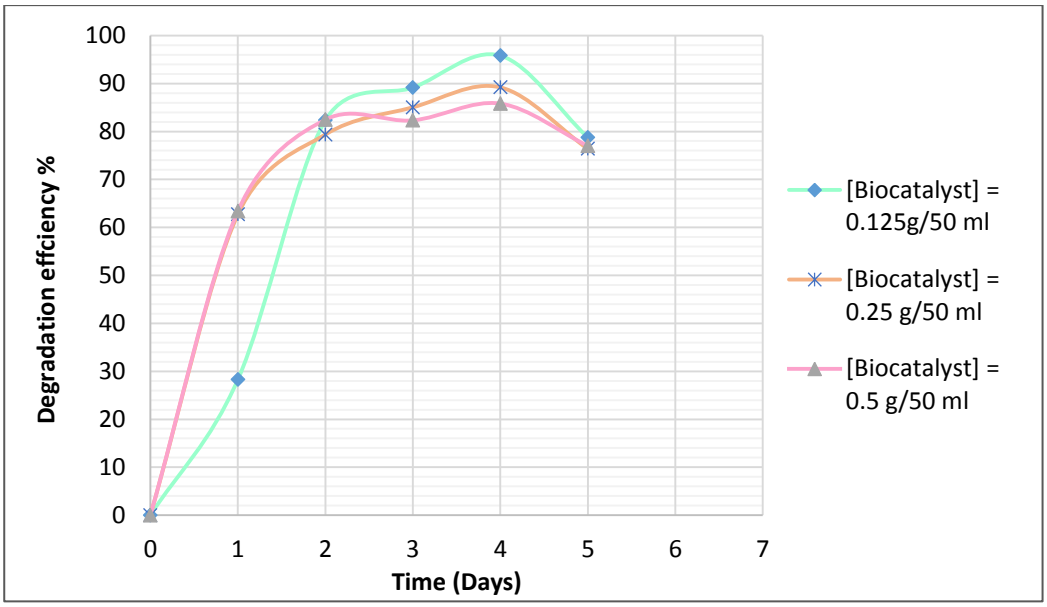

Figure 6.39 Effect of biocatalyst loading for ([BA]=50 ppm, T=25°C)

Effect of glucose concentration:

The experiments investigating the effect of glucose concentration showed that final degradation efficiencies decreased slightly from 90 to 65 %with increase in glucose concentration from 0.25 to 1.5 g/L. The beginning of the death phase were in 4 days for all experiments consistent with biocatalyst loading experiments and the decrease observed because of that was sharper for higher glucose concentrations. Moreover absence of glucose in reaction medium lead the highest degradation. The reason for that was the severe glucose inhibition which is commonly observed in biological studies (Masumoto et al., 2003). In this case, the reason of the inhibition was acidic glucose end products which decrease pH of intracellular reaction medium and reduce enzymatic activity (Chen et al., 2003). The inhibition was highest for the highest glucose concentration which is consistent with the inhibition theory. Hence it was concluded that absence of glucose is necessary to avoid inhibition and achieve high degradation efficiencies (Figure 6.40).

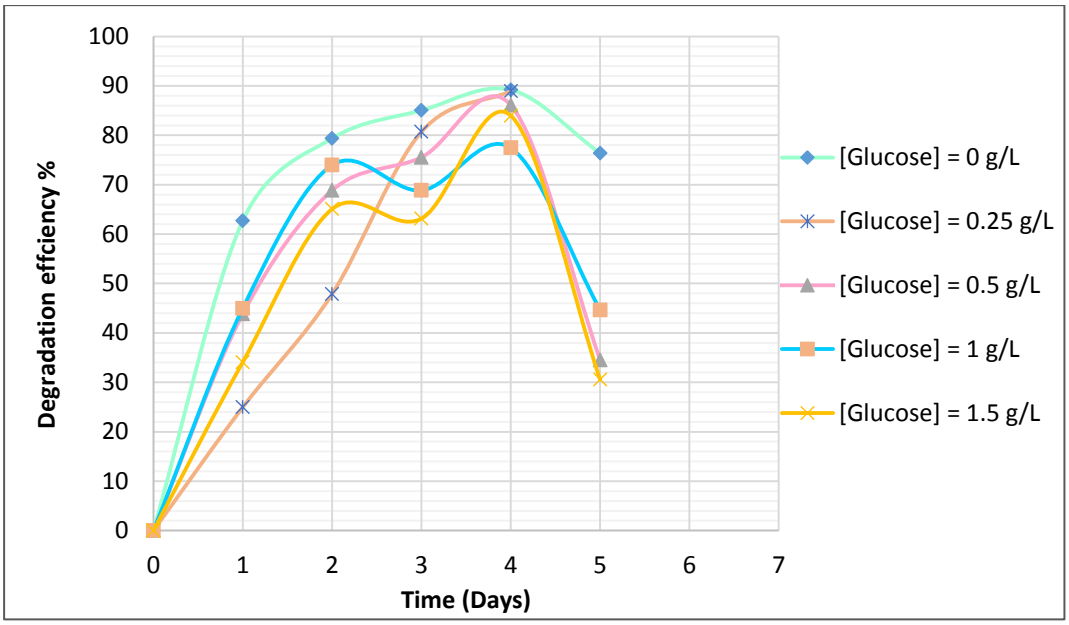

Figure 6.40 Effect of glucose concentration ([BA]=50 ppm, [Biocatalyst]=0.25 g/50 ml, T=25°C)

The optimum values of operating parameters for biological oxidation of BA with an initial concentration of 50 mg/L were determined as 0.25 g/50 mL for biocatalyst loading, and absence of glucose with a final degradation efficiency of approximately 90 % in 4 days.

6.3 Terephthalic Acid Degradation

6.3.1 Fenton-like oxidation

Catalyst screening experiments were carried out using Fe/AC catalysts obtained by physical and chemical (acidic, neutral, basic) activation for Fenton-like oxidation. For each Fe/AC catalyst, two different catalyst loadings (0.1 and 0.2 g/L) and hydrogen peroxide (H_2O_2) concentrations (3 and 4 mM) were studied.

Unfortunately, almost no degradation was observed with all catalysts. Hence further parametric study was not performed for Fenton-like oxidation.

6.3.2 Photocatalytic and photo-Fenton-like oxidation

6.3.2.1 Catalyst screening

Experiments were carried out using Fe/AC and Fe-TiO_2/AC catalysts obtained by physical and chemical (acidic, neutral, basic) activation for photocatalytic oxidation. For each catalyst, two different catalyst loadings (0.25 and 0.5 g/L) and UV intensities (6 and 8 watt) were studied. The results for the effect of those different catalyst loadings and UV intensities for each catalyst are shown in Figure 6.41 to 6.47.

The results obtained for physical Fe/AC catalyst showed that degradation efficiencies were around 80–90 %. Effects of both increasing catalyst loading and UV light intensity on degradation were very insignificant. Despite high degradation efficiencies in general, the degradation wasn't stable and many osciallations were observed with rather slower degradation rates. Additionally no parametric effect could have been observed, so this catalyst was considered as not appropriate for further parametric study (Figure 6.41).

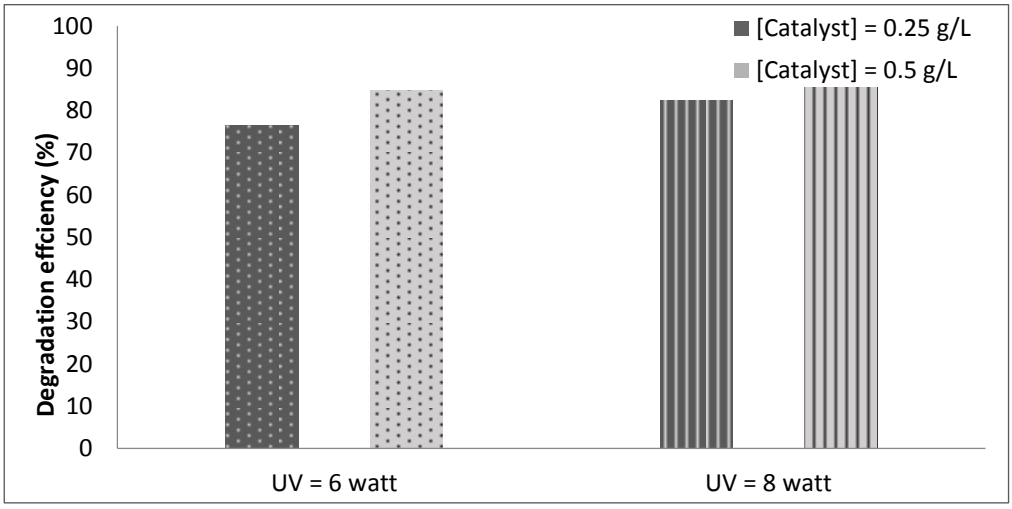

Figure 6.41 Degradation efficiencies obtained by physical Fe/AC ([TPA]=50 ppm, T=25°C, pH=4)

Results obtained with acidic Fe/AC catalyst showed that degradation efficiencies were around 50 % for low UV light intensity and 80 % for high catalyst loading. Effect of UV light intensity was observed for both catalyst

loadings very significantly. However positive effect of catalyst loading wasn't observed, increasing catalyst loading slightly decreased degradation for both UV light intensities (Figure 6.42).

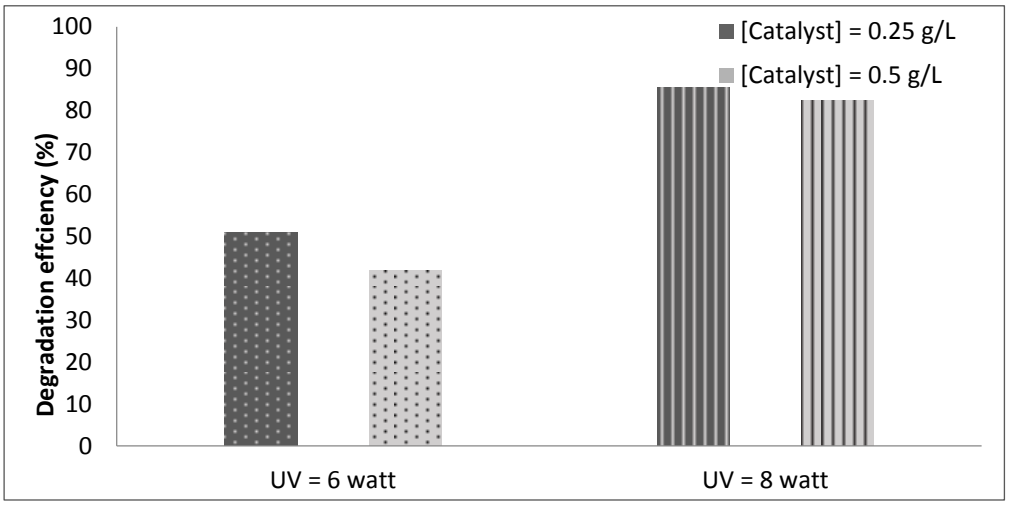

Figure 6.42 Degradation efficiencies obtained by acidic Fe/AC ([TPA]=50 ppm, T=25°C, pH=4)

Results obtained by neutral Fe/AC catalyst revealed that almost same degradation efficiencies were obtained around 70 % except for low catalyst loading and high UV light intensity. Increasing catalyst loading was not effective when UV light intensity was low. When the UV light intensity was low, the two parameters (UV light intensity and catalyst loading) were in good competition, whereas at high UV light intensity due to the possible low penetration of UV light, this competition could not be investigated (Figure 6.43).

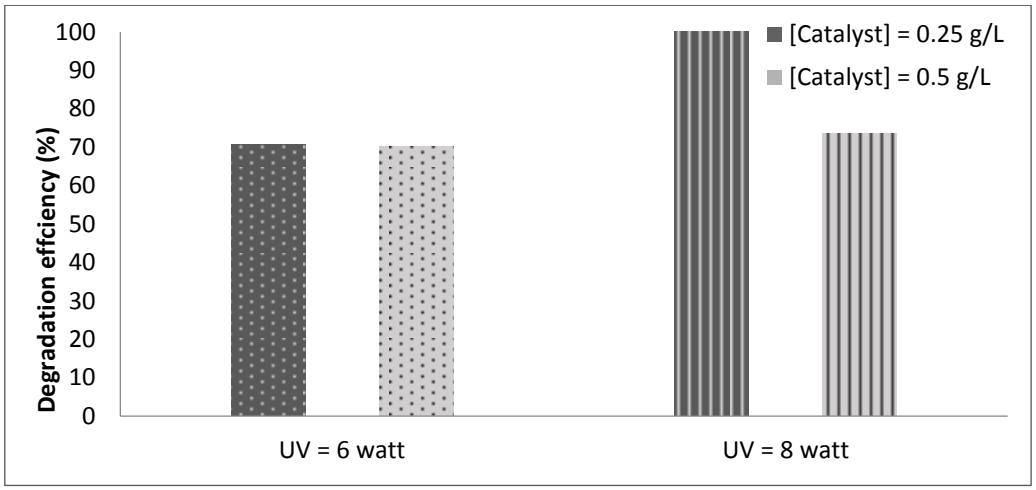

Figure 6.43 Degradation efficiencies obtained by neutral Fe/AC ([TPA]=50 ppm, T=25°C, pH=4)

The results obtained for basic Fe/AC showed that degradation efficiencies varied from 50 to 70 % depending on experimental conditions. For low UV light intensity, a decrease in degradation was observed due to the increase in catalyst loading as a consequence of possible formation of intermediates by preventing complete mineralization. But for high UV light intensity, considerable increase in degradation was observed by increasing catalyst loading which means byproducts weren't formed (Figure 6.44).

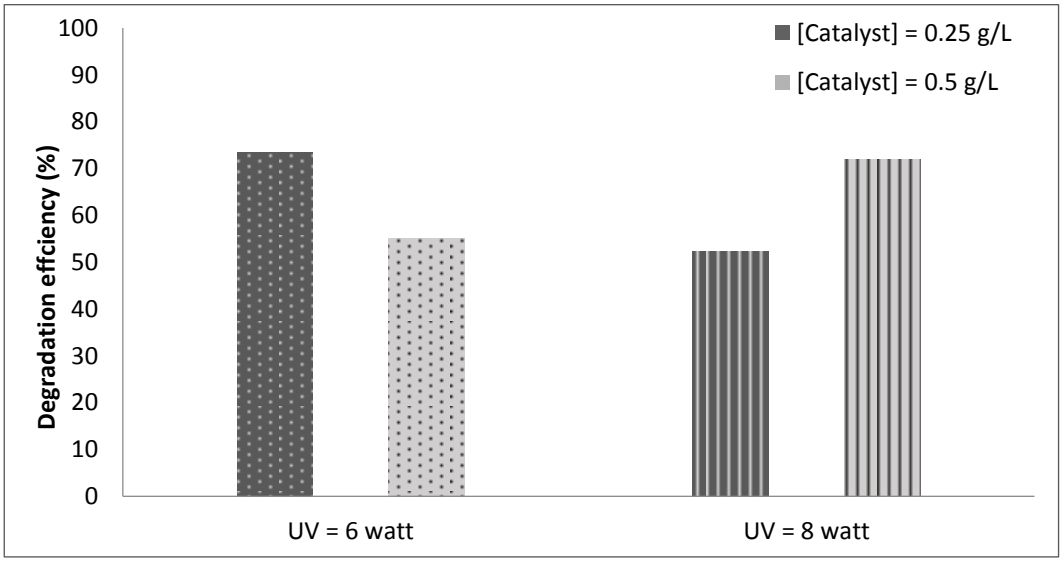

Figure 6.44 Degradation efficiencies obtained by basic Fe/AC ([TPA]=50 ppm, T=25°C, pH=4

Further catalyst screening experiments were performed to investigate effect of TiO_2 doping to the catalyst on degradation efficiency.

Degradation efficiencies for physical Fe-TiO_2/AC catalyst were around 80–90 %. Even high degradation efficiencies were achieved; both catalyst loading and UV light intensity didn't have any significant effect on degradation. Hence, no parametric effect was observed. So it was concluded that this catalyst wasn't appropriate for further parametric study (Figure 6.45).

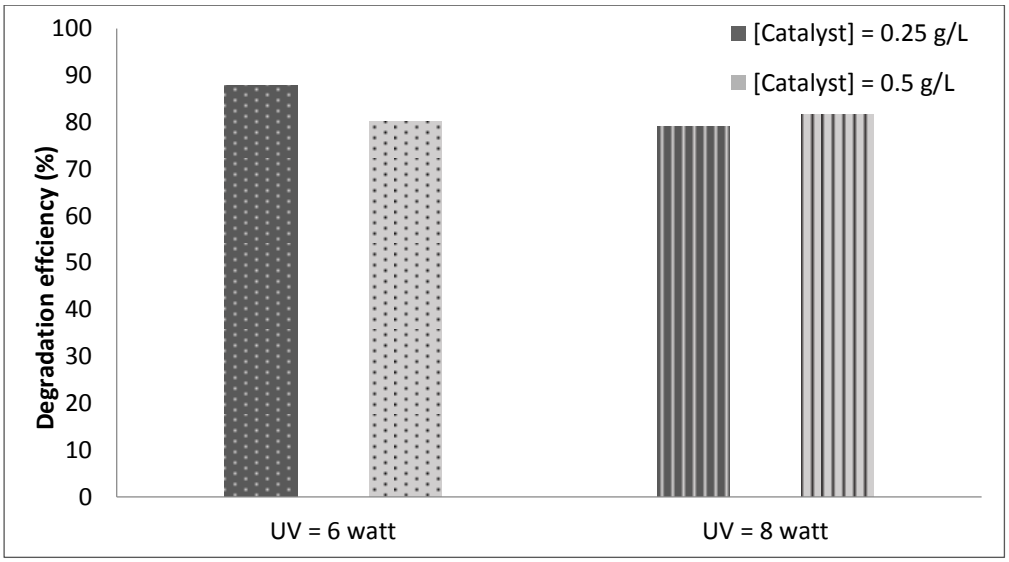

Figure 6.45 Degradation efficiencies obtained by physical Fe-TiO_2/AC ([TPA]=50 ppm, T=25°C, pH=4)

For acidic Fe-TiO_2 catalyst, degradation efficiencies obtained was around 60–90 %. UV light intensity was only effective for low catalyst loading. Moreover catalyst loading was also significantly effective for low UV light intensity. This was because of high UV light intensity concealed the effect of catalyst loading. Either high catalyst loading and low UV intensity or low catalyst loading and high UV light intensity was enough for high degradation efficiencies (Figure 6.46).

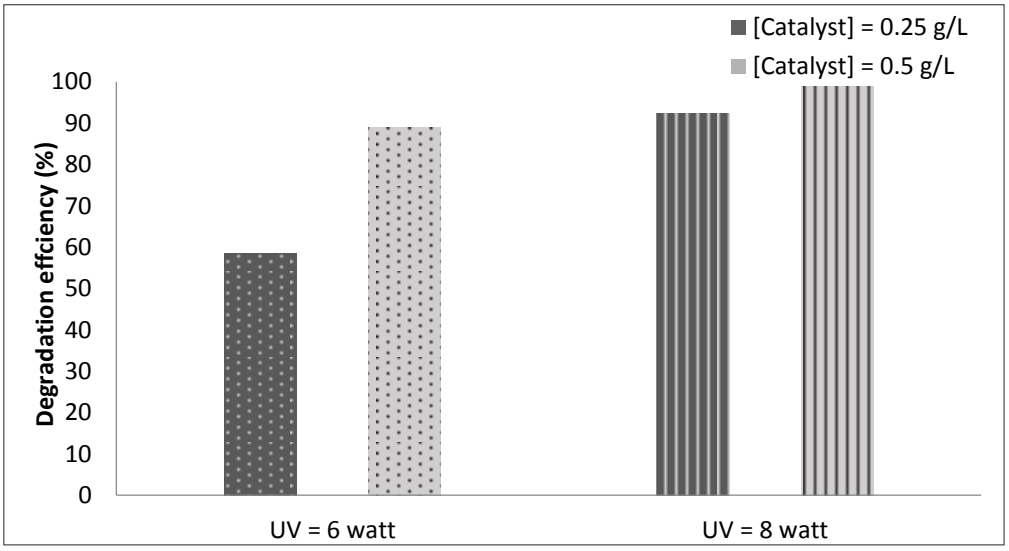

Figure 6.46 Degradation efficiencies obtained by acidic Fe-TiO_2/AC ([TPA]=50 ppm, T=25°C, pH=4)

Degradation efficiencies achieved for neutral Fe-TiO_2/AC catalyst was around 70–80 % but with high catalyst loading and high UV light intensity up to 90 % degradation was achieved. Increasing UV light intensity at low catalyst loadings wasn't effective due to absence of sufficient amount of catalyst in reaction medium. However it was very effective when catalyst loading was high to achieve higher degradation. For all experiments especially for high catalyst loading and high UV light intensity, the degradation efficiencies reached its maximum almost in 60 minutes which is the half duration time of the experiment. It remained constant after 60 minutes and stable degradation was observed (Figure 6.47).

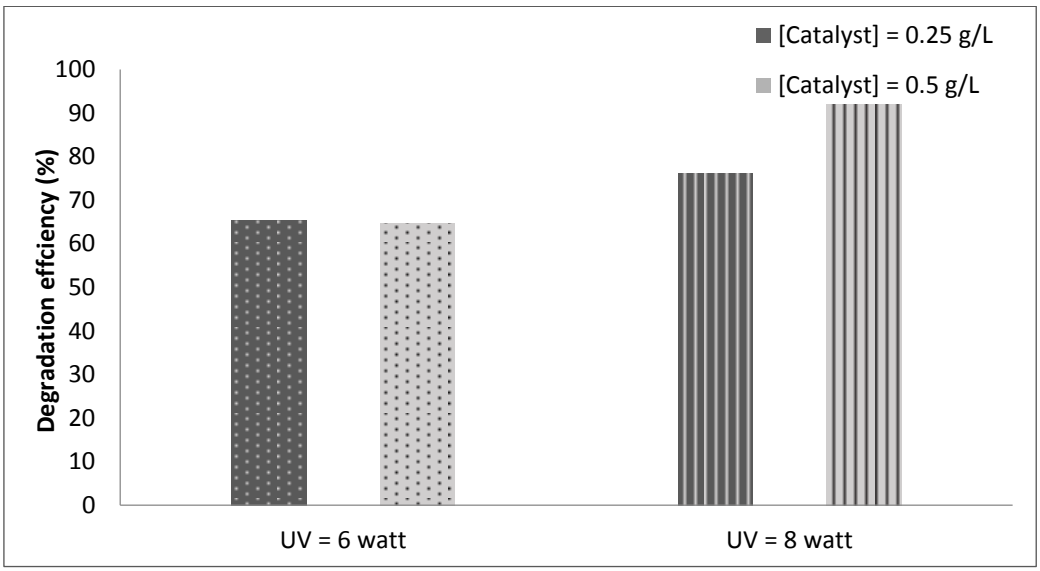

Figure 6.47 Degradation efficiencies obtained by neutral Fe-TiO_2/AC ([TPA]=50 ppm, T=25°C, pH=4)

The results obtained by acidic and neutral Fe-TiO_2/AC catalysts are the highest among all catalysts with 80–90 % degradation efficiencies. But for physical Fe/AC, physical Fe-TiO_2/AC, and acidic Fe-TiO_2/AC catalysts, very unstable degradation efficiencies were observed. For neutral Fe-TiO_2/AC however, same final degradation efficiencies were observed with stable degradation that degradation efficiencies remained generally constant after 60–80 minutes. Hence further parametric study was performed in the presence of neutral Fe-TiO_2/AC catalyst for photocatalytic oxidation by considering stability.

6.3.2.2 Parametric study for photocatalytic oxidation

Photocatalytic oxidation screening experiments showed that the highest degradation efficiency (up to 90%) achieved by Fe-TiO_2/AC catalyst prepared by neutral activation. Hence the parametric study for this method was performed in the presence of neutral Fe-TiO_2/AC. In this context, the effects of operational parameters such as catalyst loading ([Catalyst]), UV light intensity and initial pH on degradation efficiency were investigated.

Effect of catalyst loading:

The results for effect of catalyst loading showed that presence of catalyst increased degradation very remarkably compared to the degradation obtained with no catalyst. Addition of catalyst with a loading of 0.25 g/L increased degradation up to 40 % where only 20 % degradation was achieved by UV light without catalyst. This was achieved in 40 minutes then remained approximately same until 120 minutes. Almost same degradation profile was observed for 0.5 g/L catalyst loading and final degradation efficiency increased from 40 to 65 % because of active sites of catalyst increased which accelerated degradation (Ramirez et al., 2010, Rusevova et al., 2012). Further increase in catalyst loading to 1 or 2 g/L resulted almost same final degradation efficiencies but degradation for 1 g/L catalyst loading was rather slow. The reason for achieving same final degradation efficiencies for two catalyst loadings can be explained by low penetration of UV light at high catalyst loading because of turbid reaction medium as also observed for photocatalytic oxidation of BA with same catalyst (Chen et al. 2009, Rusevova et al, 2012). Since 20 % increase in degradation efficiency was observed with 1 g/L and further increase is unnecessary, optimum catalyst loading was determined as [Catalyst]=1 g/L (Figure 6.48).

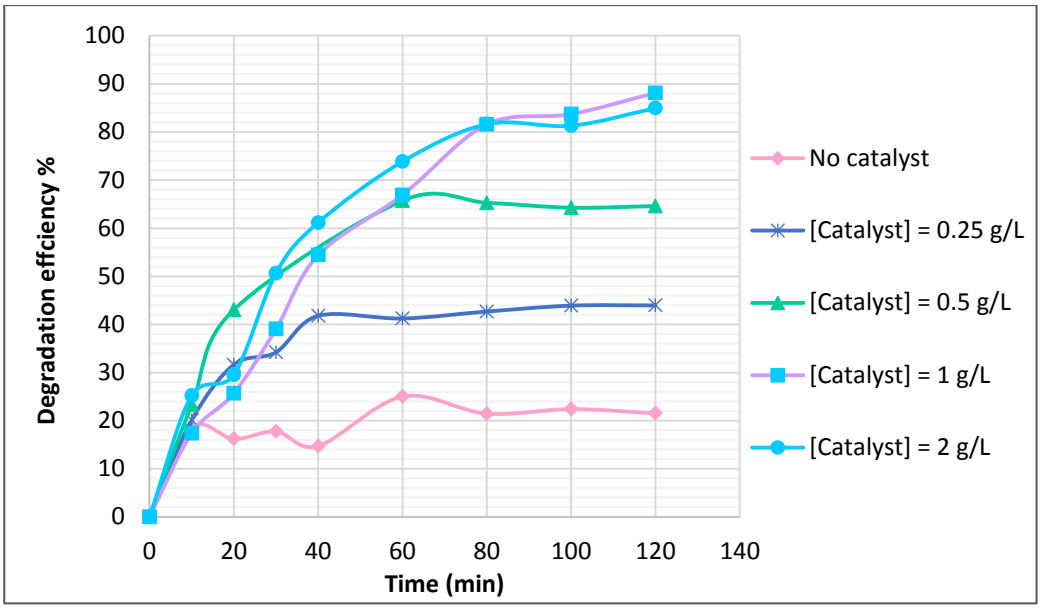

Figure 6.48 Effect of catalyst loading for neutral Fe-TiO_2/AC ([TPA]=50 ppm, UV light intensity=6 watt, T=25°C, pH=4)

Effect of UV light intensity:

According to the results obtained for effect of UV light intensity showed that presence of UV light has a great influence on degradation. As mentioned above, only 20 % degradation was achieved in presence of UV light without catalyst and almost 20 % degradation was also achieved in presence of catalyst without UV light. Moreover the degradation was around 5 % for first 60 minutes and slightly increased to 20 %. This proves the synergetic effect of catalyst and UV light that up to 90 % degradation efficiency was accomplished as observed in previous studies (Ramirez et al., 2010). When UV light was applied with 6 watt intensity, very fast degradation observed with a final degradation efficiency of up to 90 %. However increase in UV light intensity from 6 to 8 watt caused a slight decrease in final degradation efficiency and slower degradation rate. This was probably caused by formation of reaction intermediates which inhibit degradation of TPA. So it was concluded that presence of UV light was highly essential but increase in light intensity was not necessary. Hence optimum UV light intensity was determined as 6 watt (Figure 6.49).

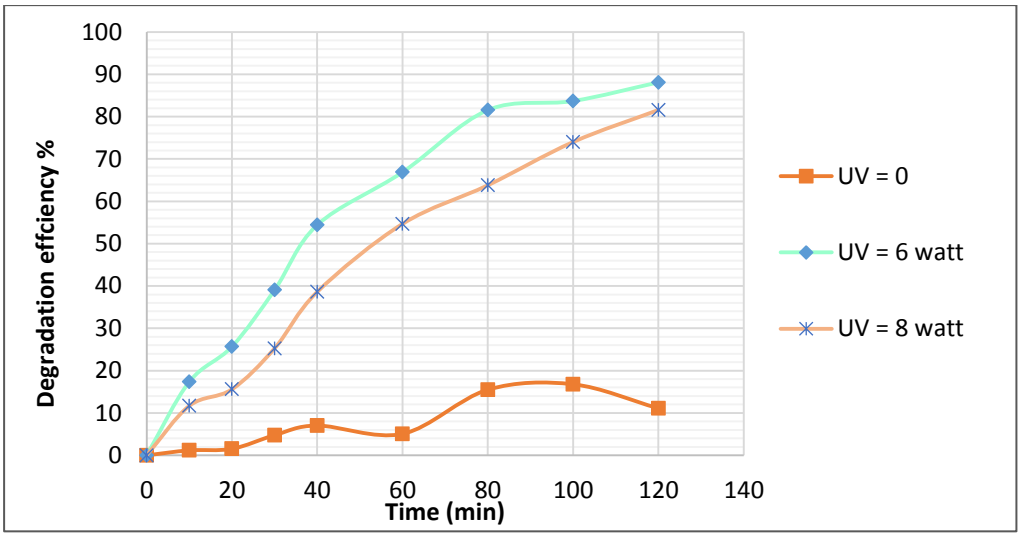

Figure 6.49 Effect of UV light intensity for neutral Fe-TiO_2/AC ([TPA]=50 ppm, [Catalyst]=1 g/L, T=25°C, pH=4)

Effect of initial pH:

Results for investigating effect of initial pH for photocatalytic oxidation of TPA showed that same observations as photocatalytic oxidation of BA were also obtained. Degradation efficiencies and degradation rate were almost same for initial pH=3 and pH=4 in first 40 minutes. After 40 minutes, faster and higher degradation was achieved for pH=4. The reason why slower and lower degradation was observed for pH=3 is formation of acidic intermediates after 40 minutes which reduced photocatalytic activity of Fe^{3+} doped TiO_2 catalyst as explained in detail previously (Chen et al., 2009, Ramirez et al., 2010). Unlike BA, when initial pH=6, there was no degradation until 30 minutes. After 30 minutes very sharp increase was observed and degradation kept increasing with a high degradation rate. At the end of 120 minutes same final degradation efficiency was obtained as initial pH=3. It is concluded that for first 40 minutes acidic intermediates weren't formed yet so pH remained high and precipitation of $Fe(OH)_3$ occurred which reduced catalytic activity. After acidic intermediates were formed, probably pH decreased to 4-5 which was still rather high since the highest catalytic activity is observed when pH=3, in theory (Chen et al., 2009, Ramirez et al., 2010). Therefore initial pH=4 provided sufficient decrease in pH to 3 and resulted with highest degradation efficiency (90 %). Both pH adjustments decreased degradation efficiency but insignificantly. If degradation

rate is essential, optimum initial pH can be taken as pH=4 since the degradation efficiency was around 50–60 % in first 30 minutes where there was no degradation for pH=6 within the same time interval. But corrosion is another important issue for chemical processes so if it is needed to be certainly avoided and low degradation rate can be neglected, optimum initial pH can be taken as pH=6 (Figure 6.50).

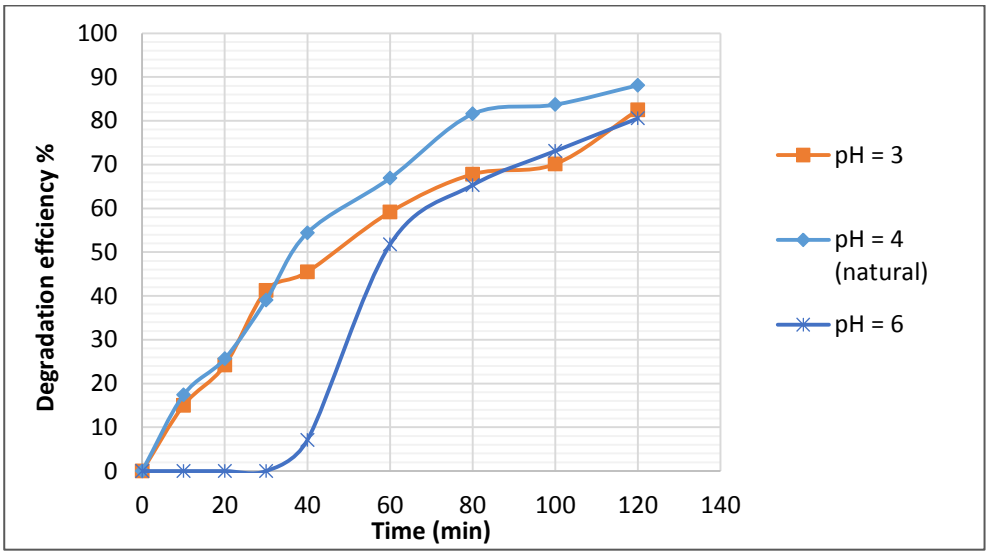

Figure 6.50 Effect of initial pH for neutral Fe-TiO_2/AC ([TPA]=50 ppm, [Catalyst]=1 g/L, UV light intensity=6 watt, T=25°C)

The optimum values of operating parameters for photocatalytic oxidation of TPA with an initial concentraton of 50 mg/L in the presence of neutral Fe-TiO_2/AC were determined as 1 g/L for catalyst loading, 6 watt for UV light intensity, and 4 or 6 for initial pH with a final degradation efficiency of approximately 90 % in 120 minutes.

6.3.2.3 Parametric study for photo-Fenton-like oxidation

The parametric study for photo-Fenton like oxidation was performed by using the same catalyst (neutral Fe-TiO_2/AC) determined from photocatalytic oxidation catalyst screening experiments. Hence the optimum values of operational parameters such as catalyst loading ([Catalyst]) and UV light intensity determined previously for photocatalytic oxidation were applied for

this method. Additionally, effect of H_2O_2 concentration and initial pH were investigated.

Effect of H_2O_2 concentration:

When there was no H_2O_2 in reaction medium, considerable degradation efficiency was achieved (around 80 %) but the degradation rate was slower in first 20 minutes comparing to presence of H_2O_2 with a concentration of 1 or 2 mM. Addition of H_2O_2 in reaction medium caused faster degradation but final degradation efficiencies obtained at the end of 120 minutes were same for no H_2O_2, 1 and 2 mM H_2O_2 concentrations (90 %). The reason for that was probable formation of hydroxyperoxyl radicals (HO_2•) due to the local excess of H_2O_2 after 80 minutes as explained in detail previously. So addition of H_2O_2 was effective for faster degradation but not for final degradation efficiency. Further increase to 3 and 4 mM showed the scavenging effect of H_2O_2 by very sharp decrease in degradation rate (Duarte et al., 2011). Final degradation efficiency was almost same again for 3 mM but it was very low for 4 mM where the scavenging effect was very severe. It also affected degradation rate as there was no degradation at first 40 minutes for 4 mM H_2O_2 concentration. Generally, it can be concluded that H_2O_2 addition was not very necessary, however optimum H_2O_2 concentration was chosen as [H_2O_2]=1 mM in order to investigate the synergetic effect of presence of H_2O_2 and initial pH (Figure 6.51).

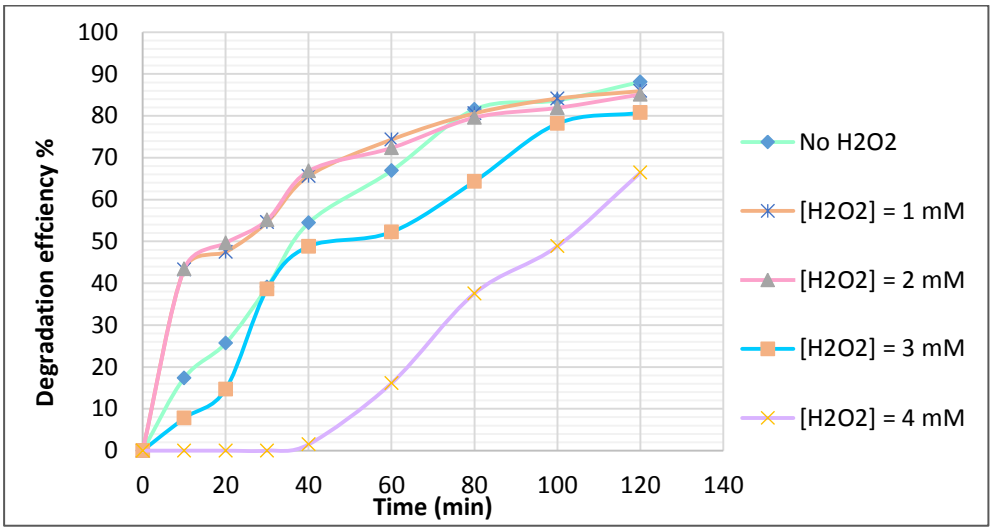

Figure 6.51 Effect of H_2O_2 concentration for neutral Fe-TiO_2/AC ([TPA]=50 ppm, [Catalyst]=1 g/L, UV light intensity=6 watt, T=25°C, pH=4)

Effect of initial pH:

The effect of initial pH experiments showed that same final degradation efficiencies obtained for all pH values but degradation rates were quite different. As explained in detail previously, pH=4 caused the fastest degradation due to the acidic intermediate formation. Since final degradation efficiencies were same, the optimum initial pH is highly dependent on the scope of the study. If degradation rate is essential than optimum initial pH can be taken as pH=4. But initial pH=6 is much closer to the neutral pH which eliminates corrosion. Hence, if corrosion must be definitely avoided and degradation rate is not that important, then optimum initial pH can be taken as pH=6 (Figure 6.52).

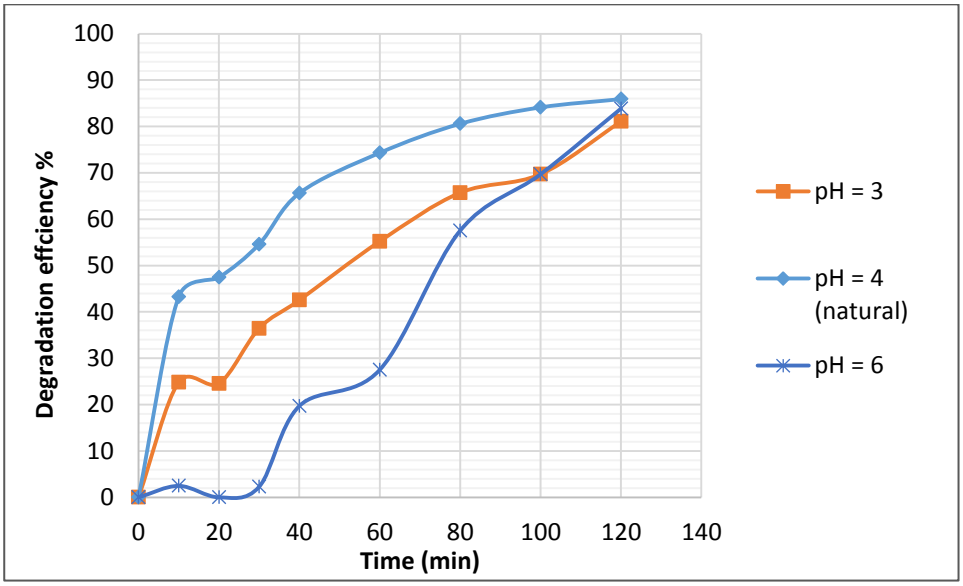

Figure 6.52 Effect of initial pH for neutral Fe-TiO_2/AC ([TPA]=50 ppm, [Catalyst] = 1 g/L, UV light intensity=6 watt, [H_2O_2]= 1 mM, T=25°C)

The optimum values of operating parameters for photo-Fenton-like oxidation of TPA with an initial concentration of 50 mg/L were determined as 1 g/L for cata1yst loading and 6 watt for UV light intensity from parametric study for photocatalytic oxidation and 1 mM for hydrogen peroxide concentration, and 4 or 6 for initial pH from parametric study of photo-Fenton-like oxidation with a final degradation efficiency of approximately 85 % in 120 minutes.

6.4 p-Toluic Acid Degradation

6.4.1 Fenton-like oxidation

Catalyst screening experiments were carried out using Fe/AC catalysts obtained by physical and chemical (acidic, neutral, basic) activation for Fenton-like oxidation. For each Fe/AC catalyst, two different catalyst loadings (0.1 and 0.2 g/L) and hydrogen peroxide (H_2O_2) concentrations (3 and 4 mM) were studied.

Unfortunately, almost no degradation was observed with all catalysts. Hence further parametric study was not performed for Fenton-like oxidation.

6.4.2 Photocatalytic oxidation

6.4.2.1 Catalyst screening

Experiments were carried out using Fe/AC and Fe-TiO_2/AC catalysts obtained by physical and chemical (acidic, neutral, basic) activation for photocatalytic oxidation. For each catalyst, two different catalyst loadings (0.25 and 0.5 g/L) and UV intensities (6 and 8 watt) were studied. The results for the effect of those different catalyst loadings and UV intensities for each catalyst are shown in Figure 6.53 to 6.59.

Results of experiments obtained by physical Fe/AC catalyst showed that the degradation efficiencies were around 30 % for low UV light intensity. But it varies between 10 to 50 % for high UV light intensity. So, catalyst loading wasn't effective for low UV light intensity. At low catalyst loading, degradation efficiency increased when UV intensity increased since UV light is highly essential for catalytic activity. For catalyst loading of 0.5 g/L however, degradation of p-Tol sharply decreased as UV intensity increased. For catalyst loading, increase in loading caused decrease in degradation because of possible low penetration of UV light due to the turbidity of solution. The final

degradation efficiencies obtained were very low, so it was concluded that this catalyst was not appropriate for parametric study (Figure 6.53).

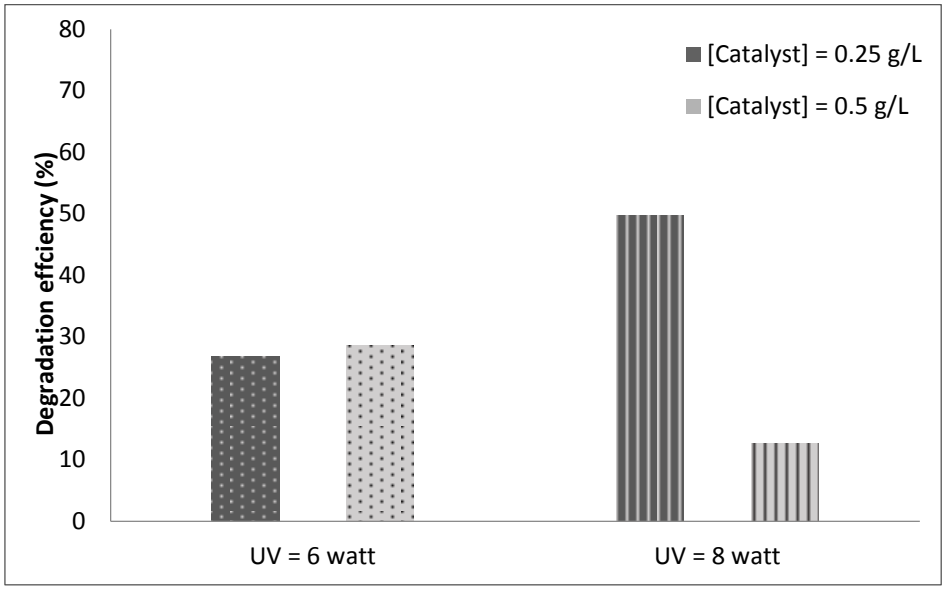

Figure 6.53 Degradation efficiencies obtained by physical Fe/AC ([p-TOL]=50 ppm, T=25°C, pH=4)

Results of experiments obtained by acidic Fe/AC catalyst showed that degradation efficiencies were between 30–40 %. For low UV light intensity, effect of catalyst loading was observed. But for high UV light intensity, increase in UV light intensity concealed the effect of catalyst loading. Additionally low penetration caused slight decrease due to the increase in catalyst loading for high UV light intensity. Either high catalyst loading and low UV light intensity or low catalyst loading and high UV light intensity can be preferred. This catalyst also achieved rather low degradation. Consequently it was also not used in parametric study (Figure 6.54).

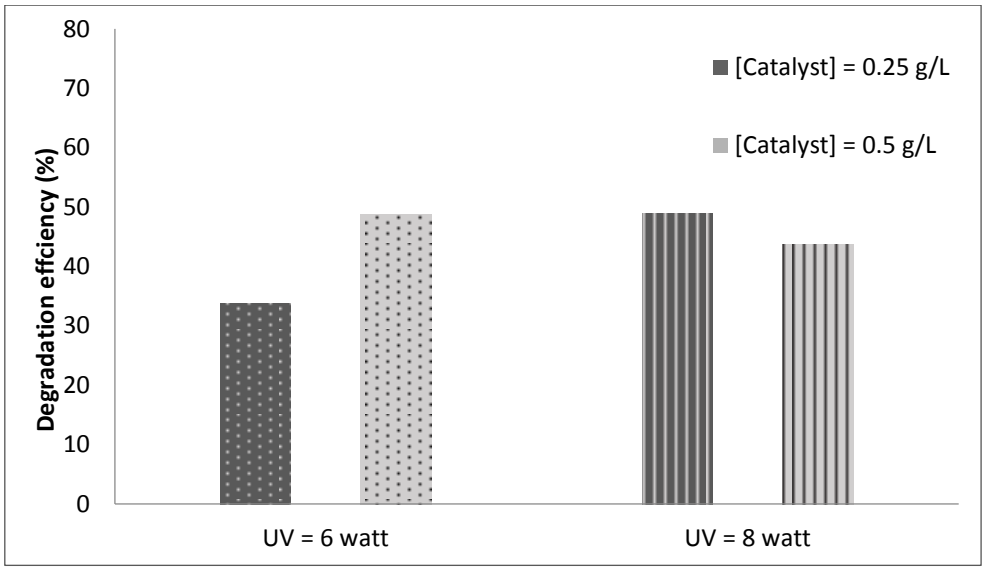

Figure 6.54 Degradation efficiencies obtained by acidic Fe/AC ([p-TOL]=50 ppm, T=25°C, pH=4)

Results of experiments obtained by neutral Fe/AC catalyst showed that the degradation efficiencies were around 40 % except for low catalyst loading at high UV light intensity. For the effect of UV intensity, at low catalyst loading, increasing UV intensity had a considerable increase on degradation, as fulfilling the expectations from theory that UV light intensity accelerating catalysis. On the other hand, for high catalyst loading, UV intensity had negative effect. By considering low UV light intensity, catalyst loading was more effective. Final degradation efficiencies obtained was quite low and this catalyst was not appropriate for parametric study, too (Figure 6.55).

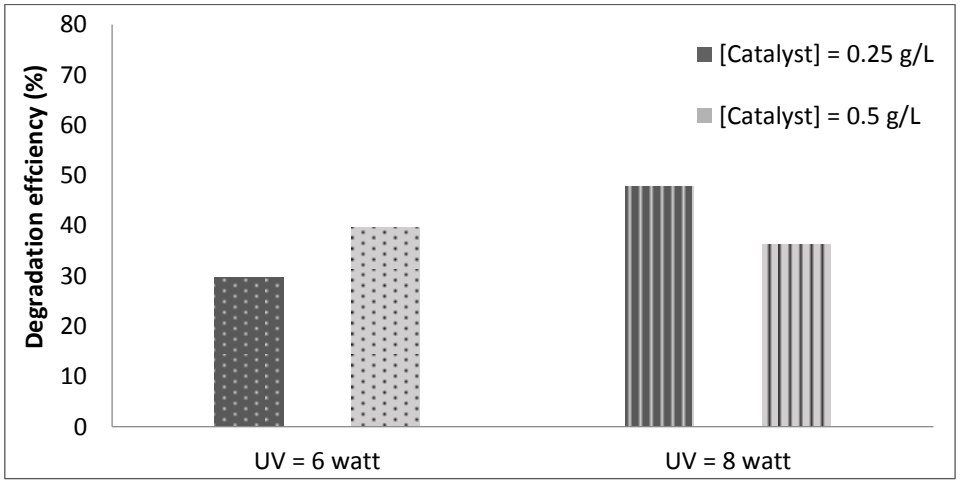

Figure 6.55 Degradation efficiencies obtained by neutral Fe/AC ([p-TOL]=50 ppm, T=25°C, pH=4)

Results of experiments obtained by basic Fe/AC catalyst showed that there weren't any remarkable changes in degradation due to the change in operating parameters and the degradation efficiencies were around 30 to 50 %. When UV intensity was increased, final degradation efficiency slightly increased for low catalyst loading, but it decreased for high catalyst loading. This could be because of formation of several byproducts. Generally, high UV intensity caused slower degradation at the beginning of the experiments. However for low catalyst loading, higher UV intensity yielded relatively higher degradation efficiency at the end. For catalyst loading effect, degradation remained almost same for high UV light intensity but it increased when UV light intensity was low. This might be because of the same reason as observed for UV light intensity. This catalyst also achieved quite low degradation efficiencies and was not selected for parametric study (Figure 6.56).

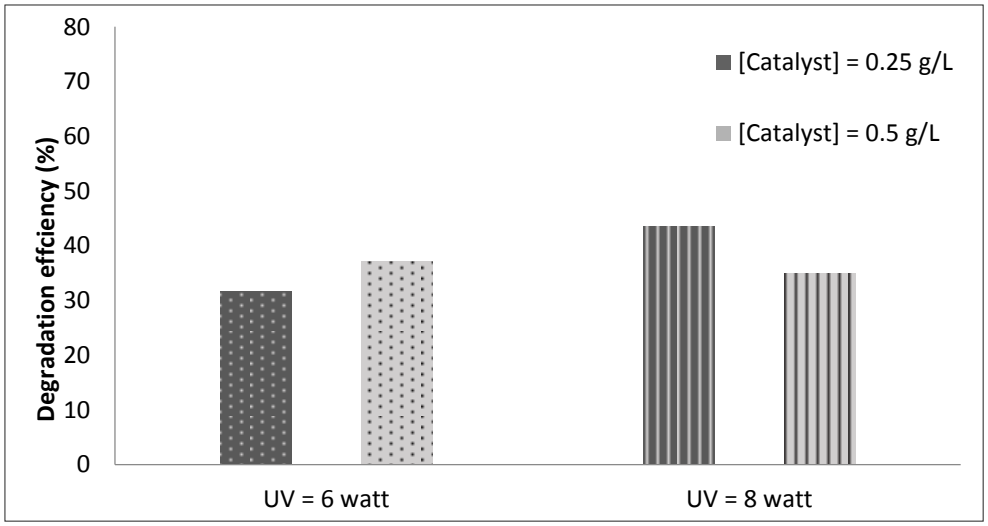

Figure 6.56 Degradation efficiencies obtained by basic Fe/AC ([p-TOL]=50 ppm, T=25°C, pH=4

Further catalyst screening experiments were performed to investigate effect of TiO_2 doping to the catalyst on degradation efficiency.

Results obtained by physical Fe-TiO_2/AC catalyst showed that all degradation efficiencies were around 40 %. Generally, high UV intensity yielded slower degradation for this catalyst. At low catalyst loadings, low UV intensity achieved around 25 % degradation where high UV light intensity achieved around 35 % in first 60 minutes. But in terms of final degradation efficiencies,

increasing catalyst loading or UV intensity had no considerable effect on degradation. It slightly increased by increasing UV intensity for high catalyst loading but that increase wasn't significant. This catalyst was also considered as not successful and not used in further parametric study (Figure 6.57).

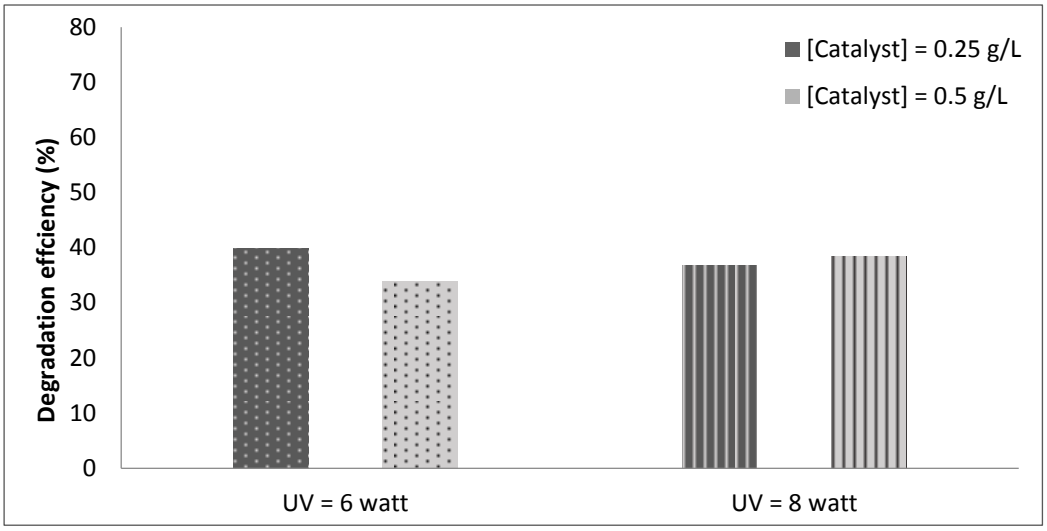

Figure 6.57 Degradation efficiencies obtained by physical Fe-TiO_2/AC ([p-TOL]=50 ppm, T=25°C, pH=4)

For acidic Fe-TiO_2/AC catalyst, the final degradation efficiencies varied between 30–50 %. The increase in UV light intensity caused considerable increase in degradation for high catalyst loading. Increasing catalyst loading had significant effect for high UV light intensity. Due to the increase in UV light intensity, degradation increased for high catalyst loading. In contrast, for low catalyst loading increasing UV light intensity caused a slight decrease in degradation probably caused by byproducts. This catalyst also achieved rather low degradation, so it was considered as not appropriate for parametric study (Figure 6.58).

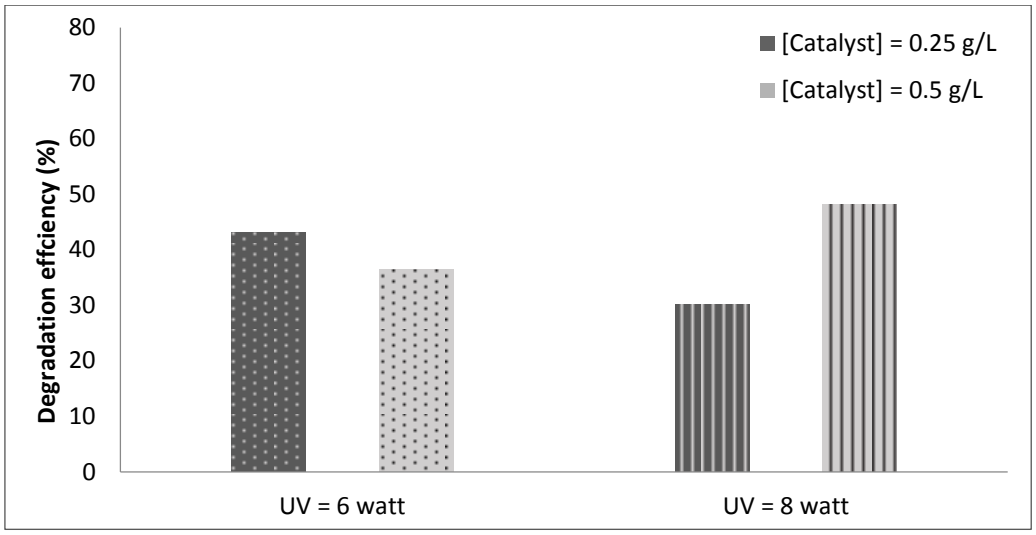

Figure 6.58 Degradation efficiencies obtained by acidic Fe-TiO_2/AC ([p-TOL]=50 ppm, T=25°C, pH=4)

The highest degradation efficiencies were obtained by neutral Fe-TiO_2/AC catalyst compared to the other catalysts. Both increasing catalyst loading and UV light intensity had remarkable effect on degradation and 70 % degradation efficiency was achieved. But lower degradation was obtained for high catalyst loading. Furthermore the degradation behaviors due to the increase in UV light intensity weren't same for two catalyst loadings. Degradation increased sharply at low catalyst loading where it slightly decreased at high catalyst loading. These were because of low penetration of UV light which is very effective on degradation. Even increase in UV light couldn't eliminate this problem. Therefore there was a great increase in degradation due to the increase in UV light intensity when catalyst loading was low and UV light penetrated efficiently. So it was concluded that either increasing catalyst loading or UV light intensity was sufficient enough for high degradation efficiencies (Figure 6.59).

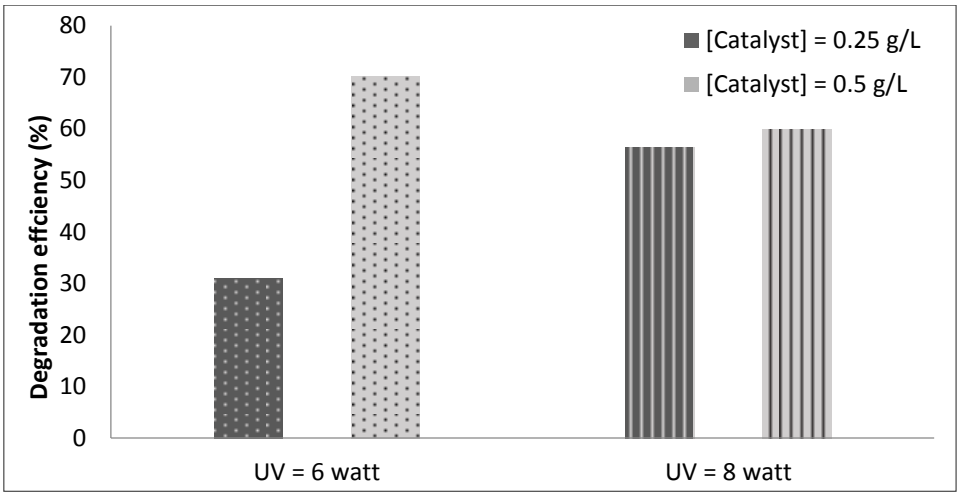

Figure 6.59 Degradation efficiencies obtained by neutral Fe-TiO_2/AC ([p-TOL]=50 ppm, T=25°C, pH=4)

Since the results obtained by neutral Fe-TiO_2/AC catalyst were highest among all catalysts with 60–70 % degradation efficiency, further parametric study was performed in the presence of neutral Fe-TiO_2/AC catalyst for photocatalytic and photo-Fenton-like oxidation.

6.4.2.2 Parametric study for photocatalytic oxidation

Photocatalytic oxidation screening experiments showed that the highest degradation efficiency (up to 70 %) achieved by Fe-TiO_2/AC catalyst prepared by neutral activation. Hence the parametric study for this method to was performed in the presence of neutral Fe-TiO_2/AC. In this context, the effects of operational parameters such as catalyst loading ([Catalyst]), UV light intensity and initial pH on degradation efficiency were investigated.

Effect of catalyst loading:

The results of the experiments for effect of catalyst loading showed that no degradation was observed when no catalyst was present in reaction medium. Addition of catalyst with a loading of 0.25 g/L achieved a final degradation efficiency around 30 %. When catalyst loading was increased from 0.25 to 0.5 g/L, final degradation efficiency increased from 30 to 70 %. Degradation rate was also much faster at 0.5 g/L catalyst loading as degradation reached its

maximum in 60 minutes and remained constant after where it was constant in last 20 minutes at 0.25 g/L loading. However further increase from 0.5 to 1 g/L caused a drastic decrease both in final degradation efficiency and degradation rate. The final degradation efficiencies were both same at 0.25 and 1 g/L catalyst loadings. Only it was faster at 1 g/L loading since degradation remained almost constant after 40 minutes where it kept increasing until 100 minutes and was only constant in last 20 minutes at 0.25 g/L catalyst loading. The degradation behavior observed at 1 g/L catalyst loading was because of very turbid reaction solution which inhibited the catalytic activity by reducing penetration of UV light. By considering degradation rates and final degradation efficiencies, 0.5 g/L catalyst loading was selected as optimum with a degradation efficiency of 70 % (Figure 6.60).

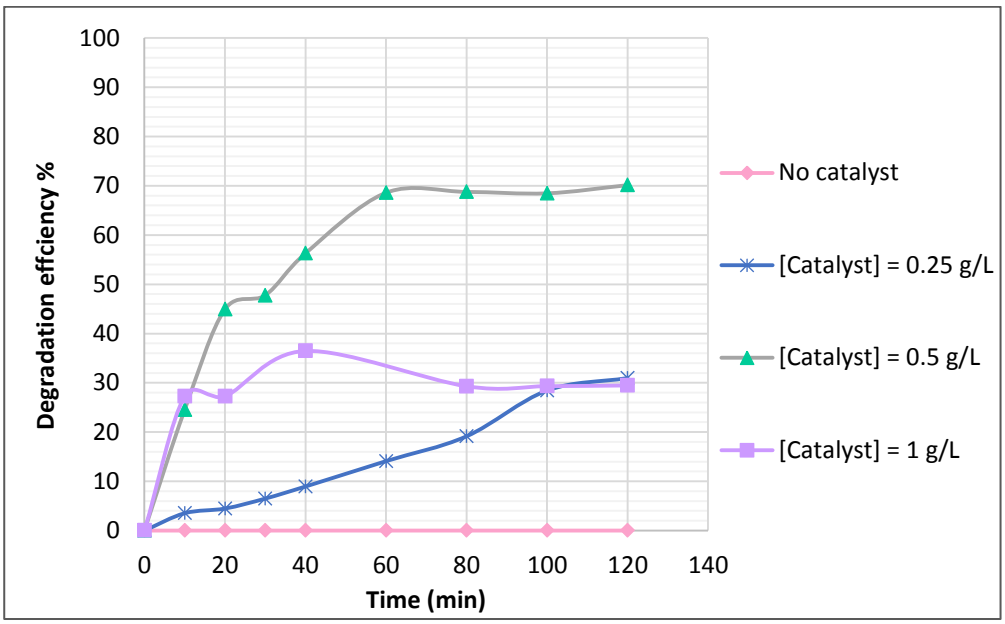

Figure 6.60 Effect of catalyst loading for neutral Fe-TiO_2/AC ([p-TOL]=50 ppm, UV light intensity=6 watt, T=25°C, pH=4)

Effect of UV light intensity:

The results of the experiments investigating effect of UV light intensity showed that no degradation was observed when no UV light was used. By using a UV light with an intensity of 6 watt, 70 % degradation was achieved and it remained constant after 60 minutes with significant degradation rate until 60 minutes. For 8 watt however slower and lower degradation was observed. This

was also observed in catalyst screening experiments as penetration problem occurred when catalyst loading was 0.5 g/L and more. By considering degradation rate for UV light intensity of 8 watt, degradation remained constant around 40 % between 10 to 80 minutes and a slight increase from 40 to 50 % was observed at 80 minutes. As degradation rate was slower and final degradation efficiency was lower with 8 watt UV light intensity, further parametric study was carried out with UV light intensity = 6 watt (Figure 6.61).

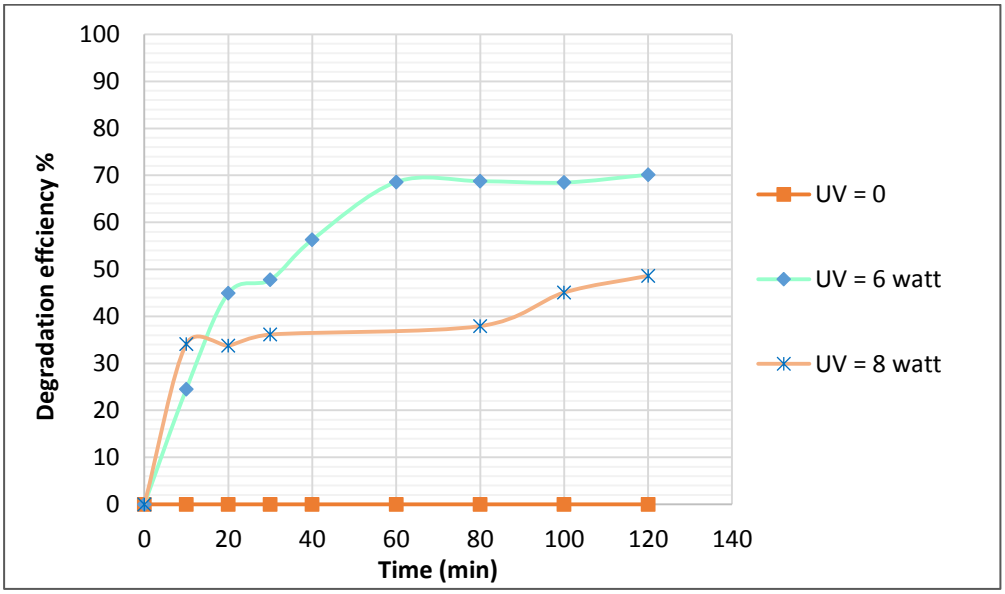

Figure 6.61 Effect of UV light intensity for neutral Fe-TiO_2/AC ([p-TOL]=50 ppm, [Catalyst]=0.5 g/L, T=25°C, pH=4)

Effect of initial pH:

For the experiments investigating effect of initial pH showed that only experiment that degradation could be achieved the experiment carried out with an initial pH=4 with a degradation efficiency of 70 %. Unfortunately no degradation was achieved when pH was adjusted to 3 or 6. This was probably because of decomposition of p-toluic acid by the chemicals used for pH adjustment. Hence optimum initial pH was determined as 4 with a degradation efficiency of 70 % (Figure 6.62).

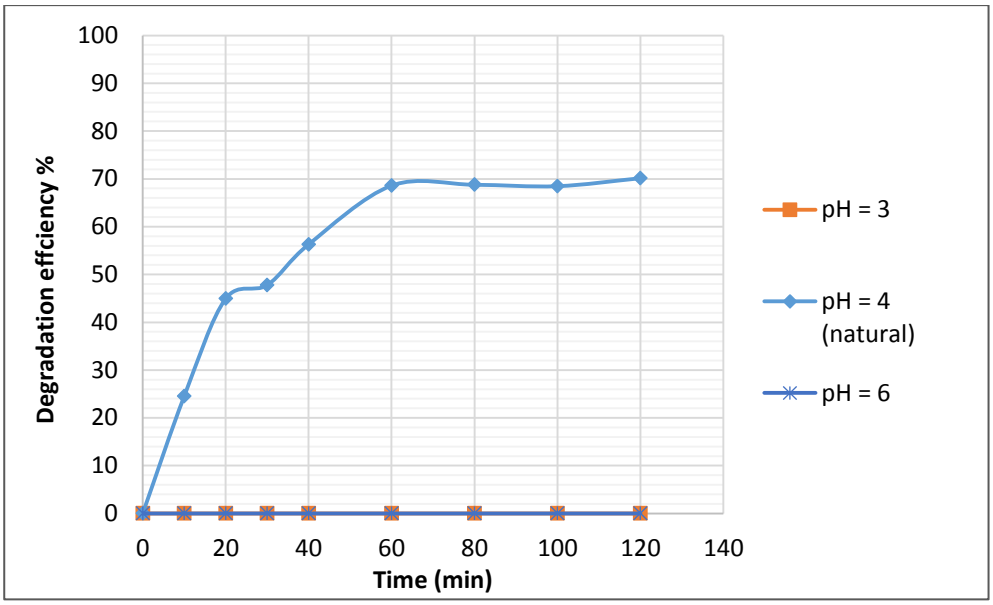

Figure 6.62 Effect of initial pH for neutral Fe-TiO_2/AC ([p-TOL]=50 ppm, [Catalyst]=0.5 g/L, UV light intensity=6 watt, T=25°C)

The optimum values of operating parameters for photocatalytic oxidation of p-Tol with an initial concentration of 50 mg/L in the presence of neutral Fe-TiO_2/AC were determined as 0.5 g/L for catalyst loading, 6 watt for UV light intensity, and 4 for pH with a final degradation efficiency of approximately 70 % in 60 minutes.

6.4.2.3 Parametric study for photo-Fenton-like oxidation

The parametric study for photo-Fenton like oxidation was performed by using the same catalyst (neutral Fe-TiO_2/AC) determined from photocatalytic oxidation catalyst screening experiments. Hence the optimum values of operational parameters such as catalyst loading ([Catalyst]) and UV light intensity determined previously for photocatalytic oxidation were applied for this method. Additionally, effect of H_2O_2 concentration and initial pH were investigated.

Effect of H_2O_2 concentration:

In the experiment for absence of H_2O_2 in reaction medium, considerable degradation was achieved with a final degradation efficiency of 70 %. When H_2O_2 was added with a concentration of 1 mM much slower degradation was observed and the final degradation efficiency reached around 40 % at the end of 120 minutes. The increase from 1 to 2 mM increased degradation rate especially in first 10 minutes comparing to no H_2O_2 or 1 mM H_2O_2 but with rather lower final degradation efficiency than no H_2O_2 . Further increase from 2 to 3 mM caused the same final degradation efficiency (≈65 %), and it was that degradation rate for 2 mM was lower. Consequently it was concluded that addition of H_2O_2 was not necessary. Despite the observation that the highest final degradation efficiency was achieved with absence of H_2O_2, rest of the parametric study was performed for $[H_2O_2]$=2 mM in order to investigate the synergetic effect of addition of H_2O_2 with pH adjustment (Figure 6.63).

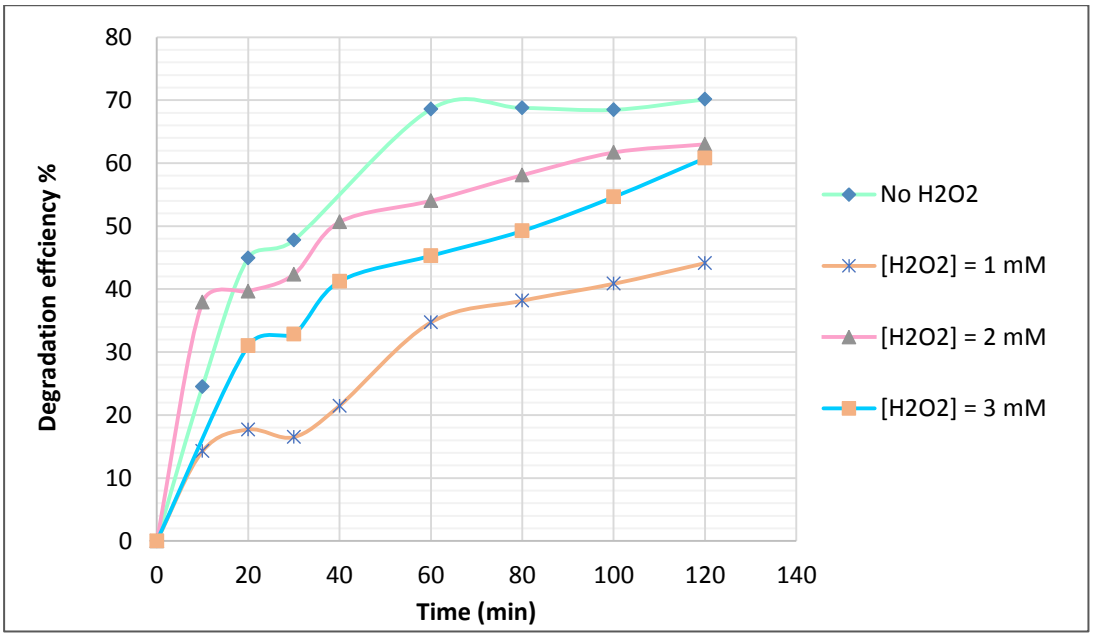

Figure 6.63 Effect of H_2O_2 concentration for neutral Fe-TiO_2/AC ([p-TOL]=50 ppm, [Catalyst]=0.5 g/L, UV light intensity=6 watt, T=25°C, pH=4)

Effect of initial pH:

The results obtained for investigating effect of initial pH showed that the highest and fastest degradation efficiency achieved when natural pH of aqueous

p-Tol solution was taken as initial pH with a final degradation efficiency of approximately 65 %. pH adjustment caused slower degradation rate with lower final degradation efficiencies. When initial pH was adjusted to 6, the degradation was too slow and unstable in the first 40 minutes. After 40 minutes, it was more stable and reached the same final degradation efficiency with the experiment for initial pH=4. The reason slower and lower degradation behavior especially in first 40 minutes was probably causes by reduction in photocatalytic activity due to the precipitation of Fe^{3+} ions as previously explained in detail. For initial pH=3, degradation was rather stable and faster comparing to initial pH=6, but it was still slower with lower degradation efficiencies than initial pH=4. The reason for that was also formation of acidic intermediates previously discussed in detail. By considering these, optimum initial pH was determined as 4 (Figure 6.64).

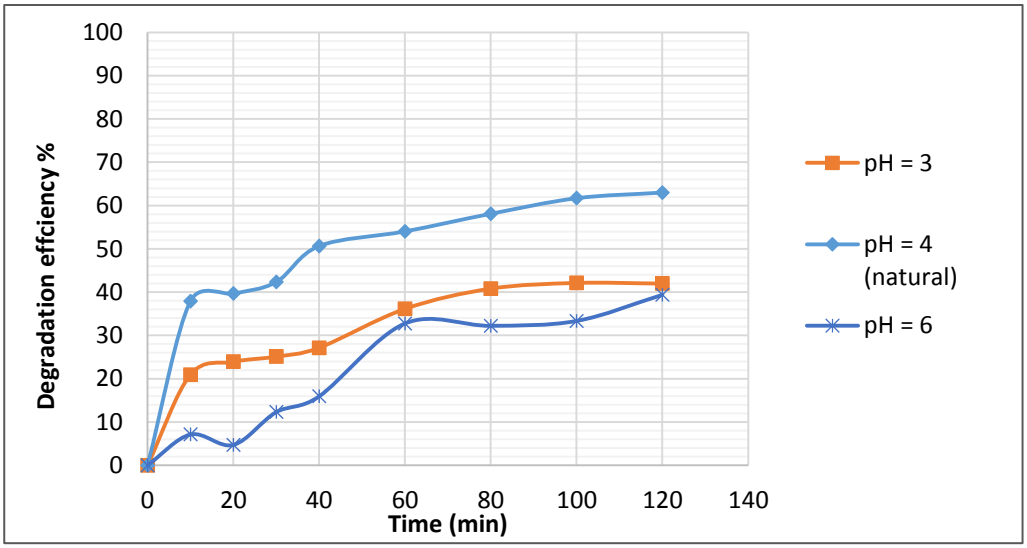

Figure 6.64 Effect of initial pH for neutral Fe-TiO_2/AC ([p-TOL]=50 ppm, [Catalyst]=0.5 g/L, UV light intensity=6 watt, [H_2O_2]= 2 mM, T=25°C)

The optimum values of operating parameters for photo-Fenton-like oxidation of p-Tol with an initial concentration of 50 mg/L were determined as 0.5 g/L for cata1yst loading and 6 watt for UV light intensity from parametric study for photocatalytic oxidation and 2 mM for hydrogen peroxide concentration, and 4 for initial pH from parametric study of photo-Fenton-like oxidation with a final degradation efficiency of approximately 65 % in 60 minutes.

7.0 GENERAL CONSIDERATIONS

In first part of the study catalyst preparation and characterization steps for AOPs were performed. In this context, Fe/AC and Fe-TiO_2/AC catalysts were prepared. Firstly, activated carbons which used as catalyst support both for Fe/AC and Fe-TiO_2/AC catalysts were prepared by different physical and chemical activation methods such as physical, acidic, neutral and basic activation. Fe/AC catalysts were prepared by impregnation method and Fe-TiO_2/AC catalysts were prepared by Sol-gel method.

Three different target compounds that represent TPA wastewater were selected as benzoic acid, terephthalic acid, and p-toluic acid. Methods applied were various AOPs such as Fenton-like oxidation, catalytic wet air oxidation, photocatalyic oxidation, and photo-Fenton-like oxidation. Additionally biological oxidation for benzoic acid was also applied. Degradation experiments for all target compounds were carried out in two steps and they are explained in detail below.

In catalyst screenings for AOPs for each target compound, Fe/AC catalysts were tested for Fenton-like oxidation and catalytic wet air oxidation and both Fe/AC and Fe-TiO_2/AC catalysts were tested for photocatalytic and photo-Fenton-like oxidation by varying several operating conditions. Most successful catalysts determined in this part were used for further parametric studies.

In parametric studies for AOPs for each target compound, values of operating conditions were varied for each method and optimum operating conditions were determined by considering final degradation.

For biological oxidation, firstly growing and immobilization of microorganisms were performed. Two different microorganisms were tested for catalyst screening and optimum values of operating conditions such as biocatalyst (immobilized microorganism) loading and glucose concentration were determined for parametric study.

The comparison of with optimum operating conditions methods for each target compound BA, TPA and p-Tol with maximum degradation efficiencies achieved are shown in Table 7.1 in detail.

Table 7.1 Maximum degradation efficiencies for each target compound.

Target Compound	Method	Catalyst	Optimum values of operating conditions							Time (min)	Degradation Efficiency (%)
			[Catalyst] (g/L)	Temperature (°C)	Pressure (bar)	Air flowrate (ml/min)	UV light intensity (watt)	$[H_2O_2]$ (mM)	Initial pH		
BA	Fenton-like oxidation	Basic Fe/AC	0.3	25	-	-	-	2	3 or 4	40	60
	Catalytic wet air oxidation	Basic Fe/AC	1	50	1	0.92	-	-	-	120	70
	Photocatalytic oxidation	Neutral Fe-TiO_2/AC	0.5	25	-	-	8	-	4 or 6	60	90
	Photo-Fenton-like oxidation	**Neutral Fe-TiO_2/AC**	**0.5**	**25**	**-**	**-**	**8**	**2**	**3 or 6**	**80**	**95**
	Biological oxidation	Immobilized *P.chrysosporium*	5	25	-	-	-	-	-	4 days	90
TPA	**Photocatalytic oxidation**	**Neutral Fe-TiO_2/AC**	**1**	**25**	**-**	**-**	**6**	**-**	**4 or 6**	**120**	**90**
	Photo-Fenton-like oxidation	Neutral Fe-TiO_2/AC	1	25	-	-	6	1	4 or 6	120	85
p-TOL	**Photocatalytic oxidation**	**Neutral Fe-TiO_2/AC**	**0.5**	**25**	**-**	**-**	**6**	**-**	**4**	**60**	**70**
	Photo-Fenton-like oxidation	Neutral Fe-TiO_2/AC	0.5	25	-	-	6	2	4	60	65

117

8.0 CONCLUSIONS

This study aimed at investigation on the treatment of terephthalic acid plant wastewater by applying advanced oxidation methods using metal doped walnut shells as catalyst and comparing biological oxidation.

For catalyst preparation as the first part of study, physical and acidic, neutral and basic activation that represents chemical activation methods were applied for preparation of activated carbon. Effects of activation method were to be searched for in terms of porous structure, specific surface area and catalytic activity. Porous structure and high surface area were required properties for activated carbons and catalysts for effective adsorption of metals and target compounds. The characterization results of prepared catalysts showed that both for activated carbons and catalysts have porous structure and high surface area. For comparison of activated carbons, neutral and basic activation methods were determined as the most successful activation methods since the most porous structure was obtained for basic activated carbon according to SEM analysis and highest surface area was obtained for neutral AC according to BET analysis. Additionally, catalytic performances of the catalysts in which these activated carbons were used as support were also more successful. BET analysis results showed that basic AC with BET surface area of 961.06 m^2/mg and neutral AC with BET surface area of 1370.30 m^2/mg which are considered as consistent with similar studies in literature. Also loading of metal catalysts to the catalyst support were performed successfully according to the peaks in XRD patterns of all catalysts and also decrease in BET surface area results for basic Fe/AC and neutral Fe-TiO_2/AC catalysts with BET surface areas of 724.86 and 1229.54 m^2/mg, respectively. Comparisons of catalytic performances of Fe/AC and Fe-TiO_2 AC catalysts are explained below in detail for different target compounds and methods.

In the second part of the study, firstly the effect of activation method on catalytic performance for degradation of benzoic acid, terephthalic acid and p-toluic acid was investigated by determining the most efficient catalyst which yielded higher degradation for Fenton-like oxidation, catalytic wet air oxidation

and photocatalytic oxidation. Different cases by changing operational conditions of each method were applied for each catalyst and the degradation efficiencies were compared. After catalyst screening experiments, parametric studies were carried out to determine the optimum operating conditions and improve degradation efficiencies by using the most efficient catalyst.

Benzoic acid treatment results

Catalyst screening experiments for Fenton-like oxidation and catalytic wet air oxidation of BA revealed that basic Fe/AC catalyst was more successful. Catalyst screening experiments for photocatalytic and photo-Fenton-like oxidation showed that neutral Fe-TiO_2/AC catalyst was more successful. Hence parametric studies for Fenton-like oxidation and catalytic wet air oxidation were carried out with basic Fe/AC catalyst and parametric studies for photocatalytic oxidation and photo-Fenton-like oxidation were carried out with neutral Fe-TiO_2/AC catalyst.

For parametric studies, 60 % degradation efficiency was achieved by Fenton-like oxidation in the presence of basic Fe/AC catalyst at optimum operating conditions as 0.3 g/L for catalyst loading, 2 mM for H_2O_2 concentration, 3 for initial pH, and 25°C (room temperature) for temperature. By catalytic wet air oxidation, 70 % was achieved in the presence of same catalyst, basic Fe/AC at optimum operating conditions as 1 g/L for catalyst loading, 50°C for temperature, 1 bar for pressure, 0.92 ml/min for air flowrate. However despite the degradation efficiency achieved by CWAO was relatively higher, the optimum catalyst loading was three times the optimum catalyst loading for Fenton-like oxidation. Moreover Fenton-like oxidation was carried out in milder conditions, in other words at room temperature and atmospheric pressure. For photocatalytic and photo-Fenton-like oxidation in the presence of neutral Fe-TiO_2/AC catalyst, much higher degradation efficiencies up to 90–95 % were achieved and the highest degradation efficiency was achieved by photo-Fenton-like oxidation with a final degradation efficiency of 95 % in 80 minutes at optimum operating conditions as 0.5 g/L catalyst loading, 8 watt for UV light intensity, 2 mM for H_2O_2 concentration, and 3 or 6 for initial pH. Comparing

Fenton-like oxidation and photo-Fenton-like oxidation (which is basically UV assisted Fenton-like oxidation) in terms of degradation rate and degradation efficiencies, degradation rates were almost same but final degradation efficiencies increased from 60 to 95 % only by additional UV assisted TiO_2 doped catalyst.

The most efficient method for benzoic acid was selected as photo-Fenton-like oxidation in the presence of neutral Fe-TiO_2/AC catalyst with a final degradation efficiency of 95 % at optimum operating conditions as 0.5 g/L catalyst loading, 8 watt for UV light intensity, 2 mM for H_2O_2 concentration, and 3 or 6 for initial pH.

Terephthalic acid treatment results

Catalyst screening experiments for Fenton-like oxidation showed that unfortunately no degradation observed with any catalyst. Catalytic wet air oxidation couldn't be performed because of use of Tetrahydrofuran in aqueous solution of TPA which has very low flaming temperature. For catalyst screening for photocatalytic and photo-Fenton-like oxidation, neutral Fe-TiO_2/AC catalyst was more successful same as BA. Hence parametric studies parametric studies for photocatalytic oxidation and photo-Fenton-like oxidation were carried out with neutral Fe-TiO_2/AC catalyst.

For parametric studies in the presence of neutral Fe-TiO_2/AC catalyst, for photocatalytic and photo-Fenton-like oxidation, 85–90 % degradation efficiencies were achieved at optimum operating conditions as 1 g/L catalyst loading, 6 watt for UV light intensity, 1 mM for H_2O_2 concentration, and 4 or 6 for initial pH. The highest degradation efficiency was achieved by photocatalytic oxidation with a final degradation efficiency of 90 % and a slight decrease was observed for photo-Fenton-like oxidation as the final degradation efficiency was 85 % but degradation rates were almost same.

The most efficient method for terephthalic acid was selected as photocatalytic oxidation in the presence of neutral Fe-TiO_2/AC catalyst with a

final degradation efficiency of 90 % at optimum operating conditions as 1 g/L catalyst loading, 6 watt for UV light intensity, 1 mM for H_2O_2 concentration, and 4 or 6 for initial pH.

p-Toluic acid treatment results

Catalyst screening experiments for Fenton-like oxidation of p-Tol showed that unfortunately no degradation was accomplished with any catalyst. Catalytic wet air oxidation also couldn't be performed because of same reason as TPA. Neutral Fe-TiO_2/AC catalyst was again more successful for catalyst screening for photocatalytic and photo-Fenton-like oxidation same as BA and TPA. Hence parametric studies parametric studies for photocatalytic oxidation and photo-Fenton-like oxidation were carried out with neutral Fe-TiO_2/AC catalyst.

For parametric studies in the presence of neutral Fe-TiO_2/AC catalyst, up to 65–70 % degradation efficiencies were achieved for photocatalytic and photo-Fenton-like oxidation at optimum operating conditions as 0.5 g/L catalyst loading, 6 watt for UV light intensity, 2 mM for H_2O_2 concentration, and 4 for initial pH. The highest degradation efficiency was achieved by photocatalytic oxidation with a final degradation efficiency of 70 % and the same decrease observed for TPA was also observed for photo-Fenton-like oxidation as the final degradation efficiency was 65 % but degradation rates were also almost same.

The most efficient method for p-toluic acid was selected as photocatalytic oxidation in the presence of neutral Fe-TiO_2/AC catalyst with a final degradation efficiency of 70 % at optimum conditions as 0.5 g/L catalyst loading, 6 watt for UV light intensity, 2 mM for H_2O_2 concentration, and 4 for initial pH.

General comparison for catalysts and AOPs

As a general comparison of activation methods for efficient degradation of target compounds by AOPs is one of the main goals of this study:

- Physical and acidic activation for activated carbon preparation were considered as less successful than neutral and basic activation in terms of catalytic activity according to the catalyst screening experiments
- The highest catalytic activities for Fenton-like oxidation and catalytic wet air oxidation belong to basic Fe/AC catalyst and it can be possibly explained that basic Fe/AC catalyst has high surface area with higher adsorption capacity which provided contact for target compounds as pollutants and metals as catalysts
- Neutral Fe-TiO_2/AC catalyst was successful for photocatalysis based AOPs probably because of Zn ions remained from activated carbon preparation by neutral activation which is also known to be efficient semiconductor photocatalyst as TiO_2

For a detailed comparison of AOPs according to catalyst screenings and parametric studies:

- Fenton-like oxidation achieved moderate degradation efficiencies only for BA and even no degradation for TPA and p-Tol. Despite the advantages it provides such as easy operation and mild operating conditions, unfortunately this method was considered as not successful for these target compounds.
- Photocatalytic and photo-Fenton-like oxidation methods were much more successful for all target compounds and achieved 90–95 % degradation efficiencies for BA and TPA and 70 % for p-Tol. This can be considered as a great accomplishment since there weren't so many studies obtained very high degradation efficiencies especially for p-Toluic acid which was known to be the most refractive compound with very poor degradation.
- For comparing photocatalytic and photo-Fenton-like oxidation, photo-Fenton-like oxidation was more successful than photocatalytic oxidation only for BA since scavenging effect of H_2O_2 was more severe for TPA and p-Tol than BA.
- Catalytic wet air oxidation also achieved high degradation efficiency up to 70 % for BA, but this was still below than the degradation efficiency achieved by photocatalysis based AOPs.

Benzoic acid treatment results by biological oxidation

As the third part of the study, catalyst screening experiments for biological oxidation of BA showed that *P.chrysosporium* accomplished higher degradation efficiencies than *T.versicolor*. This fulfilled the expectations since few studies applied biological oxidation to TPA and its derivatives mostly preferred this microorganism. Biological oxidation seems to be successful as 90–95 % degradation efficiencies in parametric study for BA were observed. But the required time to achieve these degradation efficiencies were up to 4 days where same degradation efficiencies were achieved in 2 hours by photocatalytic and photo-Fenton-like oxidation.

Unfortunately biological oxidation couldn't be applied for TPA and p-Tol because of toxicity of THF for microorganisms.

General Conclusions

For general conclusions extracted from this study can be expressed as:

- Neutral and basic activation are more successful activation methods in terms of catalytic activity,
- Photocatalysis based on AOPs are the most successful methods for all target compounds and very high degradation efficiencies with high degradation rates were accomplished,
- Biological oxidation with novel biocatalysts can be considered as more successful than conventional biological methods but it was still much slower comparing to AOPs.

The main goal of this study was the development of innovative eco-friendly methods for degradation of major pollutants present in TPA wastewater in the presence of waste derived catalyst. The open gap in degradation of TPA wastewater pollutants was successfully fulfilled since very high degradation efficiencies were obtained. Additionally walnut shells were also successfully reused as green catalyst which led application of AOPs in milder conditions and

decreasing operating costs and prevented generation of secondary wastes. It is thought that this will lead a great interest for application of AOPs in industrial scale especially for treatment of refractive organic compounds such as TPA and its derivatives which still have been a great challenge for industry from both economic and environmental point of views.

REFERENCES

Abo-Farha S.A., 2010, Comparative Study of Oxidation of Some Azo Dyes by Different Advanced Oxidation Processes: Fenton, Fenton-Like, Photo-Fenton and Photo-Fenton-Like, Journal of American Science, 6(10):128-142pp.

Agarwal, G.K. and Ghoshal A.K., 2008, Packed bed Dynamics during microbial treatment of wastewater: Modelling and simulation, Bioresource Technology, 99:3765-3773pp.

Ahmadpour A. and Do D.D., 1997, The preparation of activated carbon from macadamia nutshell by chemical activation, Carbon, 35:1723-1732pp.

Ahmed M.J. and Dhedan S.K., 2012, Equilibrium isotherms and kinetics modeling of methylene blue adsorption on agricultural wastes-based activated carbons, Fluid Phase Equilibria, 317:9-14pp.

Álvarez-Merino M.A., Fontecha-Cámara M.A., López-Ramón M.V., and Moreno-Castilla C., 2008, Temperature dependence of the point of zero charge of oxidized and non-oxidized activated carbons, Carbon, 46-5:778-787pp.

Andreozzi R., Caprio V., Insola A., and Marotta R., 1999, Advanced oxidation processes (AOP) for water purification and recovery, Catalysis Today 53:51-59pp.

Andreozzi, R. and Marotta, R., 2004, Removal of benzoic acid in aqueous solution by Fe(III) homogeneous photocatalysis, Water Research, 38:1225-1236pp.

Anotai, J., Su, C., Tsai, Y., and Lu, M., 2010, Effect of hydrogen peroxide on aniline oxidation by electro-Fenton and fluidized-bed Fenton processes, Journal of Hazardous Materials 183:888-893pp.

Asiltürk M. and Şener Ş., 2012, TiO_2-Activated carbon photocatalyst: Preparation, characterization and photocatalytic activities, Chemical Engineering Journal 180:354-363pp.

REFERENCES (Continued)

Aworn A., Thiravetyan P., and Nakbanpote W., 2008, Preparation and characteristics of agricultural waste activated carbon by physical activation having micro- and mesopores, J. Anal. Appl. Pyrolysis, 82(2):279–285pp.

Babić B.M., Milonjić S.K., Polovina M.J., and Kaludierović B.V., 1999, Point of zero charge and intrinsic equilibrium constants of activated carbon cloth, Carbon, 37-3:477–481pp.

Banic N., Abramovic B., Krstic J., Sojic D., Loncarevic D., Cherkezova Z., and Guzsvany V., 2011, Photodegradation of thiacloprid using Fe-TiO_2 as a heterogenous photofenton catalyst, Applied Catalysts B:Environmental 107:363–371pp.

Carpio E., Zuniga P., Ponce S., Solis J., Rodriguez J., and Estrada W., 2005, Photocatalytic degradation of phenol using TiO_2 nanocrystals supported on activated carbon, Journal of Molecular Catalysis A: Chemical 228:293–298pp.

Chai K. and Ji H., 2012, Dual functional adsorption of benzoic acid from wastewater by biological-based chitosan grafted b-cyclodextrin, Chemical Engineering Journal, 203:309-318pp.

Chen, K., Vu, J., Liou, D., and Hwang, S., 2003, Decolorization of the textile dyes by newly isolated bacterial strains, Journal of Biotechnology, 101(1):57–68pp.

Chen, S., Sun, D., and Chung, J.S., 2007, Anaerobic treatment of highly concentrated aniline wastewater using packed-bed biofilm reactor, Process Biochemisstry, 42:1666–1670pp.

Chen, C.Y., Kao, C.M., and Chen, S.C., 2008, Application of Klebsiella oxytoca immobilized cells on the treatment of cyanide wastewater, Chemosphere, 71:133–139pp.

REFERENCES (Continued)

Chen, Q., Wu, P., Li, Y., Zhu, N., and Dang, Z., 2009, Heterogeneous photo-Fenton photodegradation of reactive brilliant orange X-GN over iron-pillared montmorillonite under visible irradiation, Journal of Hazardous Materials 168:901–908pp.

Choi W., Shim W., Ryu D., Hwang M., and Moon H., 2012, Effect of ball milling on electrochemical characteristics of walnut shell-based carbon electrodes for EDLCs, Microporous and Mesoporous Materials, 155:274–280pp.

Crittenden, J.C., Trussell, R.R., Hand, D.W., Howe, K.J., and Tchobanoglous, G., 2012, Water Treatment, Principles and Design, Part 18: Advanced Oxidation, John Wiley & Sons, Inc.

Daud, N.K. and Hameed, B.H., 2010, Decolorization of Acid Red 1 by Fenton-like process using rice husk ash-based catalyst, Journal of Hazardous Materials, 176:938–944pp.

Djilani C., Zaghdoudi R., Modarressi A., Rogalski M., Djazi F., and Lallam A., 2012, Elimination of organic micropollutants by adsorption on activated carbon prepared from agricultural waste, Chemical Engineering Journal, 189-190:203–212pp.

Duarte F., Maldonado-Hódar F.J., and Madeira L.M., 2011, Influence of the characteristics of carbon materials on their behaviour as heterogeneous Fenton catalysts for the elimination of the azo dye Orange II from aqueous solutions, Applied Catalysis B: Environmental, 103 (1-2):109–115pp.

Ekpete O.A. and Horsfall M., 2011, Preparation and characterization of activated carbon derived from fluted pumpkin stem waste, Research Journal of Chemical Sciences, 1(3):10–17pp.

REFERENCES (Continued)

El-Sheikh. A. H., Al-Degs Y. S, Nevman A. P., and Lynch D. E., 2007, Oxidized activated carbon as support for titanium dioxide in UV-assisted degradation of 3-chlorophenol, Separation and Purification Technology 54:117–123pp.

Escher, B.I., Baumgartner, R., Koller, M., Treller, K., Lienert, J., and McCardell, C.S., 2011, Environmental toxicology and risk assessment of pharmaceuticals from hospital wastewater, Water Research, 45:75–92pp.

Foo K.Y. and Hameed B.H., 2010, Decontamination of textile wastewater via TiO_2/activated carbon composite materials, Advances in Colloid and Interface Science, 159:130–143pp.

Gao, Y., Yue, Q., Gao, B., Sun, Y., Wang, W., Li, Q., and Wang, Y., 2013, Preparation of high surface area-activated carbon from lignin of papermaking black liquor by KOH activation for Ni(II) adsorption, Chemical Engineering Journal, 217:345–353pp.

Huang D., Miyamoto Y., Matsumoto T., Tojo T.,Fan T., Ding J.,Guo Q., and Zhang D., 2011, Preparation and characterization of high surface area TiO_2/activated carbon by low temperature impregnation, Separation and Purification Technology, 78:9–15pp.

Huang, H., Wei, M., Lin, Y., and Lu, P., 2009, Determining organic impurities in mother liquors from oxidative terephthalic acid synthesis by microemulsion electrokinetic chromatography, Journal of Chromatography A, 1216-12:2560–2566pp.

Huff, J.E. and Kluwe, W.M., 1984, Phthalate esters carcinogenicity in F344/N rates and B6C3 F mice, Prog. Clin. Biol. Res.,141:137–154pp.

Kalderis D., Bethanis S., Paraskeva P., and Diamadopoulos E., 2008, Production of activated carbon from bagasse and rice husk by a single-stage chemical activation method at low retention times, Bioresource Technology, 99:6809–6816pp.

REFERENCES (Continued)

Karthik, M., Dafale, N., Pathe, P., and Nandy, T., 2008, Biodegradability enhancement of purified terephthalic acid wastewater by coagulation–flocculation process as pretreatment, Journal of Hazardous Materials, 154:721–730pp.

Kim, J. Sohn, M., Kim, D., Sohn, S., and Kwon, Y., 2001, Production of granular activated carbon from waste walnut shell and its adsorption characteristics for Cu^{2+} ion, Journal of Hazardous Materials, 85-3:301–315pp.

Kim, K. and Ihm, S., 2011, Heterogeneous catalytic wet air oxidation of refractory organic pollutants in industrial wastewaters: A review, Journal of Hazardous Materials, 186:16–34pp.

Kleerebezem R., Beckers J., Hulshoff Pol, L.W., and Lettinga G., 2005, High rate treatment of terephthalic acid production wastewater in a two-stage anaerobic bioreactor, Biotechnol. Bioengr., 91(2):169-179pp.

Li, Y., Chen, J., Liu, J, Ma, M., Chen, W., and Li, L., 2010, Activated carbon supported TiO2-photocatalysis doped with Fe ions forcontinuous treatment of dye wastewater in a dynamic reactor, Journal of Environmental Sciences, 22-8:1290-1296pp.

Ling W., Qiang Z., Shi Y., Zhang T., and Dong B., 2011, Fe(III)-loaded activated carbon as catalyst to improve omethoate degradation by ozone in water, Journal of Molecular Catalysis A: Chemical, 342–343:23-29pp.

Liu S., Sun S., and Huang Z., 2010, Carbon spheres/activated carbon composite materials with high Cr (VI) adsorption capacity prepared by a hydrothermal method, Journal of Hazardous Materials, 173(1-3):377-383pp.

Matsumoto, T., Takahashi, S., Ueda, M., Tanaka, A., Fukuda, H., and Kondo, A., 2002, Preparation of high activity yeast whole cell bioctalysts by optimization of intracellular production of recombinant Rhizopus oryzae lipase, Journal of Molecular Catalysis B: Enzymatic,17(3-5):143-149pp.

REFERENCES (Continued)

Munter R., 2001, Advanced Oxidation Process–Current Status and Prospects, Proc Estonian Acad. Sci. Chem, 50-2:59-80pp.

Nowicki, P., Pietrzak, R., and Wachowska, H., 2010, Sorption properties of active carbons obtained from walnut shells by chemical and physical activation, Catalysis Today, 150(1-2):107–114pp.

Oliveira L., Pereira,Iara E., Guimaraes R., Vallone A., Pereira M.,João P., Mesquita J., and Sapag K., 2009, Preparation of activated carbons from coffee husks utilizing $FeCl_3$ and $ZnCl_2$ as activating agents, Journal of Hazardous Materials, 165(1-3):87–94pp.

Oller, I., Malato, S., and Sánchez-Pérez, J.A., 2011, Combination of Advanced Oxidation Processes and biological treatments for wastewater decontamination–A review, Science of The Total Environment, 409-20:4141–4166pp.

Ovejero, G., Rodriguez, A.,Vallet, A., and Garcia, J., 2013, Catalytic wet air oxidation of a non-azodye with Ni/MgAlO catalyst, Chemical Engineering Journal, 215-216:168–173pp.

Pariente M.I., Martinez F., Melero J.A., Botas J.A., Velegraki T., Xekoukoulotakis N., and Mantzavinos D., 2008, Heterogeneous photo-Fenton oxidation of benzoic acid in water: Effect of operating conditions, reaction by-products and coupling with biological treatment, Applied Catalysis B: Environmental, 85(1- 2):2–32pp.

Pillai K.C., Kwon, T.O., and Moon I.S., 2009, Degradation of wastewater from terephthalic acid manufacturing process by ozonation catalyzed with O_3, H_2O_2, Fe^{2+} and UV light: Direct versus indirect ozonation reactions,Applied Catalysis B: Environmental, 91:319–328pp.

Puma G.L., Bono A., Krishnaiah D., and Collin J.G., 2008, Preparation of titanium dioxide photocatalyst loaded onto activated carbon support using chemical vapor deposition: A review paper, Journal of Hazardous Materials, 157(2-3):209–219pp.

REFERENCES (Continued)

Quintanilla, A., Casas, J.A., Mohedano, A.F., and Rodriguez, J.J., 2006, Reaction pathway of the catalytic wet air oxidation of phenol with a Fe/activated carbon catalyst, Applied Catalysis B: Environmental, 67(3-4):206–216pp.

Raj C.B., Ramkumar N., Siraj M., and Chidambaram S., 1997, Biodegradation of acetic, benzoic, isophthalic, toluic an terephthalic acids using a mixed culture: Effluents of PTA Production, Trans IChemE(B), 75:246–256pp.

Rambabu R., Azargohar R., Dalai A.K., and Adjaye J., 2013, Evaluation and comparison of enrichment efficiency of physical/chemical activations and functionalized activated carbons derived from fluid petroleum coke for environmental applications, Fuel Processing Technology, 106:501–510pp.

Ramirez J. H., Maldonado-Hodar F. J., Perez-Cadenas A. F., Moreno-Castilla C., Costa C. A., and Madeira L. M., 2007, Azo-dye Orange II degradation by heterogeneous Fenton-like reaction using carbon-Fe catalysts. Applied Catalysis B: Environmental 75:312–323pp.

Ramirez J.H., Vicente, M.A., and Madeira, L.M., 2010, Heterogeneous photo-Fenton oxidation with pillared clay-based catalysts for wastewater treatment: A review, Applied Catalysis B: Environmental 98:10–26pp.

Ramirez J.H., Silva, A.M.T., Vicente M.A., Costa, C.A., and Madeira, L.M., 2011, Degradation of Acid Orange 7 using a saponite-based catalyst in wet hydrogen peroxide oxidation: Kinetic study with the Fermi's equation, Applied Catalysis B: Environmental, 101:197–205pp.

Rey A., Faraldos M. , Casas J.A., Zazo J.A., Bahamonde A., and Rodriguez J.J., 2009, Catalytic wet peroxide oxidation of phenol over Fe/AC catalysts: Influence of iron precursor and activated carbon surface, Applied Catalysis B: Environmental, 86:69–77pp.

REFERENCES (Continued)

Rey G., Carbajo J., Adán C., Faraldos M., Bahamonde A., Casas J.A., and Rodriguez J.J., 2011, Improved mineralization by combined advanced oxidation processes, Chemical Engineering Journal, 174-1:134–142pp.

Ricciardi M., 2006, Wastewater treatment by high efficiency heterogeneous photo-fenton process, The Third European Conference on Oxidation and Reduction Technologies for ex-Situ Treatment of Water, Air and Soil and in-Situ Treatment of Soil and Groundwater (ECOR-3), 90–91pp.

Rivera-Utrilla J., Bautista-Toledo I., Ferro-Garcia M.A., and Moreno-Castilla C., 2001, Activated carbon surface modifications by adsorption of bacteria and their effect on aqueous lead adsorption, Journal of Chemical Technology and biotechnology, 76:1209–1215pp.

Rusevova, K., Kopinke, F., and Georgi, A., 2012, Nano-sized magnetic iron oxides as catalysts for heterogeneous Fenton-like reactions - Influence of Fe(II)/Fe(III) ratio on catalytic performance, Journal of Hazardous Materials 241-242:433–440pp.

Saillenfait, A.M., and Laudet-Hesbert, A., 2005, Phthalates, EMC-Toxicol. Pathol. 2:1–13pp.

Senthilkumar S.T., Senthilkumar B., Balaji S., Sanjeeviraja C., and Kalai Selvan R., 2011, Preparation of activated carbon from sorghum pith and its structural and electrochemical properties, Materials Research Bulletin, 46:413–419pp.

Shafaei A., Nikazar M., and Arami M., 2010, Photocataytic degradation of terephthalic acid using titania and zinc oxide phocatalysts: Comparative study , Desalination, 252:8–16pp.

Spuhler D. , Andrés J., and Pulgarin R.H.C., The effect of Fe^{2+}, Fe^{3+}, H_2O_2 and the photo-Fenton reagent at near neutral pH on the solar disinfection (SODIS) at low temperatures of water containing Escherichia coli K12, Applied Catalysis B: Environmental, 96(1-2):126–141pp.

REFERENCES (Continued)

Tang K. S., Teng T. T., Alkarkhi A. F. M., and Li Z., 2011, Sonocatalytic degradation of rhodamine B in aqueous solution in the presence of TiO_2 coated activated carbon, APCBEE Procedia 1:110-115pp.

Tay, T., Uçar, S., and Karagöz, S., 2009, Preparation and characterization of activated carbon from waste biomass, Journal of Hazardous Materials, 165:481–485pp.

Teh C. M. and Mohamed A.R., 2011, Roles of titanium dioxide and ion-doped titanium dioxide photocatalytic degradation of organic pollutants (phenolic compounds and dyes) in aqueous solution, Journal of Alloys and Compounds, 509:1648–1660pp.

Thiruvenkatachari R., Ouk Kwon T., Chul Jun J., Balaji S., Matheswaran M., and Shik Moon I., 2007, Application of several advenced oxidation processes for the destruction of terepthalic acid (TPA), Journal of Hazardous Materials, 142:308–314pp.

Thiruvenkatachari R., Ouk Kwon T., and Shik Moon I., 2007, Degradation of phthalic acids and benzoic acid from terephthalic acid wastewater by advanced oxidation methods, Journal of Environmental Science and Health, Part A: Toxic/Hazardous Substances and Environmental Engineering, 41-8:1685–1697pp.

Tseng R., 2007, Physical and chemical properties and adsorption type of activated carbon prepared from plum kernels by NaOH activation, Journal of Hazardous Materials, 147-3:1020–1027pp.

Umar, M., Abdul, H., and Yusoff, M., 2010, Trends in the use of Fenton, electro-Fenton and photo-Fenton for the treatment of landfill leachate, Waste Management, 30-11:2113–2121pp.

USEPA, 1992, Code of Federal Regulations, 40 CFR, Part 136 (update).

REFERENCES (Continued)

Velegraki T., Xekoukoulotakis N., and Mantzavinos D., 2008, Heterogeneous photo-Fenton oxidation of benzoic acid in water: Effect of operating conditions, reaction by-products and coupling with biological treatment, Applied Catalysis B: Environmental, 85:24–32pp.

Velegraki T., Noulia E., Katsonia A., Yentekakis I.V., and Mantzavinos D., 2011, Wet oxidation of benzoic acid catalyzed by cupric ions: Key parameters affecting induction period and degradation, Applied Catalysis B: Environmental, 101(3- 4):479–485pp.

Yang, M., Xu, A., Du, H., Sun, C., and Li, C., 2007, Removal of salicylic acid on perovskite-type oxide $LaFeO_3$ catalyst in catalytic wet air oxidation process, Journal of Hazardous Materials, 139(1-2):86–92pp.

Yang T., and Lua A., 2003, Characteristics of activated carbons prepared from pistachio-nut shells by physical activation. Journal of Colloid and Interface Science, 267:408–417pp.

Yorgun S., Vural N., and Demiral H., 2009, Preparation of high-surface area activated carbons from Paulownia wood by $ZnCl_2$ activation, Microporous and Mesoporous Materials, 122(1-3):189–194pp.

Zazo J.A., Casas J.A., Mohedano A.F., and Rodriguez J.J., 2006, Catalytic wet peroxide oxidation of phenol with a Fe/active carbon catalyst, Applied Catalysis B: Environmental 65(3-4):261–268pp.

Zhang X.X., Cheng S.P., Wan Y.Q., Sun S.L., Zhu C.J., Zhao D.Y., and Pan W.Y., 2006, Degradability of five aromatic compounds in a pilot wastewater treatment system, International Biodeterioration& Biodegradation,58:94–98pp.

Zhang X., Sun S., Zhang Y., Wu B., Zhang Z., Liu B., Yang L., and Cheng S., 2010, Toxicity of purified terephthalic acid manufacturing wastewater on reproductive system of male mice (Mus musculus), Journal of Hazardous Materials, 176:300–305pp.

REFERENCES (Continued)

Zhang Y., Gan H., and Zhang G., 2011, A novel mixed-phase TiO_2/kaolinite composites and their photocatalytic activity for degradation of organic contaminants, Chemical Engineering Journal, 172:936–943pp.

Zhang Z., Liping M., Xu-Xiang Z., Weixin L., Zhang Y., and Wu B., 2010, Genomic expression profiles in liver of mice exposed to purified terephthalic acid manufacturing wastewater, Journal of Hazardous Materials, 181:1121–1126pp.

Zhou, M. and He, J., 2007, Degradation of azo dye by three clean advanced oxidation processes: Wet oxidation, electrochemical oxidation and wet electrochemical oxidation–A comparative study, Electrochimica Acta, 53-4:1902-1910pp.

PETKİM Petrokimya Holding A.Ş. Website, Manufacturing, Plants: PTA Plant - http://www.petkim.com.tr/Sayfa/1/241/URETIM-FABRIKALAR-PTA-FABRIKASI.aspx (Access date: 21.07.2014)).

RESUME

RES. ASSIST. GÜLEN TEKİN

CONTACT INFORMATION

Adress: Ege Üniversitesi Mühendislik Fakültesi
Kimya Mühendisliği Bölümü
Proses ve Reaktör Tasarımı Ana Bilim Dalı
Phone: 0-232-3114051
Mobile Phone: 0-505-5594586
E-mail: gulen.tekin@ege.edu.tr
gulentekin@gmail.com

PERSONAL INFORMATION

Nationality : Türkiye Cumhuriyeti
Place of Birth : Antalya
Date of birth Tarihi : 02/08/1988
Marital Status : Single

EDUCATIONAL BACKGROUND

2005 – 2011 : B.Sc.
Department of Chemical Engineering
Faculty of Engineering, Ankara University

2008 – 2009 : ERASMUS Exchange Programme, Dortmund-German
Department of Bioengineering and Chemical Engineering
(Fakultaet Bio-Chemieingenieurwesen)
Technical University of Dortmund
(Technische Universtaet Dortmund)

2001 – 2004 : High School
Antalya Aldemir- Atilla Konuk Anatolian High School

PROJECTS

2012 – 2015 : Researcher/Ege University – Scientific Research Project 12MÜH033 – Comparison of advanced oxidation methods and biological methods for treatment of Terephthalic acid plant wastewater

PUBLICATIONS:

National Journals (last 5 years):

G. Tekin, G. Ersöz, S. Atalay, Fenton-like oxidation of benzoic acid using Fe^{3+}doped basic activated walnut shells as a catalyst, Journal of Selçuk University Natural and Applied Science, ICOEST Conf. 2013 (Special Issue - 2), 130-137pp.

International Oral Presentations (last 5 years):

1. G. Tekin, G. Ersöz, S. Atalay, Fenton-like oxidation of benzoic acid using Fe^{3+}doped basic activated walnut shells as a catalyst, The Second International Conference on Water, Energy and Environment, ICWEE'2013,21-24 Eylül, 2013, Kuşadası, Türkiye.

2. G. Tekin, G. Ersöz, S. Atalay, "Fenton-like Oxidation of Benzoic Acid Using Fe^{3+} Doped Physically Activated Walnut Shells as a Catalyst", The international Conference on Environmental Science and Technology, the ICOEST'2013, 18 – 21 Haziran, 2013, Nevsehir, Türkiye.

National Oral Presentations (last 5 years):

1. Gülen Tekin, Gülin Ersöz, Süheyda Atalay, Ceviz Kabuğundan Farklı Aktivasyon Yöntemleri İle Hazırlanan Fe-Aktif Karbon Katalizörlerin Benzoik Asitin Katalitik Islak Hava Oksidasyonu İle Giderim Performanslarının Karşılaştırılması, On Birinci Ulusal Kimya Mühendisliği Kongresi (UKMK-11), 2-5 Eylül 2014, Eskişehir.

National Poster Presentations (last 5 years):

1. Süheyda Atalay, Gülen Tekin, Tereftalik Asit Fabrikasi Atik Sularinin Aritilmasinda İleri Oksidasyon Yöntemlerinin Kullanilmasi, Türkiye Innovasyon Haftası 2014, 29-30 Mayıs 2014, İzmir.